AN EXPERIMENTAL INVESTIGATION ON THE PROPERTIES AND PERFORMANCE OF GEOGRID AND GEOCOMPOSITE AS SUBGRADE REINFORCEMENT IN GRANULAR PAVEMENTS

Mr Glen James Barnes
Bachelor of Science (Ecosystem Management)

Submitted in fulfilment of the requirements for the degree of
Master of Philosophy (Engineering)
Faculty of Civil Engineering and Built Environment
Queensland University of Technology
2019

Keywords

Biaxial, CBR, clay soils, foundation, geocomposite, geogrid, geogrid performance, interface, pullout tests, small scale, strain gauge, subgrade, subbase, tensile, video extensometer

Abstract

The aim of this research is to address the gap in the literature that exists for small-scale laboratory testing on the performance of geogrid and geocomposite use in subgrade stabilisation. The focus of this experimental study is on developing a new small-scale laboratory testing model that will reduce the cost and expedite the performance verification process for future geosynthetic products, for use in foundation stabilisation.

An extensive literature review revealed that there has been a significant increase in research around the use of geosynthetics as foundation reinforcement, especially for unbound granular pavements. This is likely to have occurred due to the need to make pavement construction more cost effective and more environmentally sustainable under changing climatic conditions. Furthermore, due to continually changing environmental conditions increasing pavement degradation rates, a solution is required to minimise ongoing maintenance.

There are limited small-scale models discussed in the literature that are currently available to accurately assess all aspects of geogrid and geocomposite performance in pavement foundation. To perform this assessment accurately, and successfully develop future design guidelines, knowledge of the characteristics of the soil materials, geogrid and geocomposite is required. However, large-scale field trails to determine these characteristics are not always possible due to cost. Therefore, small-scale laboratory test models such as California Bearing Ratios, geogrid pullout tests and geogrid tensile tests represent a more cost effective solution.

This research investigates the performance of a biaxial polypropylene geogrid and geocomposite at the interface between a weak clay subgrade with CBR ≤ 3 and a commonly utilised granular subbase. These soil materials and physical condition were selected as they are common in Queensland. The aim of this research was achieved through methodology involving the design and manufacture of a large California Bearing Ratio (CBR) mould and geogrid tensile testing apparatus, and through a testing regime using the newly designed apparatus, as well as a bespoke geogrid pullout testing apparatus to determine interface properties. Further tests were also performed on soil materials to classify them and determine their physical properties to ensure a defined condition could be replicated for the subbase and subgrade in all facets of each test series.

The geogrid and geocomposite samples utilised in this study were subjected to a rigorous tensile testing regime to determine their performance under various strain rates. Throughout each of these test series, both contact and non-contact strain measuring techniques were experimented with, using strain gauges and a video extensometer respectively.

The subgrade and subbase soils utilised for this study were classified according to the USCS classification system as CH and ML respectively. The subgrade moisture content was manipulated to repeat a CBR ≤ 3, and the subbase condition was set at Optimum Moisture Content (OMC). During all testing phases involving these soils, above 95% compaction of field density was achieved.

The secant modulus and maximum tensile strength results from the tensile tests performed, using the newly designed and manufactured apparatus, showed good agreement with the manufacturer's claims when considering a strain rate of 20% per minute, and thus proving the success of this testing model. However, significant variation occurred when considering the 10% per minute and 30% per minute rates. The variation in these results was expected due to the usual trends observed when placing polymers under load. Furthermore, the non-contact strain measurement, using the video extensometer, showed good agreement with the contact strain measurement. However, it is recommended that other forms of non-contact strain measurement be explored.

The interface properties of each geosynthetic were successfully determined using the small scale bespoke testing model utilised in this study. By determining the friction angle and adhesion between each soil material and each geosynthetic, a calculation with an appropriate correction factor was developed. Using this model and the associated equation, predictions about geogrid and geocomposite performance in the field can be determined.

The final test series utilised the newly designed and manufactured large CBR mould with a diameter of 304mm and a height of 520mm. This test series was designed to assess the performance of geogrid with respect to subbase layer thickness, whilst attempting to minimise the boundary effect of the mould. The results of this testing showed that the inclusion of the geogrid at the interface layer did improve the overall strength of the foundation. Additionally, the boundary effect was measured qualitatively using pressure sensors, and it was determined that, under load, the boundary effect was only present at the interface layer. Furthermore, an equation was developed to determine the point at which using additional subbase materials to increase foundation strength can be

offset by using geogrid instead. This is important to minimise costs and wastage in the field.

As the new small-scale model tests proved to be a success, they have resulted in development of guidelines for assessing the performance of geogrid in a small-scale laboratory environment. More expensive, large-scale trials in the future may prove the success of these more economical testing models to accurately yield results that scale to a field condition, and show that these small-scale models can be utilised for developing guidelines for geogrid use in pavement subgrade stabilisation.

Table of Contents

List of Figures

List of Tables

List of Abbreviations

ASTM – American Society for Testing and Materials

BCR – Bearing Capacity Ratio

CBR – California Bearing Ratio

CMD – Cross Machine Direction

CNC – Computer Numerical Controlled

EN – European Norms

ISO – International Standards Organisation

LL – Liquid Limit

LVDT – Linear Variable Displacement Transducer

MD – Machine Direction

MDD – Maximum Dry Density

OMC – Optimum Moisture Content

PE - Polyethylene

PIV - Particle Image Velocimetry

PL – Plastic Limit

PP - Polypropylene

PSD – Particle size distribution

PVA - polyvinyl alcohol

QTMR – Queensland Transport and Main Roads

QTMRMTM – Queensland Transport and Main Roads Materials Testing Manual

UGM – Unbound Granular Material

UTM – Universal testing Machine

UTS – Ultimate Tensile Strength

VNCX – Video Non-Contact Extensometer

Statement of Original Authorship

The work contained in this thesis has not been previously submitted to meet requirements for an award at this or any other higher education institution. To the best of my knowledge and belief, the thesis contains no material previously published or written by another person except where due reference is made.

Signature: QUT Verified Signature Digitally signed by Glen Barnes Date: 2019.06.10 14:43:44 +10'00' _____

Date: ____10th June 2019_____

Acknowledgments

I would like to thank my principal supervisor, Dr Chaminda Gallage for his patience and valuable guidance throughout the last three years. The advice he provided helped me to piece all of my testing together to make this a cohesive and meaningful research project. I would also like to thank Dr Jay Rajapakse for being my associate supervisor.

I received some generous support from industry partners by way of providing materials for my research. These partners were Global Synthetics (geogrid and geocomposite samples), Karreman Quarry (subbase materials), and Queensland Transport and Main Roads (subgrade materials). I would also like to thank the Design and Manufacturing Centre at QUT for their support in constructing the bespoke testing apparatus.

Finally and most importantly, I would like to thank my fiancée Frances for her support and understanding throughout this research. Without her support, this study would not have been possible.

Chapter 1: Introduction

1.1 INTRODUCTION

This chapter outlines the background for this study (Section 1.2), the aims and objectives (Section 1.3), and the scope and significance of this research (Section 1.4), concluding with an outline of the remaining chapters of the thesis (Section 1.5).

1.2 BACKGROUND

Geogrid and geomembranes have been used extensively throughout Europe and the United States of America for decades, and due to this success, may represent the future direction for weak subgrade stabilisation in Queensland. The past abundance of available resources in Queensland has resulted in a lack of innovation in the civil construction industry concerning foundation stabilisation, however there is now a recognition of a need for new stabilisation materials and techniques. With the targeted use of geogrid, the quantity of virgin subbase material required for any one job can be significantly reduced (Demir et al., 2013; and Barbieri, Hoff and Mørk, 2019). As a result, this considerably reduces the cost of the construction without compromising on design quality.

In contemporary society, there is a heavy reliance on road transport and therefore a reliable undamaged pavement surface is required. With an ever increasing demand being placed on road networks, not only from increased traffic volumes but also climate change related adverse weather conditions, additional costly and time-intensive maintenance is being required (Ferrotti et al., 2011).

Queensland, specifically the southeast region, has areas where the subgrade material has a CBR value of less than three. In relation to pavement design this constitutes a poor subgrade condition and is not suitable for use as a pavement foundation material (Hufenus et al., 2006). One existing method used by Queensland Transport and Main Roads (QTMR) to reinforce a weak foundation is to compact thicker layers of a higher quality granular material over the top of the weak subgrade. The addition and compaction of these thick layers of subbase reduces the stress placed on the weak subgrade resulting from the increased load of the pavement and subsequent vehicle traffic, therefore increasing the lifespan of the pavement.

Geogrid stabilisation is one technique used to reduce the subbase layer thickness and therefore minimise the amount of virgin raw material required to create a suitable foundation condition. Placing geogrid between the subgrade and subbase layers adds strength to the foundation. The added strength is a result of the excellent tensile properties and the interlocking effect it has with the surrounding soil particles (Bergado et al., 1993).

There are a number of geogrid types available commercially that have different shapes, strengths and aperture sizes. However, despite this extensive range of products, a suitable small-scale laboratory testing method is not yet available to evaluate the performance of these new products. Therefore, development of a suitable model is required to assess geogrid performance, as field trials and large-scale model tests cannot be performed routinely.

1.3 AIM AND OBJECTIVES

The aim of the research is to develop a procedure to evaluate performance and properties of geogrid reinforced subgrade soil using a small-scale laboratory model test. This will entail development and testing of small-scale laboratory models to determine whether larger field trials are able to be scaled down and still yield accurate results. The small-scale models will consider a suitably sized CBR testing mold, a set of newly developed geogrid tensile test grips, and finally, a small-scale geogrid pullout test. This will be achieved through the following objectives:

i) development of small scale testing apparatus to determine the physical properties of geogrid and evaluate the performance of geogrid reinforced subgrade;

ii) investigation of the effects of geogrid and cover layer thickness on the performance of geogrid stabilised subgrade, using the small scale testing apparatus developed;

iii) investigation of the pullout, tensile resistance and interlocking effect of different geogrid products.

1.4 SCOPE AND SIGNIFICANCE

There is currently a significant gap in the literature regarding the testing of geogrid in a small-scale laboratory environment and using a poor-quality subgrade material – clay – as the soil medium. This study will focus on both of these aspects, allowing larger

laboratory and field trials to be completed in the future, building upon these smaller scale models.

This small-scale model is significant, as the way that each type of geogrid interacts with various soil types determines how effective it will be in the foundation design. As geogrid is most effective in soft soils, it is important to have numerical evidence of its performance. This study seeks to determine how effective a biaxial polypropylene geogrid and geocomposite will be in a Queensland clay soil with low strength conditions. Without the available experimental data, local design guidelines cannot be developed and therefore implemented.

This study will involve the development of design models to ensure more efficient and reliable testing methods for geogrid and geocomposite, therefore allowing various types to be implemented successfully in foundation designs. This will have positive short-term effects, as the initial construction will be quicker and more cost-effective. Furthermore, there are also positive long-term effects, as reduced periodic maintenance and rutting will potentially extend the life of the pavement.

1.5 THESIS OUTLINE

This thesis is prepared in seven chapters. Chapter 1 presents the background to the research problem, the research aim and objectives, scope and significance and the thesis outline. Chapter 2 reviews the currently available literature on granular pavement design procedures, subgrade improvement methods, geogrid use in pavement, design methods for geogrid reinforced pavement, laboratory methods to assess geogrid performance in pavement and addresses the implications arising from these studies. The research design methodology, the materials used in the test program and preliminary testing, procedure and timeline, analysis, and the limitations, are detailed in Chapter 3. Chapter 4 includes a detailed outline of the testing apparatus and procedures conducted. Chapters 5 and 6 present the results and discussions for the material testing and model testing respectively. Chapter 7 provides the conclusions and recommendations.

Chapter 2: Literature review

2.1 INTRODUCTION

This chapter will begin by providing a background on geogrid and geotextiles, including a brief history of their development and function. The chapter will continue with a review of the literature on granular pavement design procedures (Section 2.3) currently in use in Queensland, and how these were developed. Section 2.4 will analyse subgrade improvement methods, including their advantages and disadvantages. The following section (2.5) discusses how geogrid is used in pavement, and the properties that make it effective in adding foundation strength. Design methods for geogrid reinforced pavements, and the currently available options are evaluated in Section 2.6. Section 2.7 outlines the laboratory methods to assess geogrid performance in pavement, as well as the industry standard tests and their relevance. Finally, Section 2.8 highlights the implications from the literature that influence the direction of this study.

2.2 BACKGROUND

A British scientist and engineer Dr Brian Mercer first invented geogrid in the early 1950's (Das, 2016). Mercer had a background in the textile industry and it was from this background that he discovered the modern geogrid. Geogrid was industrialised when Mercer invented the plastic extrusion process known as the Netlon process: a process involving a single stage plastic extrusion, whereby the plastic takes on a net-like form.

Following this discovery, research began on geogrids and geomembranes from the early 1980s, as Mercer suggested that by adding his product to soil foundations, it would increase the tensile strength required for pavement foundations (Bhutta, 1998). New geogrid designs began to emerge that were not formed using the Netlon process, but instead by weaving the extruded strips together, heating the extrusions and fusing them together or even punching a regular pattern of holes in a thin sheet of polymer (Bhutta, 1998; and Das, 2016). Geogrid continued to be manufactured from various types of polymers; these include but are not limited to polyester, polyvinyl alcohol (PVA), polyethylene (PE) or polypropylene (PP)(Müller and Saathoff 2016).

Through the development of different geogrid production techniques, various designs with different shapes and thicknesses began to emerge. The most common shapes are still in production today: the square and the triangle. These designs are more commonly

recognised by their strain planes and are referred to as the square shape being biaxial, and the triangle shape being triaxial (Qian et al., 2010).

Geogrid has a diverse range of applications in the civil engineering industry. Applications include, but are not limited to: landfill capacity improvement, coastal and waterway construction and protection, control of asphalt cracking, mining, railway improvement, retaining wall and slopes, roadway drainage, pavement rehabilitation with moisture barrier protection, stabilising unpaved roadway structures, improving paved roadway structure and most importantly for this research, foundation construction and improvement.

Pavements require a strong and stable foundation to be built upon, which is not possible in every environment. Some locations necessitating road construction have very poor quality subgrade, and therefore require improvement prior to pavement construction. Failure to improve the subbase to a strong and stable condition results in pavement rutting and permanent deformation (Giroud, Ah-Line and Bonaparte, 1984). Subject to the in-situ conditions, these adverse effects can occur in a very short time frame post-construction, requiring significant ongoing maintenance.

Traditional methods of foundation improvement involve extensive excavation, backfill and compaction with a higher quality granular material. Furthermore, this higher quality granular material is not always available locally and must instead be transported to the site, thus increasing the cost of construction. However, by incorporating a geogrid into the pavement design, research has shown a significant reduction in the layer thickness of fill required by more than 30%, to achieve the strength conditions required (Hufenus et al., 2006). As a result, the amount of fill required to be transported can be minimised along with the construction costs.

Due to the vast number of geogrid and geomembrane products available commercially, and the hugely varied soil conditions existing worldwide, it is important to have accurate pavement design guidelines that have been robustly researched and tested. To achieve this objective, an understanding of the influential geogrid properties that need to be tested is required.

2.3 REVIEW OF GRANULAR PAVEMENT DESIGN PROCEDURES

In Australia, the peak governing body for pavement management is Austroads, comprising of 11 state and territory road transport and traffic agencies (Austroads, 2018). This body performs the important role of linking and providing knowledge and guidelines

to all of the members to ensure best practise nation-wide. Whilst each state or territory has slightly varied design procedures, Austroads state that their design procedures provide a balanced approach towards road planning and design (2018).

The purpose of pavement construction is to enable vehicle traffic to quickly and safely transport various loads. This is achieved through several means with the goal of even stress distribution to the subgrade soil and minimal permanent deformation (Abu-Farsakh et al., 2014). The pavement may be bound or unbound at the edges and be either sealed or unsealed on the surface.

A common pavement structure is generally comprised of four components: asphalt or concrete layers, base course layer, subbase and subgrade (Schuettpelz, Fratta and Edil, 2009). With all four of these layers working together, they are designed so that the compressive stresses are reduced on the on the lower layers and the tensile stresses are reduced in the surface layers (Abu-Farsakh et al., 2014). However, in 2015 Australia had approximately 870 000km of pavement with more than 80% classified as unpaved or granular, and not strictly conforming to this design structure (The World Factbook, 2018).

Granular pavement consists of various types of Unbound Granular Materials (UGM) that are compacted to form a trafficable surface. In order for this to be effective there needs to be minimal permanent deformation in each layer. Therefore, when considering a UGM in a pavement design, the resilient response of each material must be known to avoid uncontrolled permanent deformation (Werkmeister, Dawson and Wellner, 2004).

It is known that UGMs break down over time due to the stress placed on them from repeated traffic loads. As these materials break down, their physical properties change, which affects the way in which they interact. This therefore changes the conditions from the original design considerations, potentially increasing the rate at which permanent deformation occurs and reducing the life of the pavement (Hicks and Monismith, 1971).

In order to predict the physical changes in the UGMs, classification tests are required. These tests are laboratory-based tests that can consist of grain size distribution, compaction and Atterberg limits. Following these classification tests, the materials must be placed under load to determine how they will respond in the field. Werkmeister, Dawson and Wellner (2004) suggest that an effective way to simulate the traffic load over time (at an accelerated rate) is through repeated load triaxial tests. Therefore, if classification tests are performed before and after repeated load testing, the change in material properties can be determined and accounted for in the pavement design.

With the UGM physical properties characterised, design guidelines can be developed that allow for degradation of the soil material and extend the life of the pavement as a result. However, a pavement design is only as good as its weakest component. According to El-Ashwah et al. (2019), the weakest component is the subgrade material that sits below the UGMs. Therefore, to extend the life of the pavement it is also necessary to improve the subgrade strength.

2.4 REVIEW OF SUBGRADE IMPROVEMENT METHODS

To extend the life of a pavement structure, it is necessary to increase the strength of the weakest component: the subgrade. One example of a weak subgrade is a clay soil. Clay is weak because it is reactive, especially to climatic changes, with its strength varying greatly with moisture content. Clay soils exist all over the world in various forms, however how they respond to climatic conditions is not always consistent. Therefore, if an increase in subgrade strength is required for a pavement design, a mechanism to improve this strength is essential.

There are three common methods used globally to improve subgrade strength: excavate and fill, stabilise using lime or cementitious materials, or reinforce using geogrid. However, there are currently only two methods utilised in Queensland to increase strength in soft subgrade environments. These methods are excavation and fill, and lime or cementitious stabilisation. Each method has its advantages and disadvantages; however, geogrid stabilisation is also a viable method not yet being fully utilised.

2.4.1 Excavation and fill

Removing the weak material and replacing it with a stronger material is the most common method utilised for subgrade improvement. This approach is commonly known as the excavation and fill method. This method works very well and is the design approach implemented globally where there is a ready supply of higher strength soil material close by.

Barbieri, Hoff and Mørk (2019) discuss that in Norway, recycling materials from a location close to the construction can be a viable alternative to purchasing and transporting scarce virgin quarry materials if the location is only 20-30kms from the construction site. Whilst this may make it a viable alternative in Norway, the transport distances in Queensland between a road construction site and a suitable high strength granular material may be several hundred kilometres and therefore increases the construction cost significantly. However, cost today is not only measured in economic

value, with environmental impact increasingly becoming a consideration. As a result, transporting granular materials over long distances by truck will increase harmful emissions. Therefore, a more thorough assessment is required to develop a comprehensive cost-benefit analysis integrating life-cycle assessment.

The excavation and backfill method of subgrade improvement is the most common method specified in Australia (Paul and Grove, 2008). The challenges identified by Barbieri, Hoff and Mørk (2019) are consistent with those currently limiting pavement design guidelines in Australia (Paul and Grove, 2008). Furthermore, due to the vast distances covered by a single roadway, the in-situ soil may vary significantly. As a result, multiple onsite geotechnical tests such as a dynamic cone penetrometer and plate load tests or further laboratory tests such as CBR, Particle Size Distribution (PSD) or percentage of swell, may be required for a single project. Finally, current pavement design guidelines in Australia state that using the excavation and fill method, the minimum subbase cover layer that can be used over a highly expanse soil is 0.6-1m (Paul and Grove, 2008).

2.4.2 Lime and cementitious materials stabilisation

Stabilising and increasing the strength of a subgrade material using lime or various other cementitious materials is another common practise utilised globally and is part of the pavement design guidelines in Australia. Queensland began running trials with this technique in 1997 and confirmed its effectiveness in a study published in 2012 (Ausroads, 2012).

This method involves the mixing or injecting lime into a clay soil with a plasticity index above or equal to 10%. The lime should mix with the subgrade soil to a depth of at least 250mm and preferably up to 300mm. Using this method to improve subgrade has both positive and negative aspects, some of which occur almost immediately and other are more long term. (Ausroads, 2012)

Jameson (2008a and 2008b) describes lime stabilisation as a technique to rehabilitate and stabilise a weak subgrade soil, with other sources in agreement (Ausroads, 2012) that there are both positive and negative aspects to this technique. The most notable immediate positive aspects are a reduction in plasticity and swell, and improved compaction and bearing capacity (Celauro et al., 2012). The long-term benefits from this technique are explained by Celauro et al. (2012) as improved compressive strength and CBR and well as increased resistance to frost.

There are some negative aspects to lime stabilisation. Jahandari et al. (2017) note one specific issue and describe it as a major shortcoming: the increased brittleness that occurs is a result from the chemical reactions that occur when clay is stabilised with lime. However, Jahandari et al. (2017) suggest an appropriate method to reduce the impact of the increased brittleness and further increase the subgrade strength, which involves the inclusion of a geogrid.

2.4.3 Geogrid Reinforcement

When reviewing the available literature it is clear to see that geogrid is commonly used throughout Europe and the USA as a reinforcement product for multiple applications including railway, light structures, semi-permanent structures and pavement construction. Conversely, it is also evident, due to the lack of literature available, that geogrid products are not currently widely utilised or researched in Australia. This is likely to be the reason for a lack of available design guidelines for industry professionals to rely on.

Geogrid is defined as "a polymeric (i.e., geosynthetic) material consisting of connected parallel sets of tensile ribs with apertures of sufficient size to allow strike-through of surrounding soil, stone, or other geotechnical material" (Das, 2016, 1) and geocomposites (a geogrid with and the inclusion of an interwoven geotextile) are the dominant types of geosynthetics used in pavement construction. Each material varies in its effectiveness for any given situation. Their purpose in granular pavement design involves increasing the strength of a foundation by inserting the product in either the subbase or subgrade.

Geogrid products are more commonly used for pavement stabilisation. Kwon and Tutumluer (2009) explain that geogrid products provide higher friction values and increased confining stresses than a geocomposite, due to their interlocking ability with various soil materials. However, Kwon and Tutumluer (2009) suggest that the most effective foundation stabilisation may occur when both a geogrid and geocomposite are utilised symbiotically. This relationship is effective as Cuelho and Perkins (2017) suggest that the geocomposite provides a separation function that precludes the subbase from injecting into the subgrade when subjected to any normal stress, whilst the geogrid provides the strength gains through interlocking with the appropriately sized aggregates.

2.5 REVIEW OF GEOGRID USE IN PAVEMENT

In the mid-1980s, publications emerged aimed at evaluating the most beneficial ways geogrid could be used for soil reinforcement. Guido, Chang and Sweeney (1986)

focused on the bearing capacity ratio of strip foundations with and without geogrid reinforcement, and found a significant variation in settlement. To confirm their findings, Khing et al. (1993) conducted CBR tests in a large steel box (1100m x 304.6mm x 914mm) using sand over soil, placing geogrid layers at various intervals throughout the foundation. They determined there was a relationship between the maximum benefit and the depth of the reinforcement.

Further studies on bearing capacity and geogrid layer placement were piloted throughout the 1990s and 2000s adding to a growing body of literature on the topic. Lopes and Laderia (1996) wrote about the influence of confinement, soil density and displacement rate on soil-geogrid interactions. Adams and Colin (1997) evaluated large model spread footing load tests (also known as CBR tests) on geogrid-reinforced soils.

Perkins and Ismeik (1997) published a two-part series of technical papers summarising the available literature until 1997. This summary showed there had been several empirical models proposed by Haas, Walls and Carroll (1988), Webster (1993) and Montanelli, Zhao and Rimoldi (1997), based on experimental findings. Davies and Brindle (1990) and Sellmeijer (1990), made analytical considerations although they were not founded on experimental evidence. Perkins and Ismeik (1997, 606) summarised their research by stating, "[n]o design solutions which propose a general analytical solution that has been validated by experimental data have been identified".

Although research continued over the next decade, it has only been in the last five years that there has been a significant increase in research published on geogrids and geomembranes and their interaction with soil or sand. Research from Ferrotti et al. (2011), Ornek et al. (2012), and Cook and Andrews (2015) focused on predicting bearing capacity models of interactions between geogrid and various grades of soil. Similar laboratory based experiments on bearing capacity were conducted by Abu-Farsakh et al. (2013), Liu et al. (2014), Kumar et al. (2015) and Infante et al. (2016) with a slightly shifted focus to sand foundations.

There has been a recent increase in geogrid and geocomposite products becoming commercially available, each with their specific and varied physical properties. In order to maximise these individual properties in a granular pavement design, suitable small-scale testing models are required to determine their performance in specific conditions. Zornberg (2017) mentions some of these physical properties for a geogrid may include: reinforcement due to the tensile properties, stiffening due to the material properties of the polymer when placed under stress, and protection - as the geogrid provides a barrier

between soil layers when placing and compacting new granular material during construction. Al-Qadi et al. (2004) explain a geocomposite may have some additional physical properties due to the inclusion of the interwoven geotextile. The properties to be determined are filtration/ drainage as the geotextile allows liquids and gases to pass through without any soil material, and penetration, to determine the degree of force required from the aggregate to cause damage to the geotextile.

The physical properties of each reinforcement product directly translate to the specific benefit able to be utilised in a design guidelines for geogrid or geocomposite use in pavement. However, Powell, Keller and Brunette (1999), Berg, Christopher and Perkins (2000), Giroud and Han (2004), and Hufenus et al. (2006) all agree as to the greatest benefits of using geogrid and geocomposite to reinforce granular pavement structures. These include reducing excavation depth to remove poor quality soils, minimising the subbase layer thickness, reducing the contamination of the subgrade from the subbase material and the minimal requirement for maintenance leading to the extended life of the pavement.

2.6 REVIEW OF DESIGN METHODS FOR GEOGRID REINFORCED PAVEMENT

The addition of geogrid into pavement design methods has occurred through a necessity to reinforce weak subgrade conditions. Through this addition, the creation of a composite foundation condition occurs. The composite layer is comprised of both the granular material and the geogrid and may contain a single layer or be multi-faceted. When considering a design method for a geogrid reinforced pavement design, it is critical to know the strength of each composite layer. These parameters are likely to change with every variation in geogrid product and soil condition.

When considering changing parameters in a design method for a geogrid reinforced foundation, Patra, Das and Atalar (2005) mention there are important factors that play a role in establishing the composite strength. One factor, shown in Equation 1.1, is the Bearing Capacity Ratio (BCR), (Patra et al., 2005).

$$BCR = q_{u(R)} / q_{uu} \qquad \textbf{Equation 1.1}$$

Where

BCR = bearing capacity ratio

$q_{u(R)}$ = ultimate bearing capacity (reinforced)

q_{uu} = ultimate bearing capacity (unreinforced)

The BCR can be calculated after collecting data from a series of CBR tests on soil materials in a particular scenario. These tests consist of two conditions: the standard condition found in-situ – or unreinforced – and the same soil conditions recreated with the addition of a geogrid – or reinforced. The CBR test can be performed in-situ as Bloise and Ucciardo (2000) mention, by performing a test known as a Plate Bearing test, while the equivalent laboratory test was mentioned in section 2.5.

In 2004, Perkins et al. attempted to design a method for geosynthetic reinforcement in flexible pavements by performing a series of both field and laboratory tests, with the aim of creating a general standard to describe design methods for reinforced flexible pavements. However Perkins et al. (2004, 244) concluded that:

> while the work performed in this project showed the difficulty of distinguishing reinforcement ratios between different products and the need to develop average reinforcement ratios for reinforcement products as a whole, there may still be a need to have a limiting material specification for this application such that these reinforcement ratios are not applied to an inappropriate reinforcement product.

Since 2004, different potential design guidelines have been researched and published in an effort to include geosynthetics into flexible pavement projects. Two notable guidelines are those from The American Association of State Highway and Transportation Officials (AASHTO) and National Cooperative Highway Research Program (NCHRP).

These guidelines are based on previous research investigating the physical and mechanical properties of the geogrid (Webster, 1993; Cancelli and Montanelli, 1999; Perkins, 1999; and Berg, Christopher and Perkins, 2000), the location of the geogrid within the foundation (Haas et al., 1988; Webster, 1993; Perkins, 1999; Al-Qadi et al., 2008), and the interlocking effect that occurs between the geogrid and the soil materials (Lee and Manjunath, 2000; Abu-Farsakh, Coronel and Tao, 2007; Liu et al., 2009; McCartney, Zornberg and Swan, 2009; and Arulrajah et al., 2013). Despite numerous studies on

geogrid properties and its inclusion in a flexible pavement design, only a limited number of studies focus on the methodologies to quantify the effectiveness of this inclusion.

There are three internationally regarded methods commonly utilised when designing a flexible pavement with geogrid included as a reinforcement: The Steward, Williamson and Mohney (1977) Method, the Giroud and Noiray (1981) Method and the Giroud and Han (2004) Method. However, despite international acceptance, each method has its limitations.

The Steward et al. (1977) Method considers all geosynthetics as equal and designs are solely based on a 'with' and 'without' basis. In spite of the knowledge that not all geosynthetics are equal, this method is widely used throughout the United States of America.

The Giroud and Noiray (1981) Method, primarily utilised throughout Europe, focused on further developing the Steward et al. (1977) Method. This method was developed to determine a calculation for the granular layer thickness reduction due to the inclusion of the geosynthetic. This calculation, developed through years of various trafficking experiments, lead to an empirically based factor known as the 'stabilisation factor'. However, the limitation of this method is the only geosynthetic property considered was the tensile modulus, not how the geosynthetic interacts with the soil materials.

The Giroud and Han (2004) Method differs from the previous two methods as it allows the influence of the geogrid properties to be quantified. This method offers a mathematical framework to determine the reinforcement effectiveness from various types of geosynthetics. Although it does not require any calibration when considering a geocomposite, a limitation of this method is it does calibration for each specific type of geogrid.

The currently available literature shows that a comprehensive design criterion is still unavailable when considering using geogrid or geocomposite to reinforce granular pavement. Furthermore, as all available brands and types of geosynthetics vary in their physical properties, previous studies are limited as they are generally product and condition specific (Kwon and Tutumluer, 2009). Therefore, to address this gap in the literature a suitable small scale model is required to be developed to allow greater flexibility when evaluating the performance of a geosynthetic product in a particular condition, for example in Queensland, Australia.

2.7 METHODS TO ASSESS GEOGRID PERFORMANCE IN PAVEMENT

The performance of geogrid in pavement can be assessed using a variety of methods ranging from laboratory elemental and conditioning tests, to field trials. To assess the increase in performance due to the geogrid, it is important to test the physical properties and performance of the soil materials, and the geogrid, independently. This type of testing is advantageous as it allows completion of a series of simple and cost effective test procedures in a short timeframe.

A series of standard geotechnical tests recommended for soil materials in pavement design are outlined by Paul and Grove (2008) in their Guide to Road Design Part 7: Geotechnical Investigation and Design. These tests are designed to identify the physical or empirical properties of a soil material in any location throughout a construction site and include, but is not limited to, PSD, Liquid Limit (LL) and Plastic Limit (PL), CBR, Maximum Dry Density (MDD) and OMC (Paul and Grove, 2008).

A geogrid or geocomposite sample can also be tested in isolation, primarily using a wide-width tensile test. The wide-width tensile test is a well-defined test with both Europe and the United States of America having test standards available. Some variations between these test standards involve the use of both contact and non-contact forms of strain measurement to confirm the results obtained. Zornberg and Gupta (2010) explain that whilst this type of testing is effective for a geogrid or geocomposite, further laboratory and field tests are required to be carried out to confirm the values obtained. These tests are defined as confined tests, where a geogrid or geocomposite is confined by a soil or granular material. Examples of these types of tests used in past research to confirm these geogrid and geocomposite properties are pullout tests and CBR tests.

Publications from Bergado et al. (1993) on the interaction between cohesive frictional soil and geogrid reinforcement, and Farrag, Acar and Juran (1993) on the pullout resistance of geogrid began a new sequence of research. Farrag et al. (1993) investigated a new type of geogrid pullout box with the idea of creating a testing standard for future pullout research. Using fine-grain sand, they identified the key properties that are required when conducting a geogrid or geomembrane pullout test. The properties identified as being influential in this type of testing were “confining pressure, soil density, boundary conditions and geotextile characteristics” (Farrag, Acar and Juran, 1993, 133).

In the mid-1990s, Ochiai et al. (1996) and Lopes and Laderia (1996) extended the understanding of geogrid pullout testing by researching different sized testing apparatus as well as attempting a full scale field test. Ochiai et al. (1996) and Lopes and Laderia

(1996) both agreed that undertaking their research was significant, as there was still no established and accepted testing standard for geogrid pullout testing at that time.

Ochiai et al. (1996) used a laboratory pullout box with dimensions 600mm x 400mm x 400mm, however, did not mention what size specimen he was able to test with this apparatus. The results of this testing were compared with a full-scale instrumented field test on the same geogrid specimens with dimensions 500mm wide x 200mm and 400mm long (Ochiai et al., 1996). Ochaia et al. (1996) concluded by showing that the results from the field test were in good agreement with their laboratory tests and therefore performing the laboratory tests was an appropriate solution for determining analysis and design parameters.

Lopes and Laderia (1996) conducted laboratory geogrid pullout tests using a large shear box with dimensions 1530mm long x 1000mm wide x 800mm high. They reasoned that using such a large box was to minimise the boundary effect that may be influencing the results obtained from smaller testing apparatus. Whilst performing some successful tests they concluded that they could not be certain whether the size of the shear box was a contributing factor for the results obtained (Lopes and Ladeira, 1996).

In 2001, Sugimoto, Alagiyawanna and Kadoguchi tested a new theory about using flexible verses rigid shear box conditions for geogrid pullout testing. Their design consisted of a large shear box with internal dimensions 680mm long x 300mm wide x 625mm high, with large plates of acrylic and glass to reduce friction on the longitudinal walls (Sugimoto et al., 2001). This new design was not just unique due to the reduced friction: it also had flexible boundary conditions with air bags located both above and below the specimen. After performing a series of tests with different geogrid specimens under varying testing conditions, it was concluded that there was no significant difference between the pullout force for the rigid verses flexible shear box (Sugimoto et al., 2001).

In the last decade, geogrid pullout testing has had significant advancements regarding suitable testing methods and techniques to measure effective parameters. Kim and Frost (2011) took a new approach, and tested geotextiles using a very small pullout box. This study was based on previous literature showing that there was still no agreement that the size of the pullout box plays a role in the results obtained. Therefore, their study involved using a box with dimensions 102mm wide x 102mm long x 51mm high (Kim and Frost, 2011). After performing a series of successful tests, they were still unable to conclude that the size of the shear box played a role. However, they made some interesting

observations about the constrained versus unconstrained boundary conditions, stating that the unconstrained conditions better reflected the in-situ conditions (Kim and Frost, 2011).

Miyata and Bathurst (2012) conducted a reliability analysis of two different models commonly used in Japan using previously published data. The first model is commonly used when project-specific laboratory data is available and the second model is used when data is unavailable. The data that was published from previous tests was conducted on a shear box with dimensions 300mm long x 200mm wide x 200mm high, as this is what is published in the Japanese standard, JGS 0942-2009, for minimum dimensions (Miyata and Bathurst, 2012). The outcome of this research showed that the model used when data was not available significantly underestimated the pullout strength, compared to the model where data was available. This study has shown that currently no computer modelling software is able to accurately predict results as well as laboratory tests.

In 2016, Wang, Jacobs and Ziegler conducted both an experimental and discrete element method investigation into geogrid-soil interaction under pullout loads. After stating that "geogrid reinforcement mechanisms up till now have not been described conclusively"(Wang et al., 2016, 231), they performed their own pullout tests and used previously published data for their study. The shear box used for their study had dimensions 435mm long x 300mm wide x 200mm high, with one notable change that varied it from the ASTM D6706-01 test standard: the vertical load was applied through a rigid load plate rather than the flexible surcharge loading system (Wang et al., 2016). Following a successful study, Wang et al. (2016, 244) concluded that "the soil-geogrid interaction mechanisms might be investigated and described thoroughly with adequate models".

Bathurst continued his research with Ezzein from 2014, into geogrid pullout failures. Bathurst and Ezzein (2016) explored a better quantitative understanding of geogrid/ soil interaction using a transparent granular soil and an innovative shear box design. The shear box was the same dimensions used by Ezzein and Bathurst (2014) and had dimensions of 300mm high x 800mm wide x 3700mm long. With this large shear box already developed, they incorporated a clear bottom and using clear granular material, they attempted to use a non-contact digital image correlation technique to collect qualitative data and assess its validity (Bathurst and Ezzein, 2016). The most relevant outcome for this research was that Bathurst and Ezzein (2016) showed, for the polypropylene geogrid used, the measured in-air strain is comparable in to the in-soil strain.

The literature reviewed shows there has been some extensive studies performed to assess geogrid performance using a laboratory pullout method, however, no conclusive small scale studies have been completed on clay soils to determine interface properties for making predictions regarding field performance.

Assessment of both soil and geogrid materials in a confined situation for use in pavement design can be performed using a CBR test. The bearing capacity of a foundation can be determined both in the field via a plate load test, and in the laboratory using a UTM and mould, with the same materials tested in both circumstances yielding the same results. Over the last decade, several studies have used the CBR model to predict field conditions from laboratory experiments using bespoke methods and models to reduce some of the known limitations of this test procedure. These studies have included test variations involving reinforced and unreinforced subgrade and subbase soil samples, with variations in layer thickness for both, and finally positioning and quantity of the geogrid or geocomposite reinforcement layers.

Research by Naeini and Moayed (2009), and Singh and Gill (2012), used locally available soft clays and focused on improving the bearing capacity by embedding multiple layers of geogrid in the subgrade, and placing geogrid samples at various depths within the subgrade, respectively. Both studies resulted in showing an improvement in the bearing capacity with the inclusion of the geogrid. Similarly, research from Duncan, Williams and Attoh-Okine (2008) and Rajesh, Sajja and Chakravarth (2016) placed geogrid at the centre of their granular soil CBR tests. Once more, both studies showed a significant increase in bearing capacity due to the geogrid inclusion.

As the inclusion of a geogrid into a homogenous subbase or subgrade soil improves the bearing capacity, further studies were completed on simulated field conditions with a geogrid being placed at the interface layer between the subgrade and subbase. Moayed and Nazari (2011) performed separate CBR experiments by placing a geogrid sample in one test, and geotextile sample in the other test, at the interface layer of a clay-subgrade and sand-subbase. They compared their results and determined that the geogrid utilised for their research resulted in an increase in bearing capacity up to approximately 46%.

With geogrid proving to be a better material than geotextile for improving the bearing capacity of a foundation, research has continued with aims to minimise the limitations of the laboratory test models available and develop a suitable small scale testing

model for determining the effectiveness of any given geogrid sample, and at what point it became redundant.

Asha and Latha (2010b) performed CBR tests on soil, unreinforced and fused-junction geogrid-reinforced soil-aggregate composite system using the conventional CBR mould (150mm diameter) and a larger mould with 300mm diameter, both with a height of 175mm. The aim of this study was to determine the effect of the mould size on the resulting CBR value. Asha and Latha (2010) detailed the bearing capacity value obtained from their test method was almost 50% of the value obtained using the standard test procedure. Whilst this study yielded a significant result, the obvious limitation was the restricted height of the mould and therefore the layer thickness able to be tested.

When considering all of the literature available on assessing geogrid performance, there is unanimous agreement that the inclusion of a geogrid into a foundation design will increase its bearing capacity. However, a laboratory CBR test study is yet to be conducted for either clay or granular soil or a soil-aggregate composite system, using welded junction biaxial geogrid reinforcement at the interface layer with an appropriately proportioned large CBR mould.

Large-scale field trials are another way of assessing the performance of different geogrid products in various environments. These large-scale trials can be used to determine if the results from the small-scale trials do represent an accurate reflection of geogrid performance when considered and applied to differing environments. Due to the amount of time required and costs associated, these large scale trials are seldom undertaken without significant prior laboratory research. However, through numerous field trials conducted over the last two decades, each with a differing focus, a range of small-scale test results have been validated.

Bloise and Ucciardo (2000) completed studies on how geosynthetics are used to facilitate compaction on unpaved roads with soft subgrades. Similar research completed on a large scale, using multiple layers of geogrid to improve the bearing capacity of foundations, yielded positive results (Floss and Gold, 1994). Cancelli and Montanelli (1999) were interested in proving that the addition of a geogrid extended the life of the pavement and therefore conducted a full-scale in-ground test to collect evidence. Watts, Blackman and Jenner (2004), in a later study, were concerned with proving that with the addition of geogrid, a reduction in the necessary fill thickness layers is achievable.

Hufenus et al. (2006) published a study involving a full-scale field test on geosynthetic reinforced unpaved road on soft subgrade in Switzerland. This study

involved trialling many ideas proposed by previous smaller scale research projects and implementation on a much larger scale to determine their validity. Hufenus et al. (2006) focused their trial on investigating the bearing capacity of a soft subgrade and how it was affected by compaction and trafficking. The results of this field test showed a significant improvement in load carrying capacity for weak subgrade conditions specifically when using geogrid reinforcement in conjunction with thin subbase layers (Hufenus et al., 2006).

Demir et al. (2013) continued the earlier work conducted by Hufenus et al. (2006), and mentioned that there was still no accepted design showing the number of geogrid layers required to achieve the target strength. This full-scale field test conducted in Turkey used a plate loading method to investigate the CBR values in a series tests, using either one or two layers of geogrid, at unreinforced sites. Using the results obtained, they calculated both the subgrade modulus and the BCR. The findings from this research showed a significant improvement in the load-bearing capacity of the footing, and a decrease in the settlement, especially when using two layers of geogrid (Demir et al., 2013). Demir et al. (2013, 15) concluded by stating that "there is still no method to find out the subgrade modulus of reinforced soil layers".

2.8 IMPLICATIONS

This literature review has shown that research on geosynthetics is increasing, as they become more common for use in a wide range of applications. A notable growth area is the use of geogrid and geocomposite for stabilising pavement foundations. This is likely due to the emergent need for more cost effective and environmentally sustainable pavement design guidelines. The main consensus across this body of research is the viability of including geogrid or geocomposite in a pavement design for strengthening the foundation.

However, what is also clear is, despite the available testing models ranging from very small scale laboratory tests up to large scale field tests, there is still no internationally agreed small scale laboratory test model to assess geogrid performance. The key findings from the literature review are as follows:

- Geogrid and geocomposite can be successfully utilised in a pavement design to increase subgrade strength.

- The inclusion of geogrid in a foundation design reduces the overall costs of the pavement by minimising the amount of subbase required and extending the service life.
- Geogrid improves the strength of the subbase, subgrade and overall foundation condition when placed in multiple layers and at different locations within the foundation system.
- The overall performance of a geogrid or geocomposite pavement relies on various factors all working together. These factors, such as physical properties of both the geosynthetic and the soil material, layer thickness of subgrade and subbase, material degradation, climatic changes and magnitude of load, all require characterisation.
- The bearing capacity of a foundation is a crucial element when considering a pavement design. Researchers agree that standard laboratory CBR tests have a significant boundary effect influencing the results when considering scaling to field trials. Increasing the size of the mould has shown a reduction in CBR value, however the results are still inconclusive regarding the reduction in boundary effect.
- Geogrid pullout tests are an effective way to determine performance of geogrid in a foundation. Appropriate small-scale models are yet to be developed for efficient, cost effective testing. Therefore, design guidelines resulting from this form of testing are limited.

Through reviewing the key findings above, there are knowledge gaps in the literature that require further attention. These gaps are as follows:

- An Australian pavement design guideline utilising geogrid as a reinforcement technique is currently unavailable.
- There is a lack of appropriate small-scale laboratory testing models to assess the performance of geogrid as a granular pavement stabilisation technique.
- In order for comprehensive design guidelines including geogrid as reinforcement to be established, appropriate laboratory testing models for

CBR and pullout tests need to be developed to allow more cost effective testing.

Chapter 3: Research design

3.1 INTRODUCTION

This is an investigative study focused on new experimental methodologies for investigating geogrid and geocomposite performance in a small-scale laboratory environment. The following chapter describes the design adopted by this research to achieve the aims and objectives stated in Section 1.3. Section 3.2 details the methodology used in this research, outlining the key phases; Section 3.3 outlines the materials used throughout the research and the preliminary tests required; Section 3.4 describes how the analysis is undertaken; and Section 3.5 presents the limitations of the study.

3.2 METHODOLOGY

The objectives of this research were achieved following a methodology consisting of a number of activities. These are listed below.

- Extensive literature review to find a research gap from previous studies with a focus on small-scale laboratory studies involving geogrids and geocomposites interacting with clay soil.
- The design and manufacturing of a large size CBR mold for use in geogrid performance tests under monotonic loading conditions.
- The design and manufacture of capstan-style tensile testing clamps and associated attachment apparatus to perform materials testing on samples of geogrid and geocomposite.
- Laboratory classification testing on subgrade and subbase material to enable specific conditions to be simulated for testing following the 4th Edition of Queensland Transport and Main Roads Materials Testing Manual (QTMRMTM) that is based on Australian standard AS 1289:2014. The tests conducted were Q103A, Q103B, Q103F, Q104A, Q105, Q106, Q109 and Q145A.
- Preliminary CBR tests on both subgrade and subbase to determine density and moisture contents required to achieve a CBR ≤ 3. This test was conducted following Q113A.

- Laboratory geogrid CBR testing with a known subgrade and subbase condition with various thicknesses of subbase. The test method followed was Q113A where possible.
- Laboratory geogrid and geocomposite pullout testing on subgrade only, subbase only and simulated field condition. The test method followed, where possible, was ASTM D6706.
- Laboratory tensile testing to determine elastic properties of geogrid and geocomposite samples. The tests standard followed, where possible, was BS EN ISO 10319:2015.
- Analysis and interpretation of experimental data to evaluate properties and performance of geogrid and geocomposite-reinforced subgrades.

All laboratory testing and manufacturing was completed at Queensland University of Technology (QUT), Brisbane.

3.3 MATERIAL USED IN TEST PROGRAM

Throughout the test program four different materials were used: subgrade soil, gravel as a subbase layer, a geogrid and a geocomposite. All four of these materials required their physical properties to be investigated for various reasons. These reasons included but were not limited to ensuring repeatability of tests, ability to manipulate samples to create specific conditions, maintaining quality control of samples and ensuring accuracy in test results.

The subgrade and subbase materials required index and classification tests to be performed. These tests included particle size distribution, compaction tests and Atterberg limits, and were conducted according to the standards referenced in Section 3.2. Following these standards ensured all properties for the soils being utilised throughout the testing regimen were known and accurate.

The subgrade material provided, shown in Figure 3-1, was pre-prepared by QTMR as a representative sample of a soft soil found in the southeast region of Queensland. The material was classified in accordance with the tests mentioned previously, to ensure that the conditions could be replicated to achieve a CBR ≤ 3. This was to ensure that the conditions were consistent across all testing regimens.

Figure 3-1 Image of subgrade soil used for this research

The subbase material, shown in Figure 3.2, was provided by a local quarry as a representative sample of the high quality virgin material currently specified by QTMR in pavement designs in southeast Queensland. Approximately 600kg was required for this research and used for classification, pullout, and CBR testing.

Figure 3.2 Image of subbase soil used for this research

Geogrid and geocomposite samples were supplied by a local distributer as examples of products that may be incorporated into future pavement designs in Queensland. These two products are produced by a geotextile manufacturer based in Germany and exported worldwide. For the purpose of this research, the two products are referred to respectively as a geogrid and a geocomposite.

The geogrid sample was utilised in the tensile tests, pullout tests and the CBR tests. The geogrid is a white plastic polymer known as polypropylene. It is produced in a grid pattern with a width of 12mm and depth of 1.2mm, consisting of flat bars with welded junctions approximately 32mm apart from flat-to-flat in both directions (see Figure 3-2). The particular product used in this research had a manufacturer's claimed maximum tensile strength of ≥30kN/m in both the Machine Direction (MD) and the Cross Machine Direction (CMD).

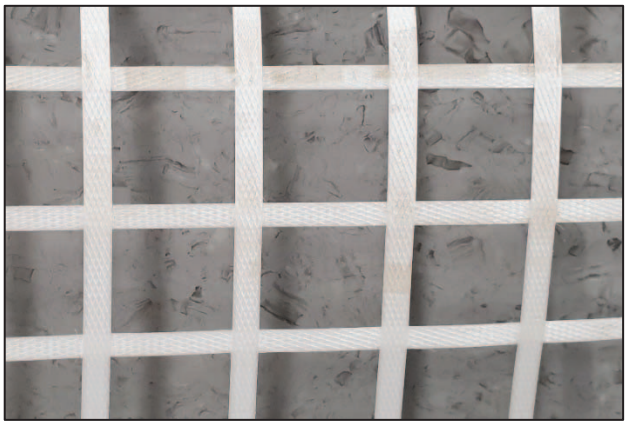

Figure 3-2 Image of geogrid used in this research

The geocomposite was utilised for the tensile tests and the pullout tests. Similar to the geogrid, the geocomposite is made of a white polypropylene polymer and produced in a grid pattern with flat bars intersecting at welded junctions. The bars have a width of 12mm and depth of 1.4mm, with the aperture again being approximately 32mm x 32mm. The geocomposite varies from the geogrid as it has a higher tensile strength rating from the manufacturer of ≥40kN/m in both the MD and CMD. It also has a geotextile woven into the grid made of polypropylene (see Figure 3-3).

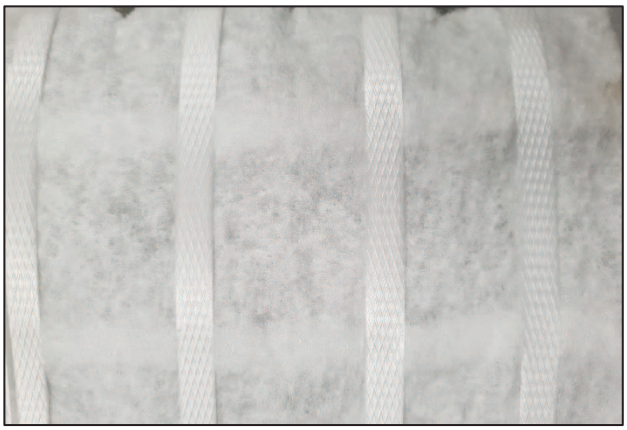

Figure 3-3 Image of geocomposite used in this research

Each sample was prepared in accordance with the relevant test standard and sized to suit the particular test and setup available. The sample sizes for each test varied slightly and the sizes used for each tests can be found in Table 3-1.

Table 3-1 Geogrid and geocomposite sample sizes used for all test series

	Sample width (mm)	Sample length (mm)	Ribs under load in the direction of force
Tensile Test	136	304 (including grip section)	4
Pullout Test	136	304 (including grip section)	4
CBR Test	220	220	6 x 6

3.4 LIMITATIONS

Throughout the research there were a number of limitations resulting from conditions or delays beyond the control of the researcher, which are outlined briefly below.

- Due to the physical properties of the subgrade material and requirement for uniform moisture content (requiring seven days for curing), there was a limit on the number of samples and individual tests that were possible in the given testing time.

- Part of this research involved the design and manufacture of new testing equipment. Delays in the manufacturing process limited the available time to conduct testing on a wide range of materials.
- Sample preparation, involving compaction of both the subgrade and subbase into the CBR mold, was a lengthy and labour-intensive process. Due to this, only the geogrid sample was able to be tested under all conditions.
- As with all experimental research involving testing equipment, there will be both human error and equipment error in each test.
- Throughout the pullout testing there were extensive delays due to equipment failure, ranging from between one and seven months on each occasion.

Chapter 4: Testing apparatus and test procedures

4.1 INTRODUCTION

Due to the nature of this research, it was necessary to have a chapter dedicated to the testing apparatus designed and used throughout. Chapter 4 presents each of these various pieces of apparatus in detail. Section 4.2 outlines the development of the model cylinder and the testing procedures used; Section 4.3 describes the geogrid tensile testing apparatus designs and the testing procedures followed; Section 4.4 includes details of the geogrid pullout apparatus with the relevant procedure; and Section 4.5 outlines the hardware and software utilised for obtaining strain measurements throughout the relevant tests.

4.2 DEVELOPMENT OF MODEL CYLINDER AND TESTING PROCEDURE

The development of this small-scale testing apparatus is critical to being able to assess the performance of various types of geogrid. This design is based on the conventional 150mm diameter CBR mold, upscaled to allow testing on a greater range of materials. The increase in size also helps to reduce the boundary effect, allowing larger geogrid samples to be tested, and allowing for variation in soil layer thickness. By allowing a larger representative sample of the geogrid to be tested, and reducing the impact of the boundary effect, the test results have a greater chance to successfully scale to future field tests for validation.

The new design has an internal diameter of 308mm and a height of 518.30mm (see Figure 4-1). The mold has been designed so that once the sample has been tested, it can be removed from the mold, undisturbed, for analysis.

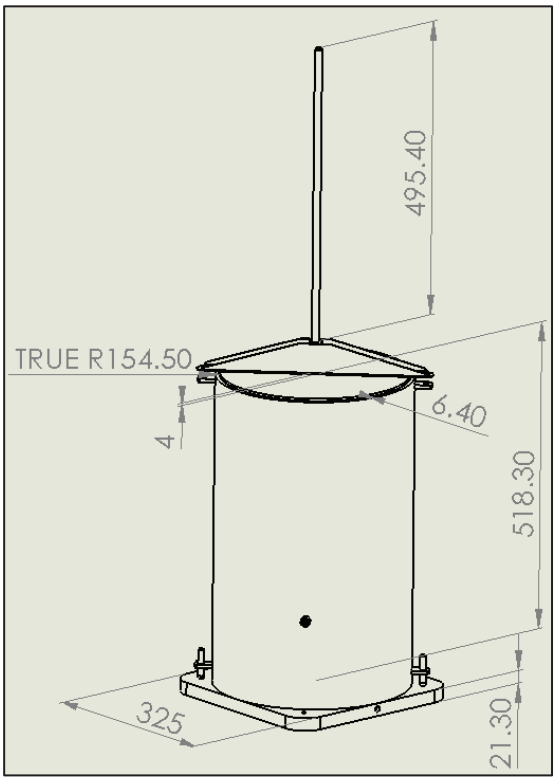

Figure 4-1: Technical drawing of new CBR mould using Solidworks (dimensions in mm)

The new mould was constructed from various materials with suitable strength and anti-corrosive properties. These materials are listed below:

- Cylinder: 6.40mm thick galvanised mild steel
- Loading Base: approximately 20mm thick anodised mild steel
- Top Cap: 4mm thick anodised mild steel
- Pneumatics: plastic hose, aluminium taps and a variety of plastic and aluminium fittings (not visible in Figure 4-1)
- Internal sleeve: 2mm thick aluminium cylinder (not visible in Figure 4-1)
- Threaded rod: 495.40mm long brass
- Top brace: 2mm thick aluminium

Due to the new mould being upscaled from the standard CBR mould, the plunger was also required to be rescaled so as to maintain the 1/5 ratio of the standard CBR testing apparatus. This was achieved by design and manufacture of an attachment to the existing standard sized CBR plunger. The new plunger attachment, shown in Figure 4-2, was

manufactured from mild steel and has a diameter of 61mm and height of 40mm. The new attachment, secured to the existing plunger with a hex head grub screw, firmly beds down onto a flat section milled into the existing plunger.

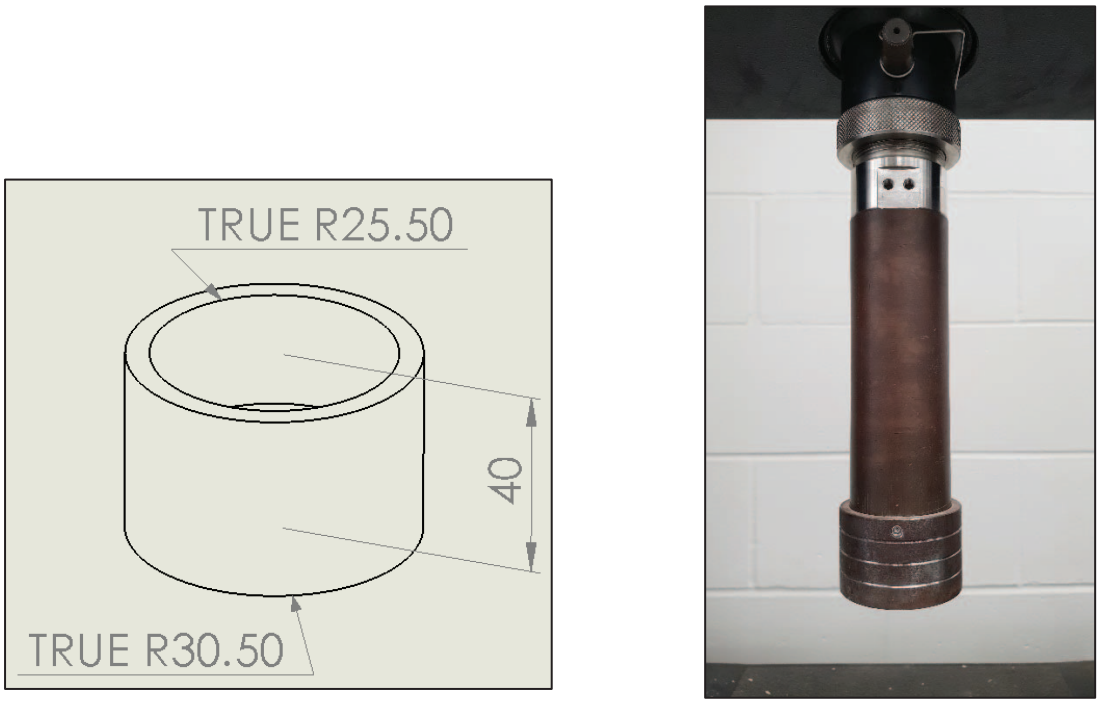

a) b)

Figure 4-2 a) Technical drawing of plunger extension using Solidworks (dimensions in mm) b) Image of CBR plunger with attachment to suit new mould dimensions

The new mold and plunger attachment were used to perform a series of CBR tests under various conditions. These tests were performed using an Instron Universal Testing Machine (UTM) model 5569A (Figure 4-3). The UTM specifications are as follows: 50kN capacity load cell in both tension and compression, 1712mm available travel, digital and analogue outputs, and controlled by a computer system running Bluehill 3 software version 3.13.1260.

Figure 4-3 Image of 50 kN Instron Universal Testing Machine used for both CBR and tensile tests

Laboratory CBR tests were performed following the test standard AS 1289.6.1.1:2014 where possible. There were significant variations to this standard including the diameter of the test mold, different compaction method and diameter of the plunger (all owing to the new design). Other variations included no surcharge weight being applied, and the fact that only unsoaked specimens were tested.

The sample preparation and testing procedure followed for this test series is outlined below and a schematic diagram of the test cell is shown in Figure 4-4.

1. The subgrade soil was oven dried to 0% moisture content and once cooled to room temperature water added to achieve predetermined moisture content. This sample was then left to achieve uniform moisture content for 7 days before being utilised for testing.
2. Subbase material was prepared in the same way as the subgrade, however only 24 hours was required to achieve uniform moisture content.

3. Where required, pressure sensors were installed on the CBR mould walls directly opposite each other.
4. Subgrade soil was compacted in 6 x 40mm thick layers in the bottom of the CBR mould.
5. Where required, geogrid (with and without strain gauges) was installed on the top layer of the subgrade.
6. Pre-prepared subbase material was compacted on top of the geogrid in 50mm, 100mm, and 150mm layers as per testing requirements.
7. CBR mould was transferred to the UTM and testing was performed.
8. Load, extension and strain measurements were collected for further analysis.

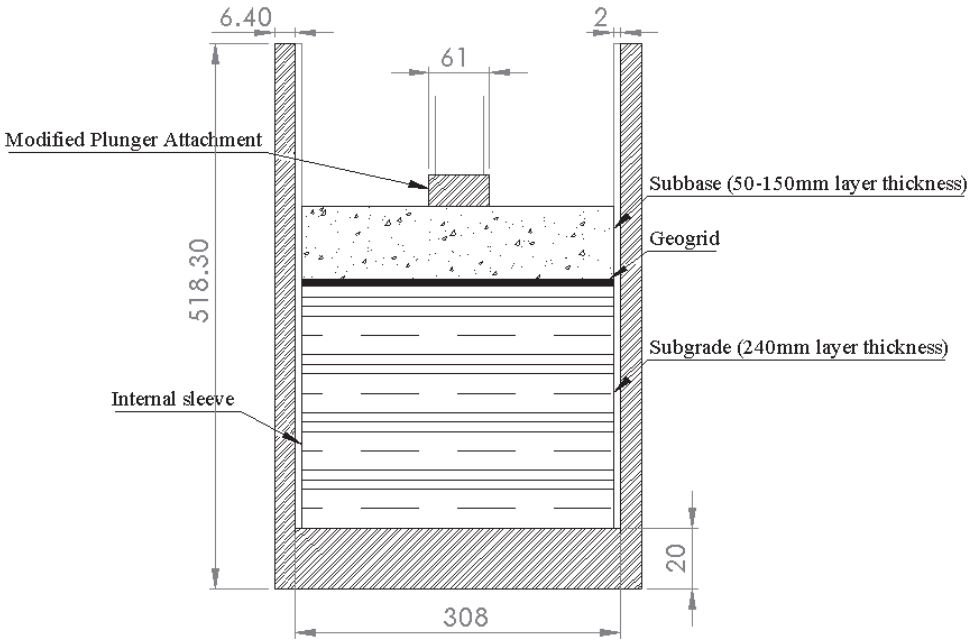

Figure 4-4 Schematic Drawing of CBR test cell setup using Solidworks (dimensions in mm)

To determine the extent of the boundary effect occurring within the new mold design, tactile pressure sensors were installed in some tests. These sensors were Tekscan model 5515 sensors attached to proprietary handles and controlled via the supplied software. Two sensors each have an effective measuring area of 343.4mm long and 86.4mm wide (shown in Figure 4-5). The sensors, installed opposite one another, were located in the cell between the soil and the inner wall (shown in Figure 4-6). These sensors collected a qualitative measurement of the pressure exerted by the soil on the inner wall, from the base of the cell to above the subgrade - subbase interface.

Figure 4-5 Image of pressure sensor used in this experimental design

a) b)

Figure 4-6 a) Image of Tekscan sensors mounted in modified CBR cell b) Image of Tekscan sensors connected to data collection hardware ready for testing

To determine the strain induced in the geogrid samples tested, strain gauges were attached to a series of specimens (see Figure 4-7). The strain gauges, software and hardware utilised, are detailed in Section 4.5. It is important to note that every test performed with strain gauges attached to the geogrid sample had a thin film of commercially available, highly flexible silicon applied to the electrical contacts to avoid any interference from the moisture in the samples.

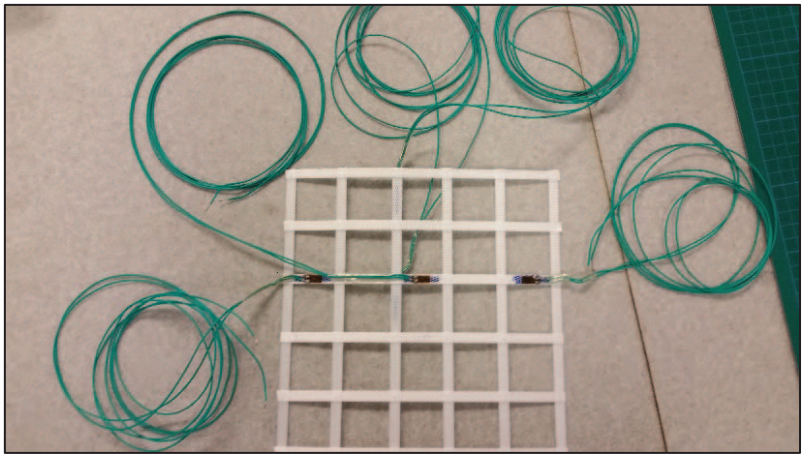

Figure 4-7 Image of geogrid sample prepared for CBR tests with strain gauges attached

4.3 GEOGRID TENSILE TESTING APPARATUS AND TESTING PROCEDURE

Understanding the physical properties of the geogrid and geocomposite samples was fundamental to analysis of the results from the pullout and CBR tests – in particular, the ultimate tensile strength (UTS) and the secant modulus (elastic modulus) of the samples. Unfortunately, the required equipment to perform tests on this scale was not all available at QUT nor available to purchase. Equipment, including clamping mechanisms and associated attachment, had to be designed and manufactured onsite before any testing could take place.

The clamping mechanism was designed to be similar to that of a capstan grip to allow a wide variety of geogrid or geocomposite materials to be tested. The dimensions of the clamp are specified as per Figure 4-8, and are the same dimensions as the clamp used in the pullout tests described in Section 4.4. Maintaining this consistency across both the tensile tests and the pullout tests meant that the test sample width would remain consistent. The clamp, constructed from mild steel, was anodised to protect the surface from corrosion. The bolts used to hold the flat section onto the cylinder were M8 x 20 caphead bolts.

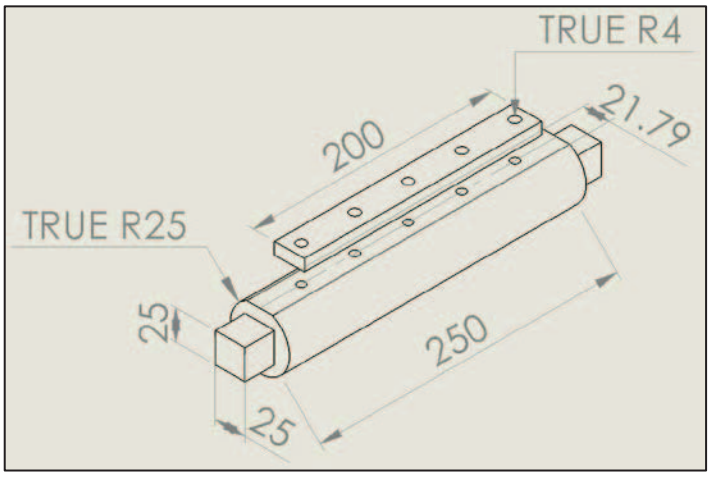

Figure 4-8 Technical drawing of geogrid clamp using Solidworks (dimensions in mm)

A mechanism, seen in Figure 4-9, to attach the geogrid clamp to the UTM was also required to be designed and manufactured. This was designed to suit both the geogrid clamp and the standard 50kN UTM jaws utilised for performing tensile tests. The attachment mechanism was produced using a 5-axis Computer Numerical Controlled (CNC) machine and constructed from mild steel, with an anodised coating to inhibit corrosion. The sides were secured using M6 x 25 flat head bolts.

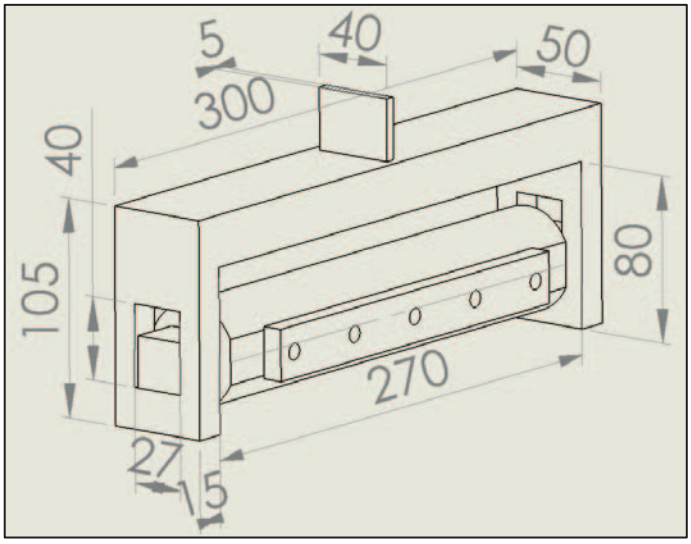

Figure 4-9 Technical drawing of complete geogrid tensile testing clamp with attachment using Solidworks (dimensions in mm)

Following the design and manufacture of the previously mentioned pieces of equipment, all items were assembled and attached to the UTM, as in Figure 4-10. The video extensometer (specifications outlined in Section 4.5) was setup and calibrated (as

per the manufacturer's guidelines) at a distance of 475mm from the front of the lens to the front of the specimen, marked with two black lines 60mm apart (30mm either side of the welded junction in the vertical direction). The UTM had identical specifications to the one outlined in Section 4.2, and the strain gauges, when utilised, were identical to the ones outlined in Section 4.5.

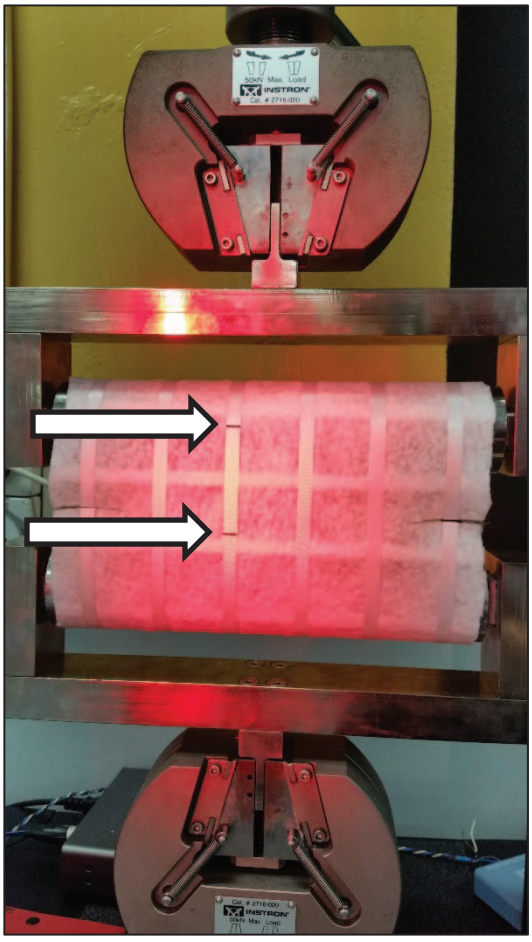

Figure 4-10 Image of tensile testing apparatus completely assembled in the UTM, showing the two black lines for strain measurement via the VNCX

A minimum of five samples of both the geogrid and the geocomposite were tested in the MD and CMD at each of the various rates. Each sample had the initial dimensions 220mm (wide) x 304mm (length), with the exterior elements cut before loading, thus reducing the active elements to a width of 136mm or four elements. The geocomposite required additional preparation to remove sections of the geotextile woven into the sample to allow the bolts to pass through for attachment to the clamp. In the case of the geocomposite for the CMD sample, some of the geotextile was removed to allow access

to the vertical elements for the video extensometer to record the strain measurements during the test (shown in Figure 4-11).

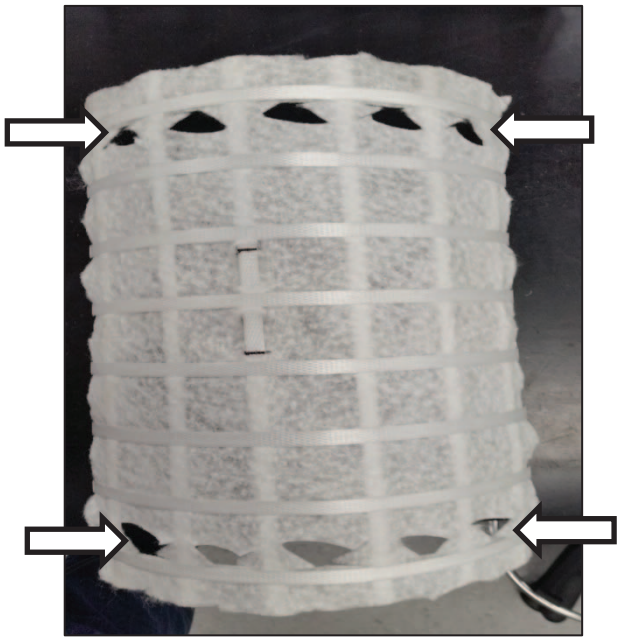

Figure 4-11 Image of geocomposite sample prepared for testing, showing geotextile sections removed

Tests were conducted according to the test standard ISO 10319:2015 with the following variation; two additional strain rates were considered 10 % per minute and 30 % per minute. All tests were conducted using the following procedure:

1. Attach grips and clamping mechanism to UTM and prepare testing method in software.
2. Setup VNCX as specified.
3. Cut correct sample size from large roll supplied by the manufacturer.
4. Trim all sides to allow 10mm of excess rib from all junctions.
5. Cut outer most ribs in the centre, as per ISO 10319:2015.
6. Prepare surface for strain gauge attachment (where required).
7. Using a fine black permanent marker, rule two lines 60mm apart on a central vertical rib in line with the VNCX lens.
8. For geocomposite samples, remove required geotextile to allow screws to pass through for clamping.

9. Attach geogrid or geocomposite sample to clamps allowing 100mm between clamp centres.
10. Perform tensile test collecting load, extension and strain data for further analysis.

4.4 GEOGRID PULLOUT TESTING APPARATUS AND TESTING PROCEDURE

Laboratory tests were conducted using apparatus available at QUT. The primary piece of equipment used was a Wykeham Farrance Shearmatic 300 direct shear tester with a geogrid pullout jig, shown in Figure 4-12. The pullout jig was custom-built by the local distributor of the equipment, and was designed to be as large as possible to suit the available test area.

a) b)

Figure 4-12 a) Image of the Wykeham Farrance Shearmatic 300 used for pullout tests, b) Plan view of pullout jig attachment designed and manufactured to suit Shearmatic 300

The shear tester with pullout jig capability was used to determine the pullout resistance and interface properties for the geogrid and geocomposite samples under various normal stresses. These tests were designed with the aim of representing specific field conditions that exist in soft subgrade environments in Queensland, with further tests completed on the subgrade only and subbase only, to determine friction properties for analysis.

The tests were conducted following the ASTM D6706 (2013) standard where possible. The significant variations to this test standard included the size of the test area, omission of wire gauge displacement devices, and the clamping mechanism. These changes were made due to the available equipment at QUT and due to these changes, there are no geogrid pullout test standards which were able to be strictly followed.

The Shearmatic 300 is a hydraulic machine that also operates on a screw drive. It has two 100kN load cells to measure the vertical and horizontal loads and two 50mm linear variable displacement transducers (LVDT) to measure the displacement. The shear box itself is operated on a screw drive, and everything is controlled by a user interface developed by CONTROLS Pty Ltd. The pullout tests were conducted at a rate of 1mm/ minute for all sample and normal stress variations.

Both the geogrid and geocomposte were held in place during the tests by a single capstan-style grip, the same design used for the tensile testing. This grip was also locally designed and manufactured to suit the size of the pullout box. The schematic diagram shown in Figure 4-13 has dimensions 150mm (w) x 150mm (l) x 200mm (d). This allowed for 70mm of soil material either side of the test specimen as the porous plate top and bottom were 30mm each.

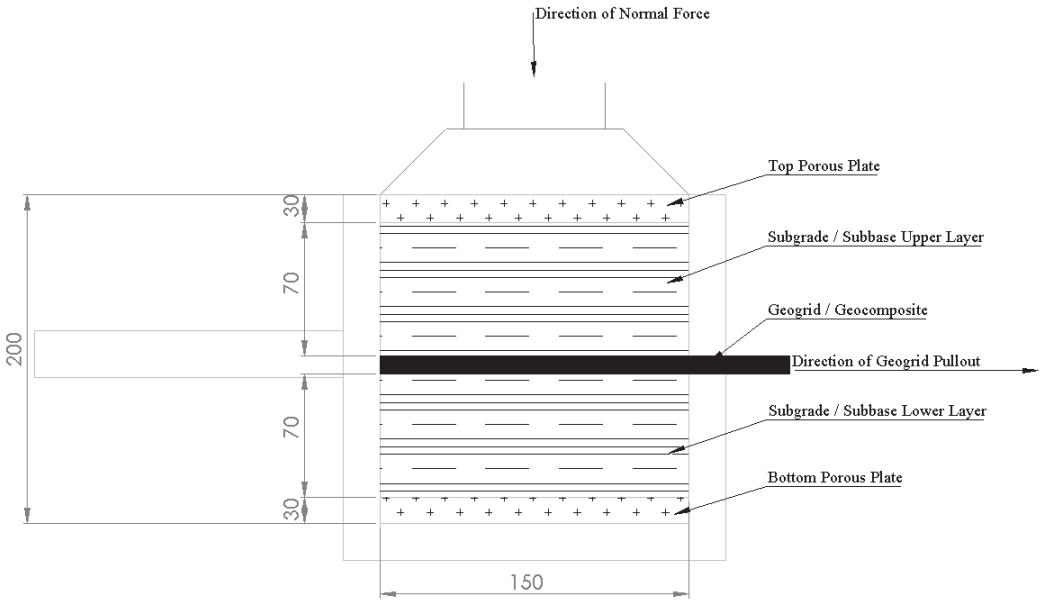

Figure 4-13 Schematic diagram of pullout box test setup using Solidworks (dimension in mm)

Consolidation and pullout tests were conducted for each sample with load and displacement data collected for both phases via the Controls software. Each test was prepared in a series of four steps, outlined here.

1. Compact the required soil in the lower half of the pullout box to ≥ 95% compaction.
2. Attach geogrid to clamp and place in holder whilst inserting the sample into the slot located centrally in the pullout box.
3. Compact the required soil in upper portion of the pullout box again to ≥ 95% compaction.
4. Reassemble upper loading platen and begin testing.

4.5 STRAIN MEASUREMENT

Strain measurement is a key component utilised within all facets of this investigation. During all tests conducted throughout the research, the apparatus recorded load and extension data as it exerted force on the sample, with additional external devices collecting other data in some tests. These additional data collection devices, operating independently of the testing equipment, were pivotal in confirming that the data provided by the apparatus was indeed accurate. As with all testing equipment there is always a degree of error associated, in spite of accurate calibration. These external independent devices were stick-on strain gauges, shown in Figure 4-14, and a non-contact video extensometer shown in Figure 4-15. Both of these strain measurement devices require additional software and hardware support to enable data collection.

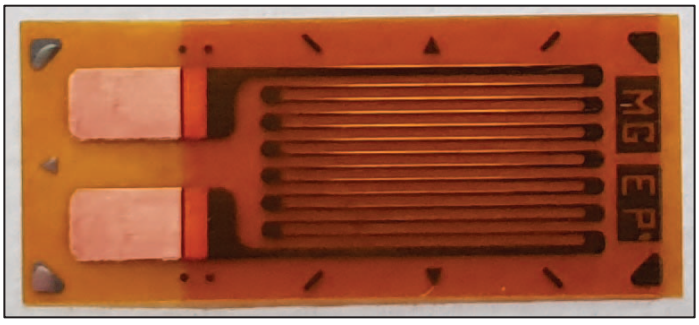

Figure 4-14: Image of stick-on strain gauge used in all testing variations for this research

The strain gauges were utilised in the tensile testing and CBR testing. The purpose of the strain gauge in each of these situations was to take a direct measurement of strain from the sample it was attached to. Each gauge was attached to the geogrid or geocomposite sample using a thin film of cyanoacrylate, and where required a thin film of

a commercially available, highly flexible, silicon over the electrical components to shield them from any moisture in the sample. For the technical specifications of the strain gauges used, see Table 4-2.

Table 4-1 Strain gauge specifications

Brand	Item code	Purpose	Dimensions (mm)	Grid resistance (Ohms)	Gauge factor at 24 DegC
Micro-measurements	6836	General purpose	6 (w) x 13 (l)	120.0 +/- 3%	2.100 +/- 0.5%

Small gauge wires were soldered to the pads located on the strain gauge in order for the electrical current to pass through the gauge and back to the data collection hardware and software. The electrical current passed through the gauge changes in resistance as the attached sample increases in strain, with the software converting this change in current to a strain value.

The hardware required to supply and collect the electrical current from the strain gauge was National Instruments branded. There were four hardware components required, two different modules (NI 9219 x 2 and NI 9205 x 1), and 1 chassis (NI eDAQ-9172). The NI 9219 modules were required to attach the strain gauge wires, and the NI 9205 was required to attach a custom cable for data communication between the Instron UTM and the National Instruments data collection apparatus, as well as an additional J-type thermocouple for temperature measurement data, in case a correction factor was required for temperature variation.

The National Instruments hardware was paired with Labview, a proprietary software. The version of Labview used for this research was version 14.0 (32-bit) 2014. Labview was utilised for combing the data from the strain gauges, Instron UTM, thermocouple and, in the case of the tensile tests, the video extensometer. Using this software was essential, as it allowed data from multiple sources to be recorded concurrently and ensured all load, displacement and strain values were captured simultaneously for each test.

The second form of strain measurement, a video extensometer, was only utilised for the tensile testing component of the research. A video extensometer is a high-resolution

video camera that is able to locate and track specific markings drawn or inscribed on a material whilst the material is in motion. This quality makes it an excellent tool for measuring strain, as the camera is able to track markings using (x, y) coordinates that are then converted to a distance measurement. The camera is able to track these markings at a micron level, and therefore provides a highly accurate optical measurement device for measuring average strain.

The primary benefit of using a video extensometer is that it is a non-contact way of measuring strain in a material. Once set up and calibrated, this test is able to be completed countless times on various samples as there is no requirement to attach strain gauges or another form of strain measurement that requires contact with the sample.

The video extensometer (shown in Figure 4-15) utilised for the tensile tests was purchased from a national engineering equipment company and was supplied with propriety software developed by the distributer. The high-speed camera itself has a minimum resolution of 1280 x 1024 pixels and is able to produce measurements at a readout rate of at least 50Hz.

Figure 4-15 Image of Video Non-Contact Extensometer (VNCX) used in this research for measuring strain in tensile tests

Chapter 5: Results and Discussion – Material Testing

5.1 INTRODUCTION

This chapter begins by showing the results obtained from testing the soil materials utilised throughout this study with a focus on the physical properties. Each of these physical attributes are discussed as the results are presented. Section 5.3 until the conclusion of the chapter focuses on the tensile properties of the geogrid and geocomposite utilised for this study. The results are discussed as they are presented.

5.2 GEOTECHNICAL PROPERTIES OF SUBGRADE AND SUBBASE MATERIALS

In order to simulate the specific field condition with a CBR value of ≤ 3, it was necessary to investigate the basic physical properties of all soil materials used throughout the testing. The tests conducted for each of the materials were particle size distribution, compaction, Atterberg Limits, CBR, particle density and shrinkage limits. All classification tests were conducted according to the methodology outlined in Section 3.2.

5.2.1 Subgrade soil

The subgrade was a heavy clay type soil with a high percentage of fines, so the particle size distribution for the subgrade was obtained through wet sieving and the use of a Malvern Mastersizer 3000 machine for the fine portion <0.075mm. The results from the particle size distribution are shown in Figure 5-1, with 61% of the soil particles passing the 0.075mm sieve. The data used to form the lower portion of the graph's curve (seen in Figure 5.1) was taken from the Malvern Mastersizer percent passing data, multiplied by 0.61.

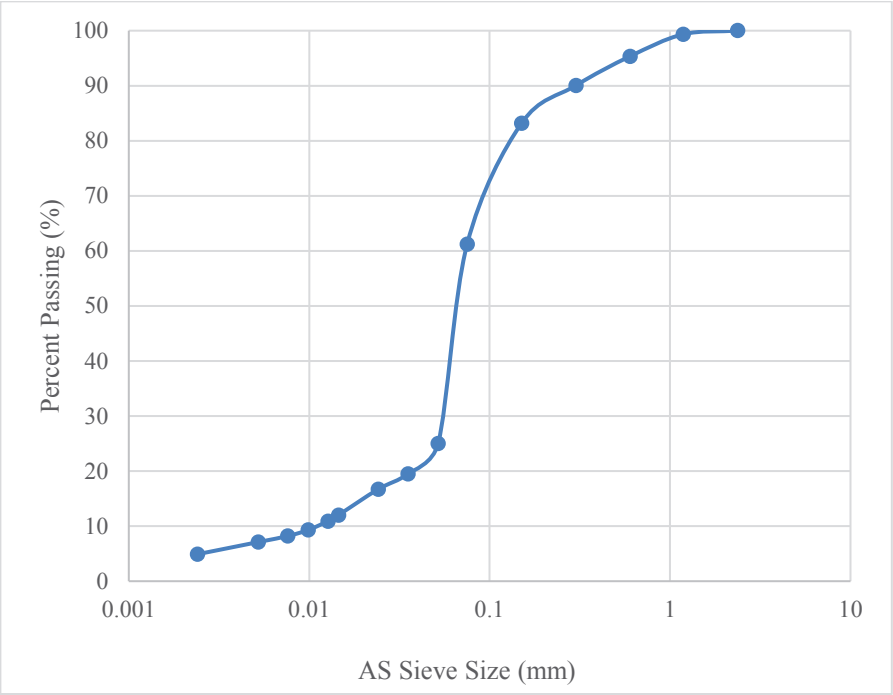

Figure 5-1 Particle size distribution curve for subgrade soil

A series of compaction tests were performed at various moisture contents ranging between 19% and 34%. These tests were performed using the standard compaction technique, in order to ascertain the values for the maximum dry density (MDD) and the optimum moisture content (OMC). The curve seen in Figure 5-2 shows the results from these tests with the peak defining the OMC as 27.65% and the MDD as 1.48t/m³.

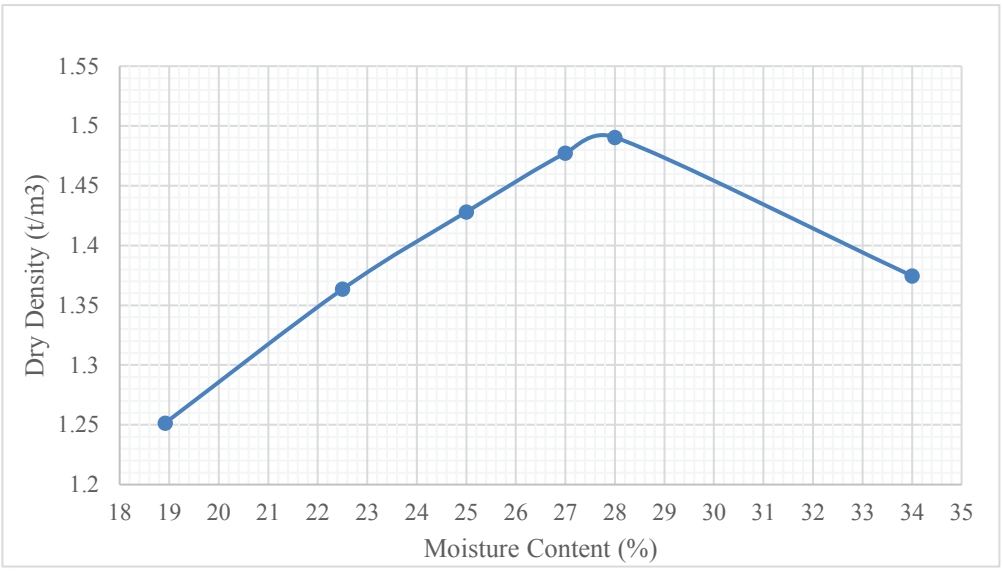

Figure 5-2 Relationship between dry density and moisture content for subgrade soil

Once the values for the OMC and MDD were known, a series of CBR tests were conducted on subgrade soil samples. The CBR values and their associated moisture content are represented graphically in Figure 5-3. The results shown in Figure 5-3 were used to determine that a moisture content of at least 33.8% was required to achieve CBR value of three or less. To ensure this condition was met for all tests, a value of 35% moisture was sought. This is the value ultimately used in this study to determine the effectiveness of geogrid as a subgrade stabiliser, in a series of model tests detailed in later sections.

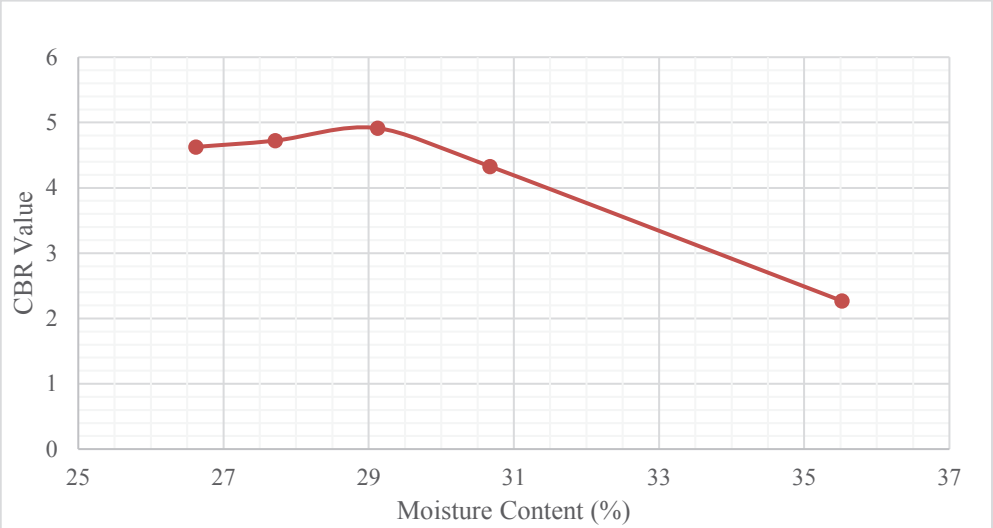

Figure 5-3 Relationship between CBR value and moisture content for subgrade soil

5.2.2 Subbase Material

The subbase was selected and sourced from a local quarry that supplies materials for road construction in southeast Queensland. The purpose of sourcing this material was because it is the same grade of material specified in pavement designs by QTMR. Classification tests mentioned in Section 5.1 were also performed on this material to ensure a high quality representative sample was used in the testing.

Due to the nature of the material, only a dry sieve analysis was required to determine the particle size distribution. Figure 5-4 shows the distribution of the subbase material with approximately 1% passing through the 0.075mm sieve. The results for the further physical classification tests are shown in Table 5-1. The subbase material was classified as ML, in accordance with the USCS.

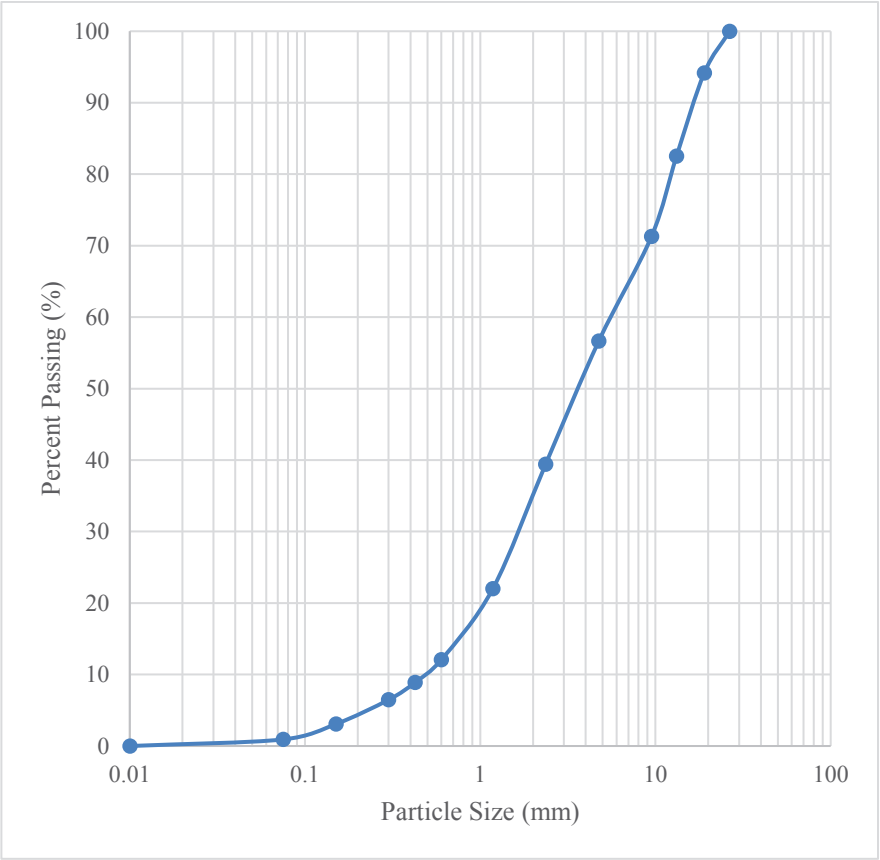

Figure 5-4 Particle size distribution for subbase material

With the physical properties know for the subbase material, a series of compaction tests were performed using the standard compaction technique. These tests were performed for moisture contents ranging between 6-10%. The curve shown in Figure 5-5 shows the results from this test defining the OMC as 8.5% and the MDD as 2.08 t/m³.

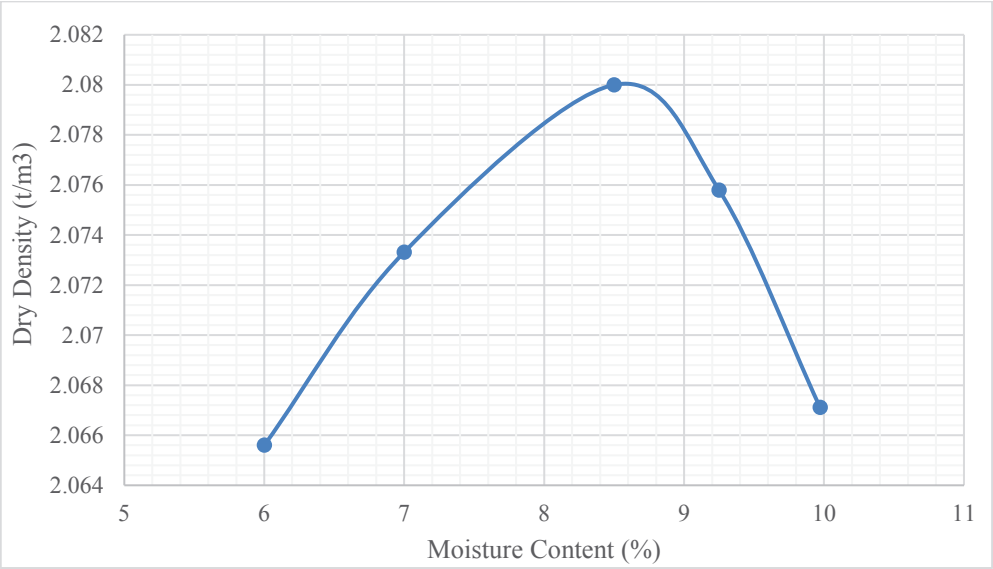

Figure 5-5 Relationship between dry density and moisture content for subbase material

With the OMC and MDD values now known for the subbase material, a series of CBR tests were performed. These tests were performed on samples with moisture contents ranging from 4-9%. The results in Figure 5-6 show that at OMC, the CBR value is 25.

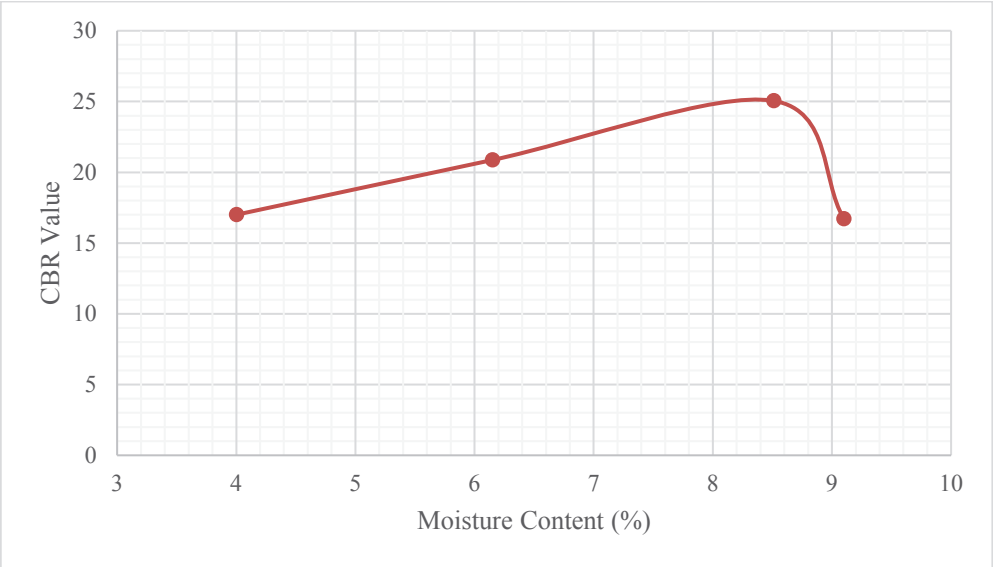

Figure 5-6 Relationship between CBR value and moisture content for subbase material

The results for the further physical classification tests are presented in Table 5-1. According to the Unified Soil Classification System (USCS), the subgrade soil used in this study is classified as CH.

Table 5-1 Physical properties of subgrade and subbase materials

Material Properties	Subgrade	Subbase
Particle Density (Gs) (t/m3)	2.78	2.57
Liquid Limit (LL) (%)	54.6	18.2
Plastic Limit (PL) (%)	17	13.6
Plasticity Index (PI) (%)	37.6	4.6
Linear Shrinkage (Ls) (%)	16	0
USCS Classification	CH	ML

5.3 TENSILE PROPERTIES OF GEOGRID AND GEOCOMPOSITE

To determine the secant modulus and the tensile strength of geogrid and geocomposite, and to investigate the effects of loading direction (machine /cross machine), loading rate (strain rate) on these properties (secant modulus and tensile strength), a series of tests were conducted according to the procedure outlined in Section 4.3.

Some geogrid specimens were instrumented with strain gauges as a physical contact form of measuring local strain when subjected to monotonic tensile load. Where required, two strain gauges were attached to each specimen: one in the MD and one in the CMD. The specifications of these gauges are outlined in Table 4-2. Further, the video extensometer was used for all tests as a non-contact form of measuring/ calculating tensile strain locally in the same specific position on the same rib as the strain gauge. Finally, the deformation measured by the UTM was used to calculate the global strain of each specimen.

Tests were performed at three different strain rates, 10 % per minute, 20 % per minute and 30 % per minute in both the MD and the CMD. Table 5-2 shows the number of tests conducted for each condition.

Table 5-2 Amount of tensile tests analysed for each tensile test series

Type	Geogrid						Geocomposite					
Loading direction	MD			CMD			MD			CMD		
Strain rate (%/min)	10	20	30	10	20	30	10	20	30	10	20	20
No. of tests with both strain gauges and video extensometer	3	3	3	3	3	3	3	3	3	3	3	3
No. of tests only with video extensometer	5	5	5	5	5	5	5	5	5	5	5	5

Note: For all tests, machine measured displacement can be used to calculate the global tensile strain

As can be seen in Table 5-2 the video extensometer was used for all tests but the strain gauges were not. This is due to the cost and reliability of the gauges for this type of testing. The reliability of the gauge was compromised due to the surface finish of the geogrid. The geogrid and the geocomposite both have a raised crosshatched finish, and whilst this increases the surface area to improve its effectiveness in a soil, it reduces the attachment surface area for the strain gauge: for good attachment, the area needs to be flat and smooth. A different method of surface preparation was attempted using sandpaper to smooth the raised crosshatching and increase the attachment area. This yielded improved results from the strain gauge; however, the strain gauges were still not consistently reliable. This method of surface preparation also introduced a risk of reducing the strength of the geogrid and geocomposite, as by sanding the ribs, the cross-sectional area of the sample was reduced.

Despite the constraints with the strain gauges, some successful tests showed a good agreement between the strain gauge results and the video extensometer results; however, the Instron global strain results showed significant variation, as shown in Figure 5-5.

The global strain results were calculated using the raw data from the Instron UTM. The typical strain results from the UTM, despite being consistent across all sample types and test rates, were significantly lower than the video extensometer and strain gauges at a specified strain, as seen in Figure 5-5. This result was expected, and there are several reasons for this.

1. The UTM is subject to error as there are a series of moving parts that all have a small degree of compliance in them. An example of this is the

knuckle joint that attaches the upper grip to the load cell, as this joint is able to freely rotate. These errors, whilst seemingly minor when considered in isolation, can collectively impact the results.

2. The UTM measures the sample indirectly, and whilst the load and displacement data output from the UTM has a Class A accuracy, the displacement data is a measure of the machine's crosshead movement, not an exact measurement of the sample.
3. The UTM measures the strain over a gauge length of 100mm, however the video extensometer measures the strain over a gauge length of 60mm. As both the geogrid and the geocomposite are polymers, it is common that the strain induced in a polymer is not always linear across the sample, which may account for differences in the result.

Due to the above mentioned sources of error for both the strain gauges and the UTM, and as the video extensometer proved to provide reliable results, the attachment of the strain gauges was discontinued and the video extensometer became the primary method for determining strain in the subsequent tests.

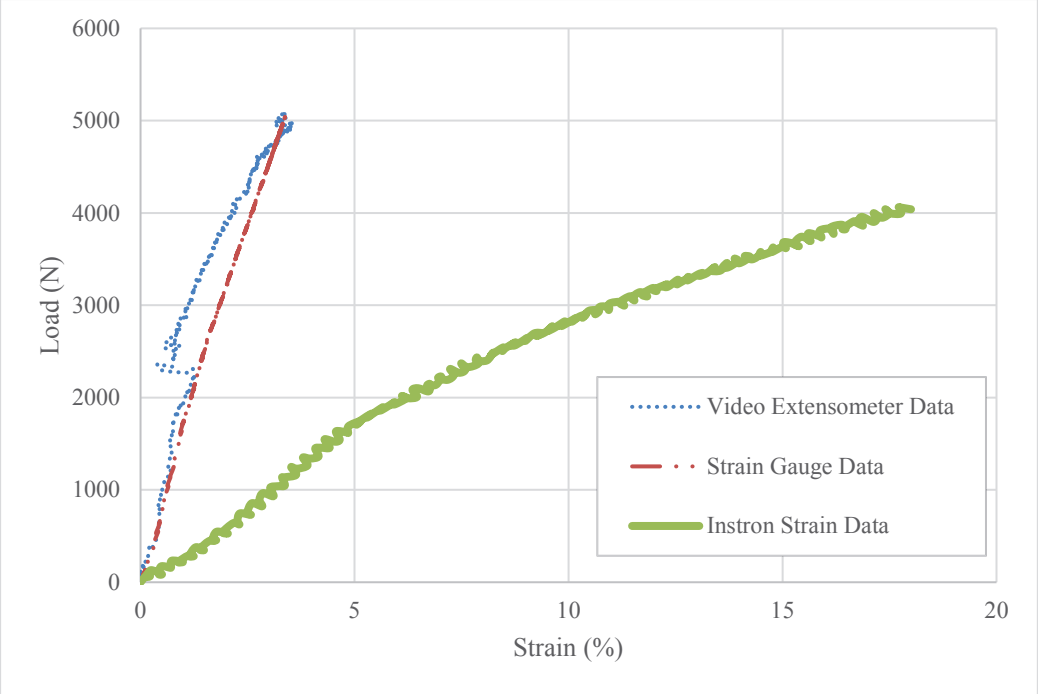

Figure 5-5 Relationship between Load and strain tensile tests results obtained from the strain gauge, video extensometer and UTM at 20% per minute strain arte

To investigate the factors affecting the tensile properties of geogrid and geocomposite, a series of tensile tests were conducted, as summarised in Table 5-2. The tests conducted with the video extensometer were used to obtain a representative (average) load and tensile strain curve for specific test conditions (e.g.: geogrid, MD, applied loading rate of 10% per minute).

Further consideration is given to the rate at which force is applied to the geogrid or geocomposite, as both samples are polymer based, and react differently depending on this rate. In order to have a good basis for comparison, three different strain rates were selected: 10 % per minute, 20 % per minute and 30 % per minute. The 10 % per minute rate is the defined rate from the ASTM D6637/D6637M—15, the 20 % per minute rate is the defined rate from the BS EN ISO 10319-2015 test standard, and to the best of the authors knowledge, there is currently no published test standard for the 30 % per minute strain rate. For each variation, initialised load-strain curves showing up to 5% strain have been created and are shown in Figures 5-6, 5-7, 5-8, 5-9.

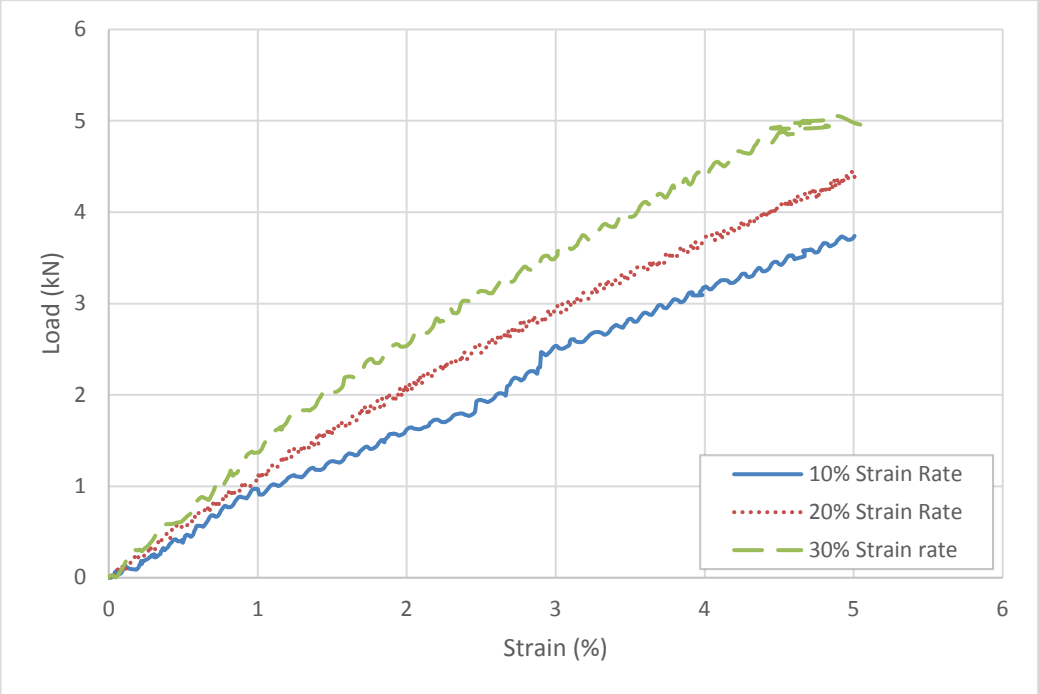

Figure 5-6 Relationship between load and strain for geogrid tensile tests, MD with all three strain rates (10%, 20%, 30%)

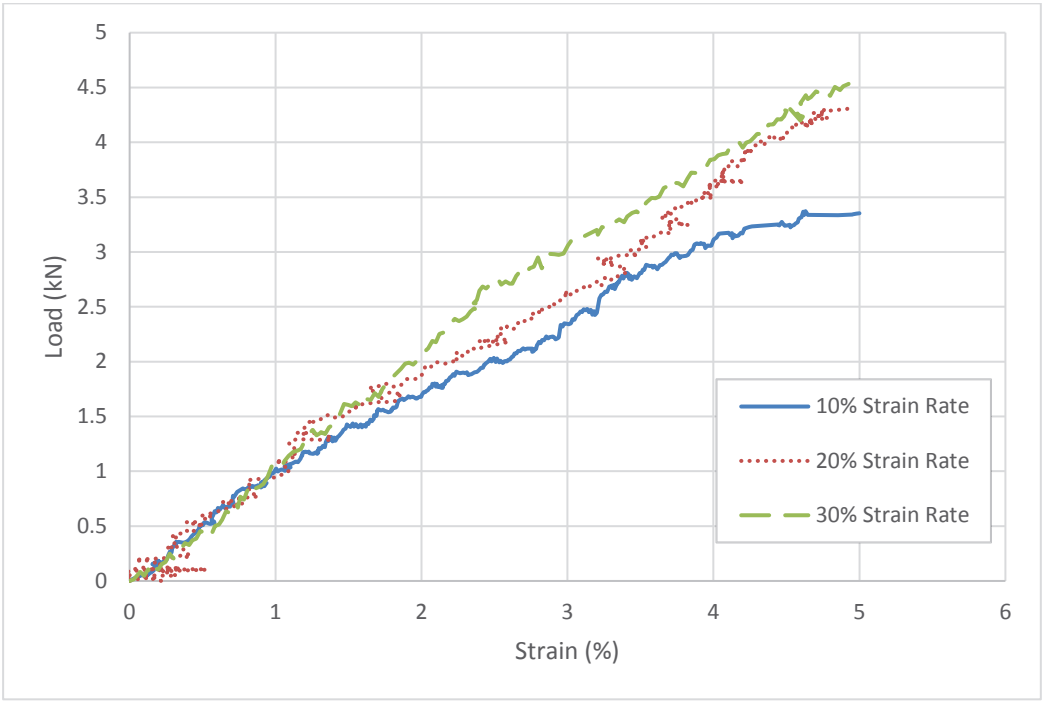

Figure 5-7 Relationship between load and strain for geogrid tensile tests, CMD with all three strain rates (10%, 20%, 30%)

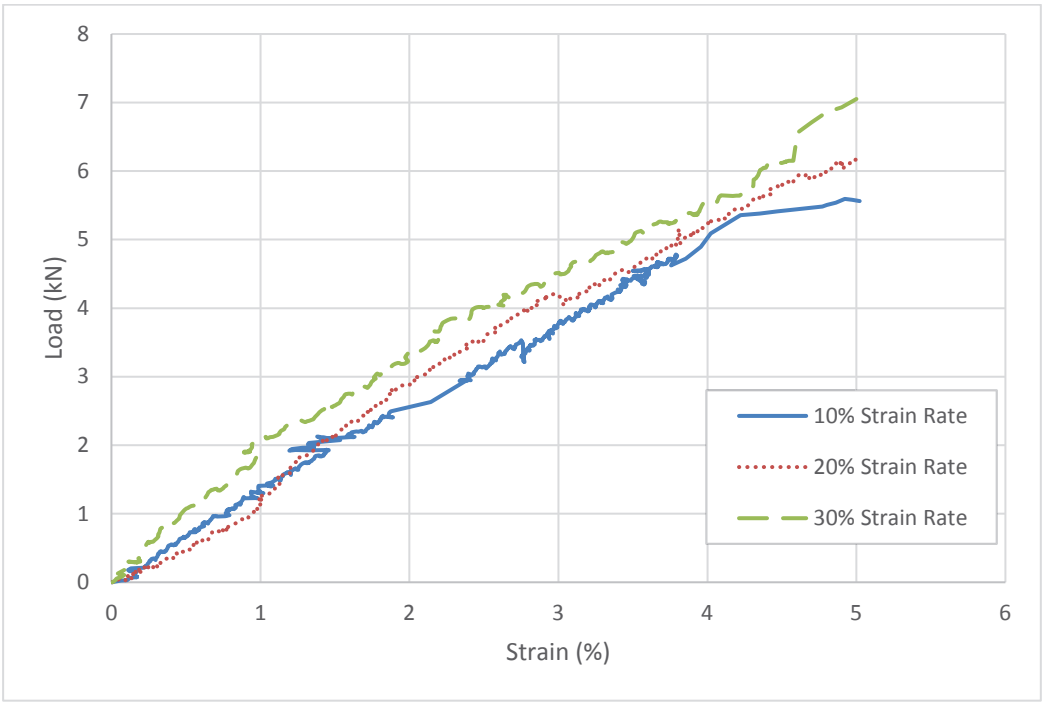

Figure 5-8 Relationship between load and strain for geocomposite tensile tests, MD with all three strain rates (10%, 20%, 30%)

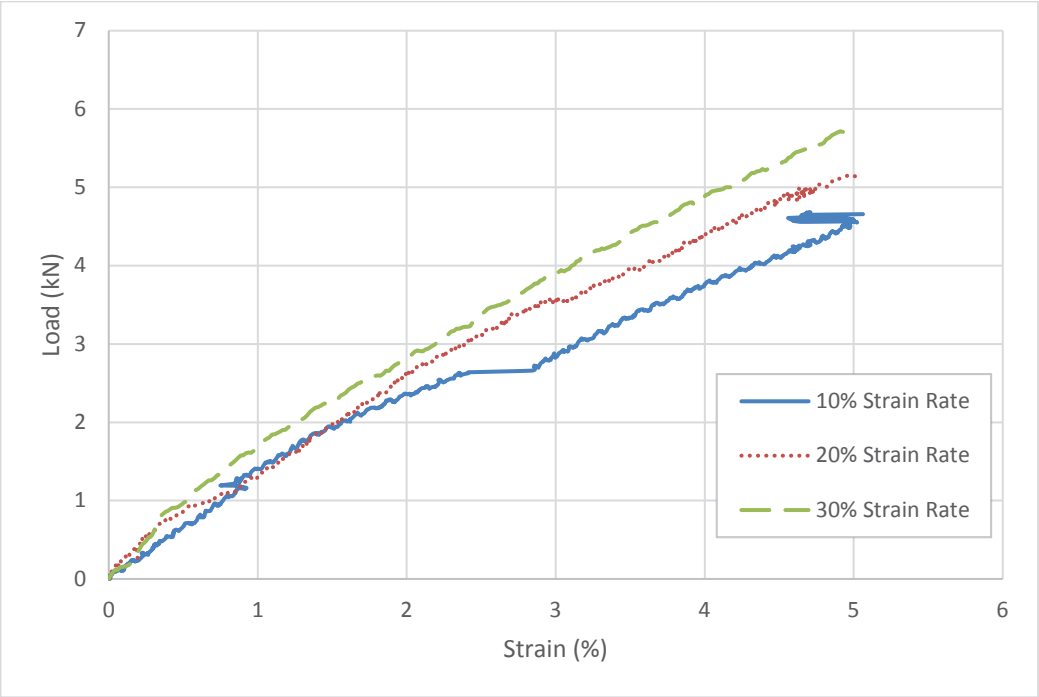

Figure 5-9 Relationship between load and strain for geocomposite tensile tests, CMD with all three strain rates (10%, 20%, 30%)

5.4 FACTORS AFFECTING THE SECANT MODULUS

When selecting a geogrid or geocomposite to suit a design criteria, one of the most important aspects of the material is how it will perform under load. The secant modulus, or secant stiffness, is how the performance of a geogrid or geocomposite is defined. This calculation from BS EN ISO 10319:2015, explains the amount of force a sample can sustain at any given strain value (see Equation 5.1).

$$J = \frac{F \times c \times 100}{\varepsilon}$$ **Equation 5.1**

Where:

J: is the secant stiffness in (kN/m)

F: is the determined force at strain, ε, in kilonewtons (kN)

ε: is the specified strain, in percent

c: is the number of tensile elements within a 1m width of the sample being tested divided by the number of tensile elements on the test specimen

5.4.1 Effects of strain rate and strain

In this study, the secant modulus was calculated at 1% strain, 2% strain and 5% strain. Generally, manufacturers publish secant modulus values at strain of 1% and 2% for geogrids and geocomposites, which is why these were selected. 5% strain was also selected by the researcher as an additional comparative value due to all samples achieving at least this strain value. Using Equation 5.1, the secant modulus was calculated and graphed for all three strain rates, at the defined strain values, for both the geogrid and geocomposite in the MD and CMD.

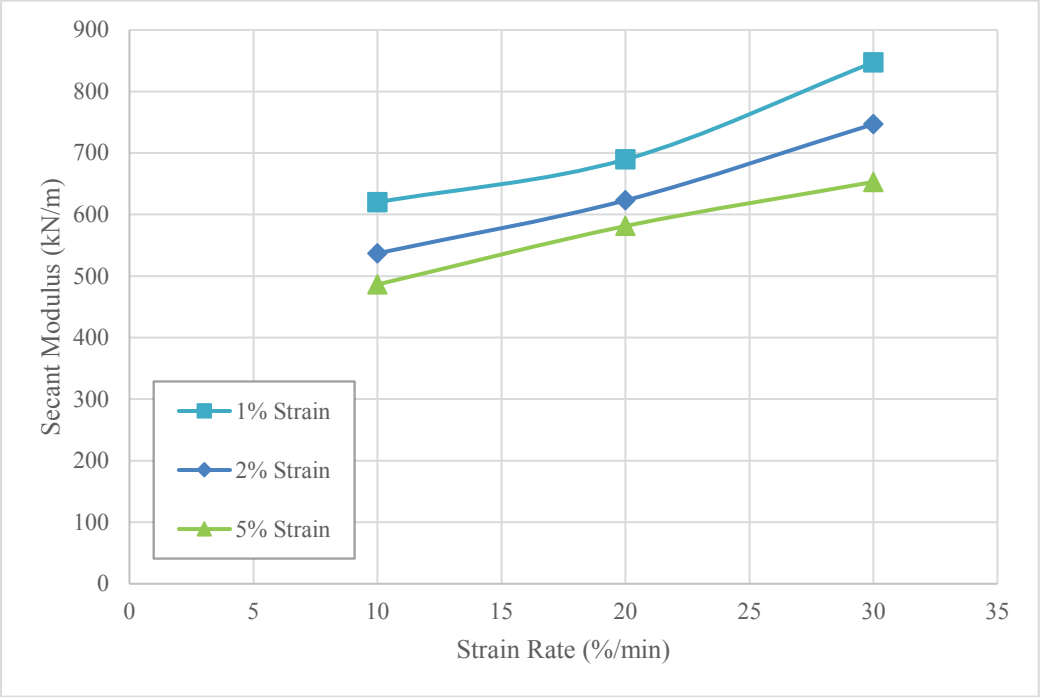

Figure 5-10 Relationship between secant modulus and strain rate for geogrid MD tensile tests

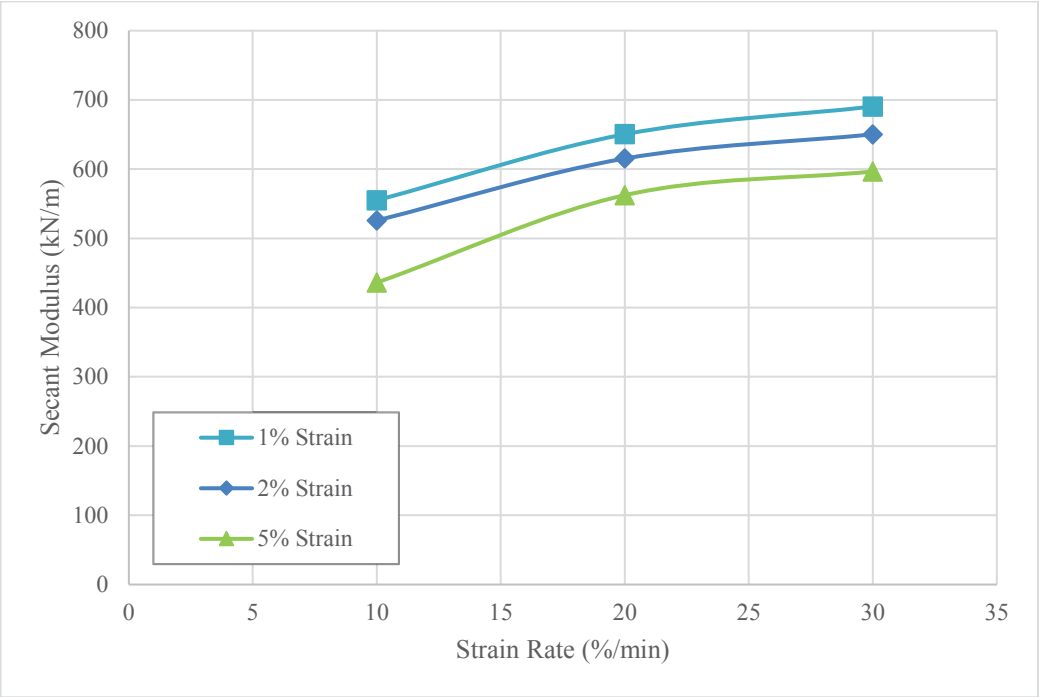

Figure 5-11 Relationship between secant modulus and strain rate for geogrid CMD tensile tests

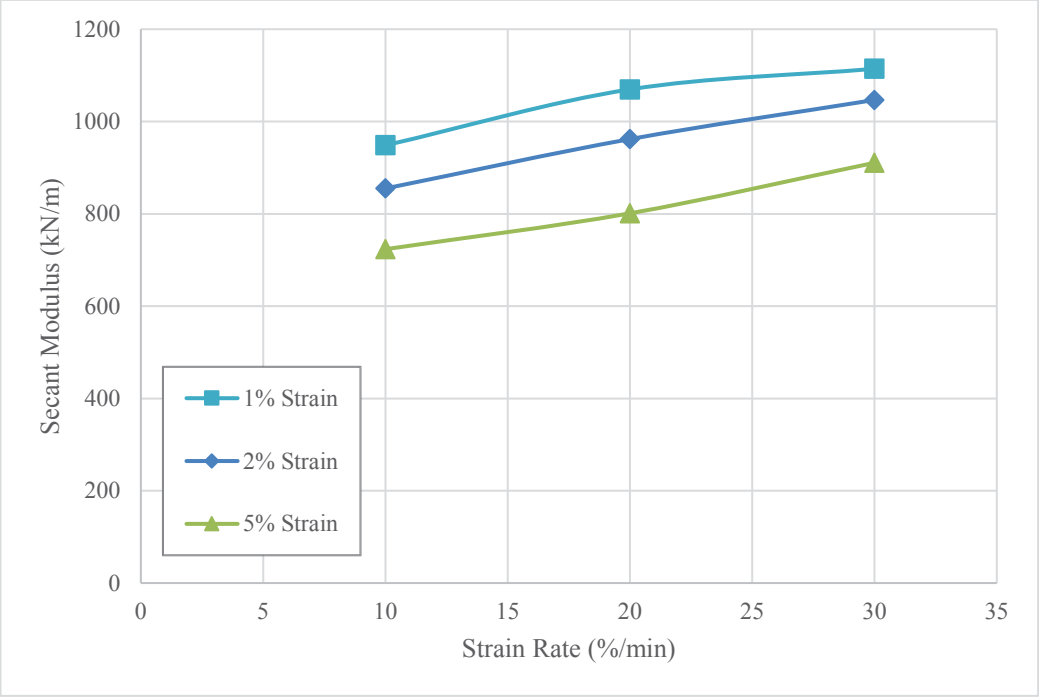

Figure 5-12 Relationship between secant modulus and strain rate for geocomposite MD tensile tests

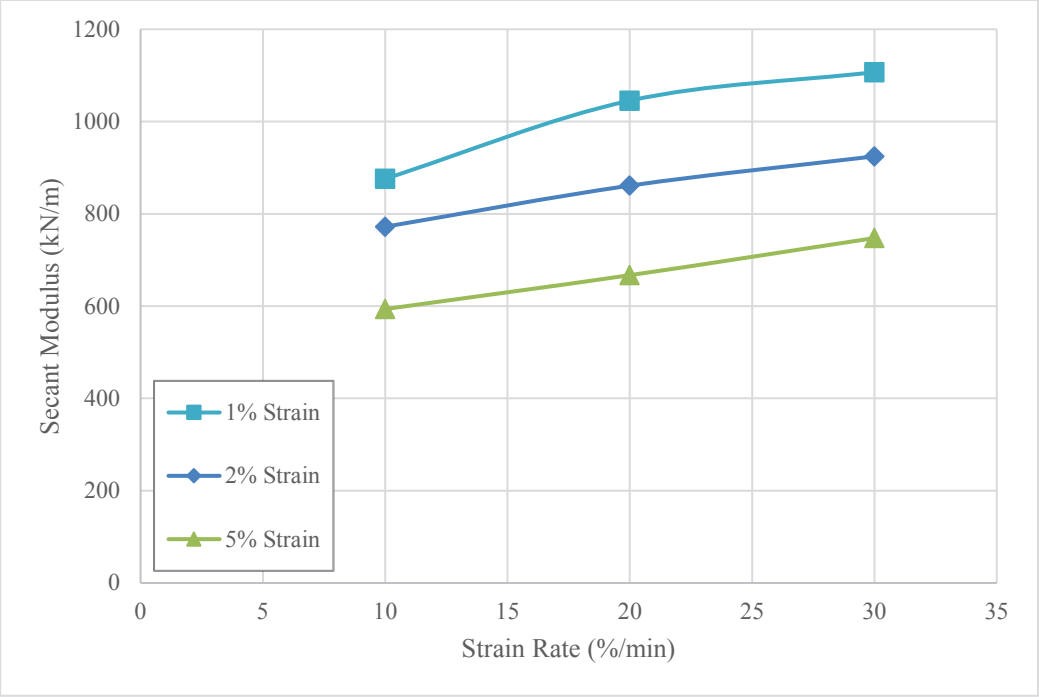

Figure 5-13 Relationship between secant modulus and strain rate for geocomposite CMD tensile tests

As shown in Figures 5-10, 5-11, 5-12 and 5-13, irrespective of geosynthetic type (geogrid or geocomposite), loading direction (MD, CMD) and the strain rate at which the secant modulus is calculated, the secant modulus increases with the increase of strain rate. This is due to the chemical properties of the PP polymer, as when subjected to a tensile load, the stiffness increases (Richeton et al., 2007). The results from this research show good agreement with Richeton et al., (2007) findings, as they further mention observing the same increase in stiffness when the geosynthetic was subjected to an increased strain rate. Due to this increase in stiffness, the modulus of the geogrid increases, and is able to withstand a higher load at a lower strain when subjected to a higher strain rate.

Evidence of this shown in Figure 5-10 where the 5% strain value achieved by the geogrid during the 30 % per minute test is similar to the 2% strain value achieved during the 20 % per minute test, and the 1% strain value achieved during the 10 % per minute test. Furthermore, despite the geocomposite being manufactured as a stiffer/ stronger material than the geogrid, a similar trend can be observed in Figure 5-9, where the 5% strain value for the 30 % per minute tests is comparable to the 1% strain value for the 20 % per minute test.

Further observations show that as the secant modulus decreases, the strain at which it is calculated increases. This is due to the non-linear variation of the load-strain curves shown in Figures 5-6, 5-7, 5-8, and 5-9. These figures show that higher load values were recorded for the faster strain rates at the same strain values. This is again attributed to the reaction of the polymer to the increased load rate providing higher strength properties at equivalent strain values. This observation is important to note as the load value is divided by the corresponding strain values in Equation 5.1, directly affecting the magnitude of the secant modulus, and thus showing the influence that a faster strain rate has on a polymer based geosynthetic.

5.4.2 Effects of loading direction

Both the geogrid and the geocomposite are welded junction products manufactured in 4.75m wide x 100m long rolls. Due to the sheer number of junctions and the manufacturing method, there is likely to be some variation throughout the sample. This is most likely to occur between the MD – the direction that the product is manufactured and packaged in – and the CMD, which is perpendicular to the MD.

When each product is specified in a design, it is laid in a particular direction, either MD or CMD, usually in the direction of expected load to maximise the benefit. Therefore, it is important to know if there is any variation in the secant modulus between the MD and CMD, so that this can be accounted for in the design specifications.

To investigate the effects of loading direction on the secant modulus, the secant modulus calculated at 2% strain was plotted against the strain rate (10% per minute, 20% per minute, and 30% per minute) for both loading directions (MD and CMD) for both geogrid and geocomposite. These results are shown in Figure 5-14, and 5-15.

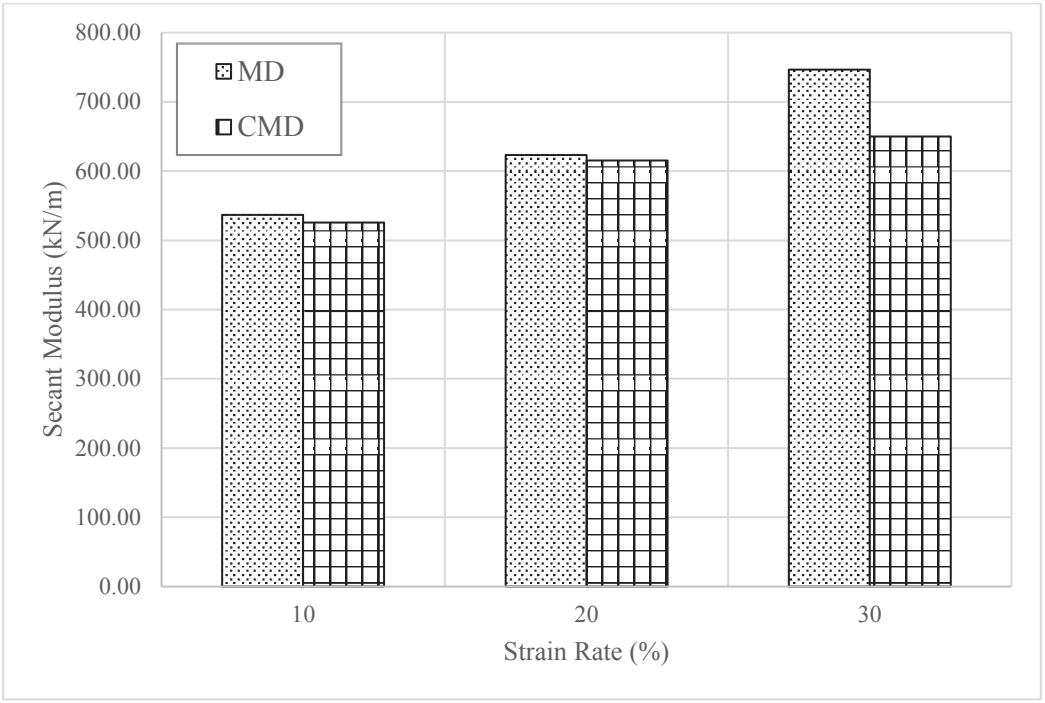

Figure 5-14 Relationship between secant modulus and strain rate at 2% strain for geogrid MD and CMD tensile tests

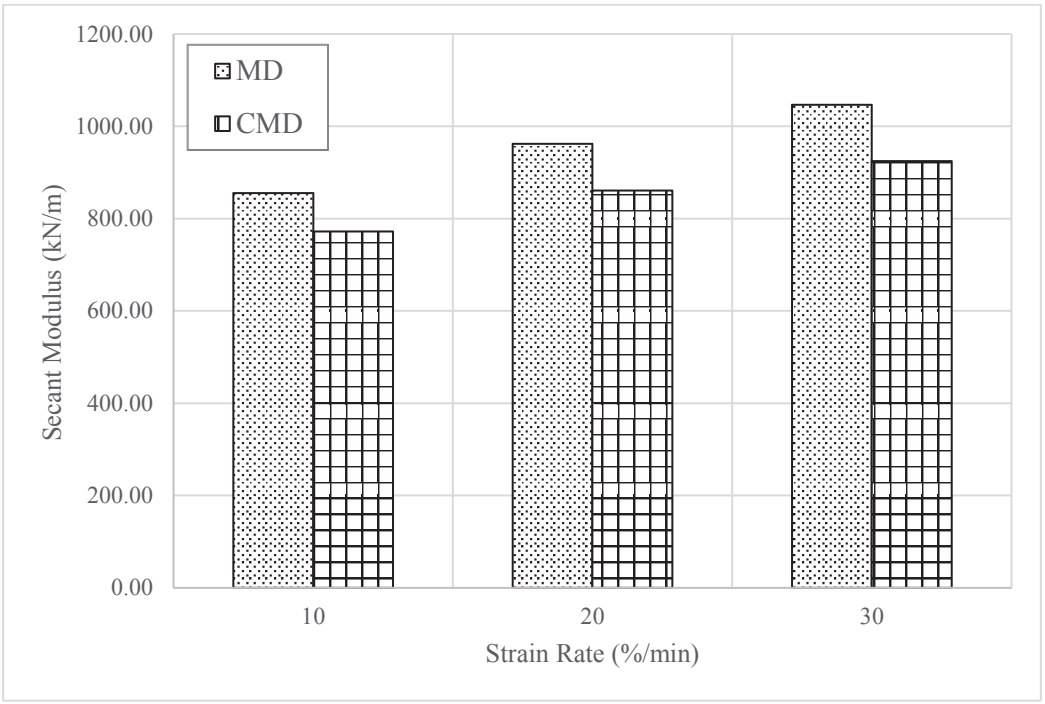

Figure 5-15 Relationship between secant modulus and strain rate at 2% strain for geocomposite MD and CMD tensile tests

As shown in Figures 5-14 and 5-15, irrespective of strain rate and geosynthetic type (geogrid or geocomposite), it can be seen that the secant modulus calculated in the MD is always higher than that recorded in the CMD. The secant modulus for the geocomposite in the CMD is 10-12% less than that of the MD. However, the geogrid is approximately 1-2% less for the strain rate of 10% per minute and 20% per minute and is about 13% less for the strain rate of 30% per minute in the CMD compared with the MD.

These results are interesting to note as the manufacturer claims that both geosynthetics are isotropic, however, this study has shown they as slightly anisotropic as the MD and CMD are not equal. The manufacturer's claimed secant modulus for the MD and CMD, at 2% strain when tested at a strain rate of 20% per minute, are equal for both the geogrid and geocomposite, although lower than the calculated values in the research. These values are shown in Table 5-3, along with the variation between the claimed and calculated values.

Table 5-3 Comparison of claimed and measured MD and CMD values for both geogrid and geocomposite tested at 20% per minute strain rate

Sample data	Geogrid		Geocomposite	
Loading direction	**MD**	**CMD**	**MD**	**CMD**
Manufacturers claimed secant modulus at 2% strain (kN/m)	600	600	800	800
Calculated secant modulus at 2% strain (kN/m)	623	615	961	861
Variation between claimed and calculated at 2% strain (kN/m)	23	15	161	61

Despite the differing values shown in Table 5-3, all calculated values exceed the manufacturer's claimed values irrespective of testing direction or geosynthetic type. The reason for this variation is unclear, and to the best of the researchers' knowledge, this has not yet been investigated in the current body of literature.

5.5 FACTORS AFFECTING THE TENSILE STRENGTH

When choosing between different geogrid or geocomposite products it is important to know what the tensile strength of the product is, and what factors may cause an increase or decrease in this strength. This research investigated the effects of strain, strain rate and loading direction as potential factors.

5.5.1 Effects of strain and strain rate

As most geogrid or geocomposite products are made up of primarily polymers, one factor is the rate at which load is applied to the sample. The reason this is a concern is that as load is applied to a polymer and it is stretched, an exothermic reaction occurs and the polymer increases in stiffness. The faster the polymer stretches the quicker this process occurs. This is particularly important when deciding between different products for specific applications when the known load is at a fast or slow rate.

Therefore, if the strain rate of the test is increased, the geogrid or geocomposite sample shows an increased load at a lower strain value. However, a side effect of this reaction is the geogrid or geocomposite will fail at a higher load value for a specified strain, but have an overall lower peak load value. These peak load values, shown in Figures 5-18 and 5-19, and show the decrease in peak load as the strain rate increases.

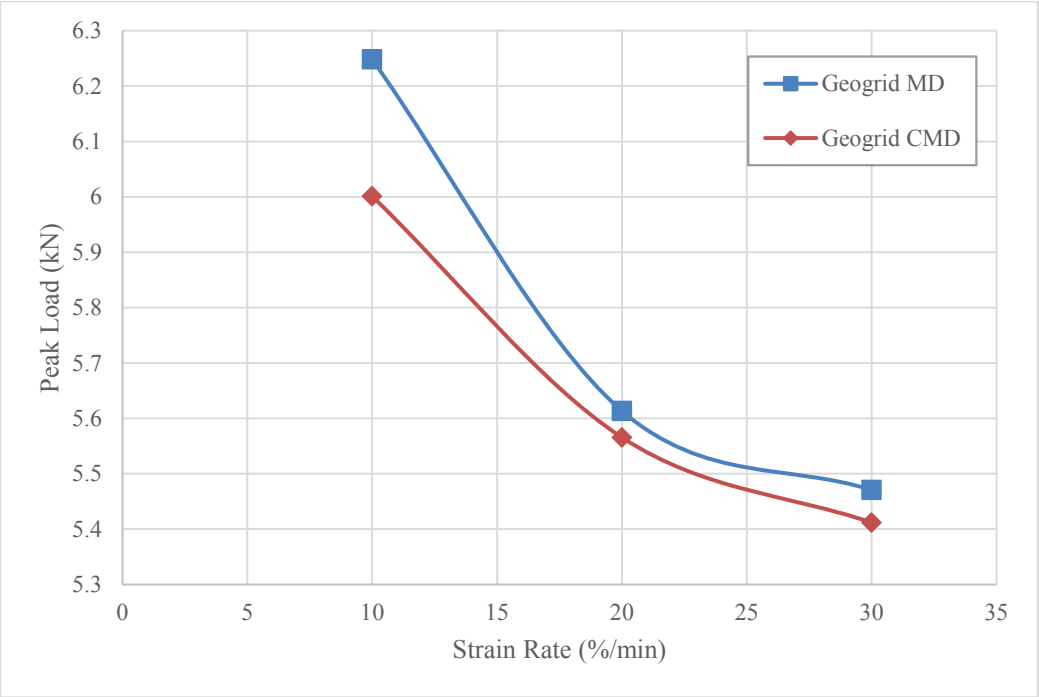

Figure 5-18 Relationship between peak load and strain rate for geogrid MD and CMD tensile tests

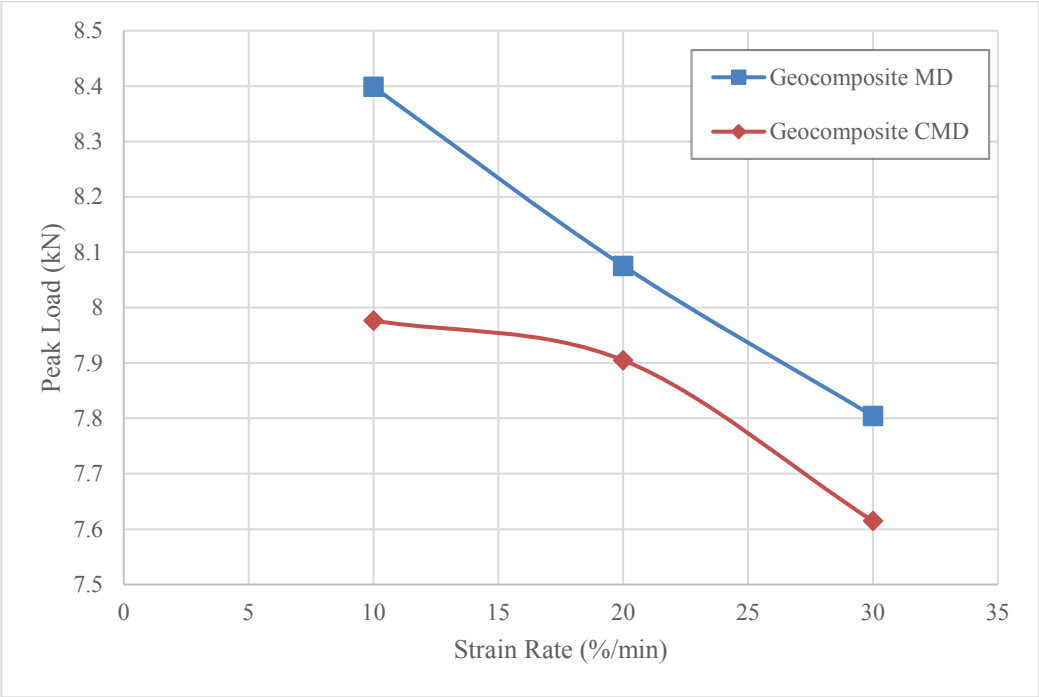

Figure 5-19 Relationship between peak load and strain rate for geocomposite MD and CMD tensile tests

Figures 5-18 and 5-19 clearly show the effect of the change in polymer properties with respect to increasing strain rate. These figures show that regardless of geosynthetic type, strain rate or testing direction, the peak load decreased as the strain rate increased from 10 % per minute up to 30 % per minute. For both the geogrid and geocomposite, the peak loads decreased 9-10% for both testing directions due to this increase in strain rate.

To calculate the tensile strength of the geogrid and geocomposite, load and displacement data was taken directly from the UTM and calculated using Equation 5.2 (BS EN ISO 10319:2015).

$$Tmax = Fmax \times c$$ **Equation 5.2**

Where:

Tmax: is the tensile strength expressed in (kN/m)

Fmax: is the recorded maximum tensile force in (kN)

c: is the average number of tensile elements in a 1m width of the specimen divided by the number of tensile elements in the sample tested

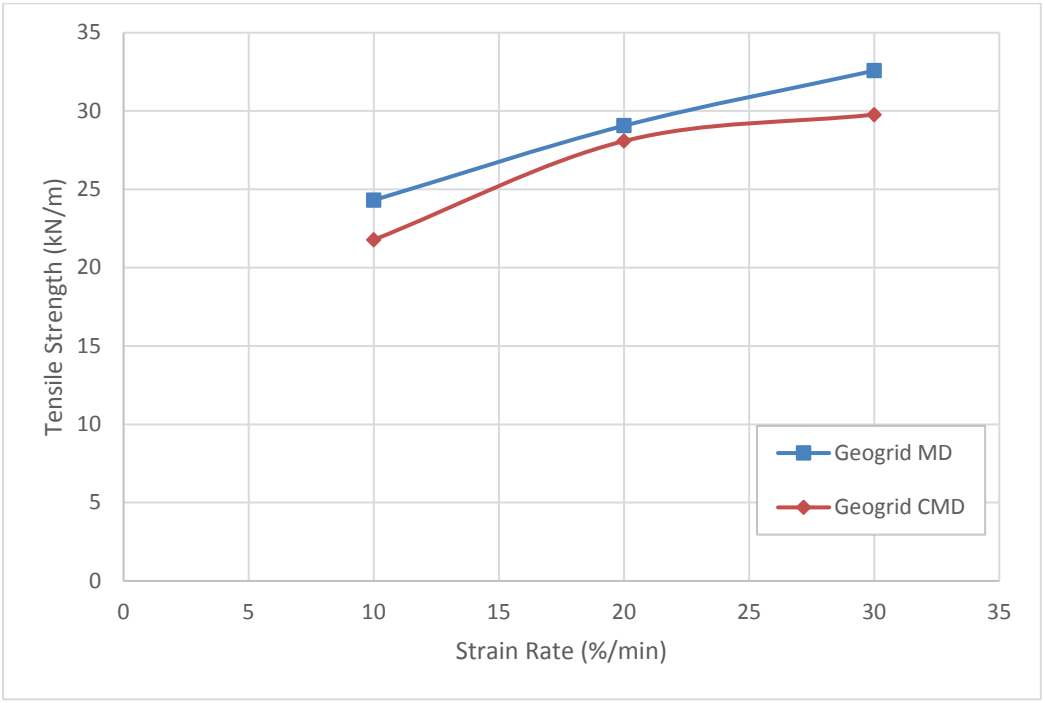

Figure 5-20 Relationship between tensile strength and strain rate for geogrid MD and CMD tensile tests at 5% strain

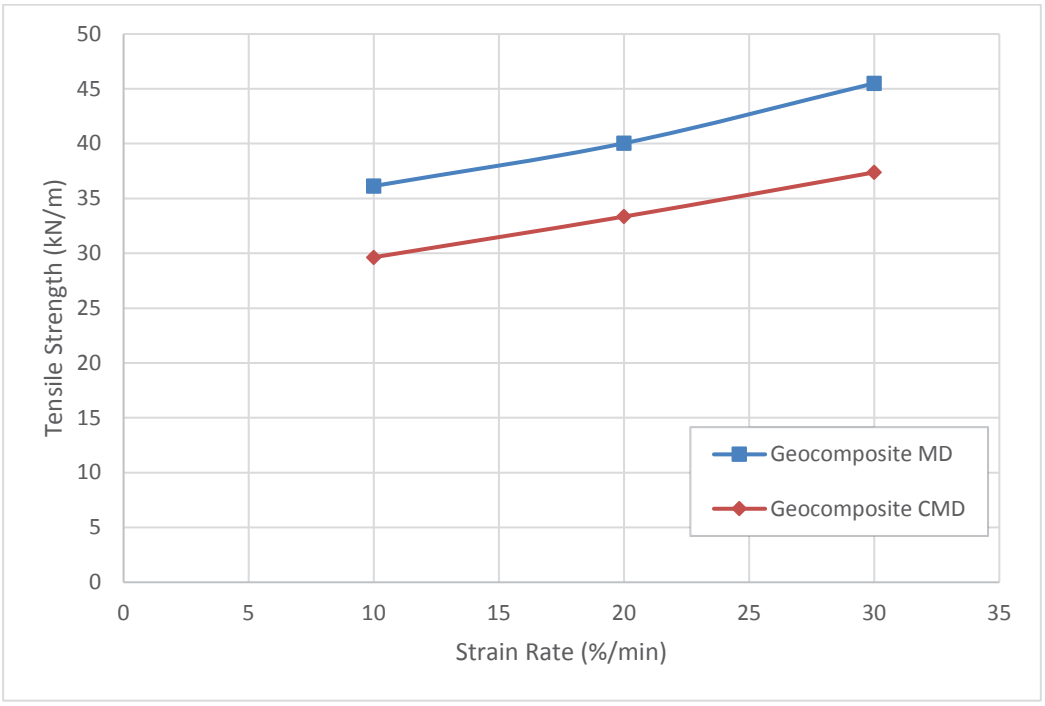

Figure 5-21 Relationship between tensile strength and strain rate for geocomposite MD and CMD tensile tests at 5% strain

Figures 5-20 and 5-21 show that irrespective of geosynthetic (geogrid or geocomposite) or testing direction (MD or CMD) or strain rate (10% per minute, 20% per minute, 30% per minute) at 5% strain there was an increase in tensile strength with strain rate. The geogrid showed approximately a 27% increase between the 10% per minute strain rate and the 30% per minute strain rate for both the MD and CMD. For the same condition, the geocomposite showed approximately a 20% increase for both the CMD and MD.

The geocomposite behaved similar to the geogrid, although exhibited less variation in the values between strain rates and testing direction. As the geocomposite was manufactured as a stiffer material with a higher tensile strength, less variation in the results at 5% strain was expected.

5.5.2 Effects of loading direction

It is an important consideration when looking at design criteria to know whether the geogrid or geocomposite product being specified has consistent tensile strength in all directions. This can vary between products due to the manufacturing process. Despite most manufacturers of geogrids and geocomposites generally claiming isotropic behaviour stating that the MD and CMD of their products have the same tensile strength, it is an important criterion to confirm.

Figures 5-21 and 5-22 show the results of both geosynthetics comparing their machine loading direction tensile strengths with the various strain rates.

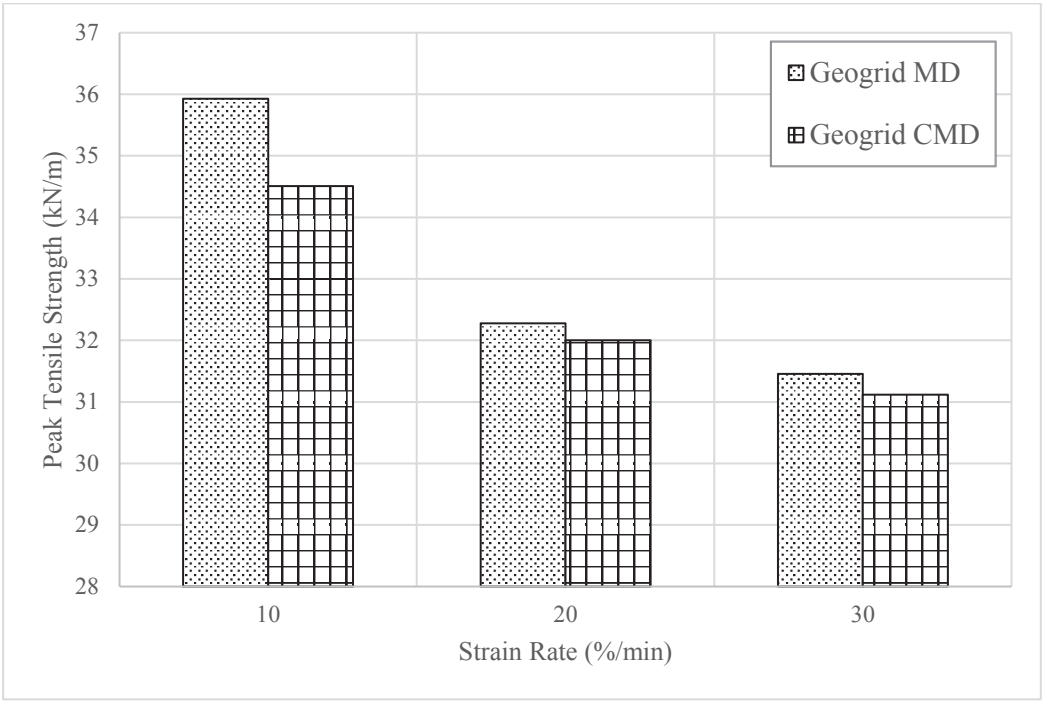

Figure 5-21 Relationship between peak tensile strength and strain rate for geogrid MD and CMD tensile tests

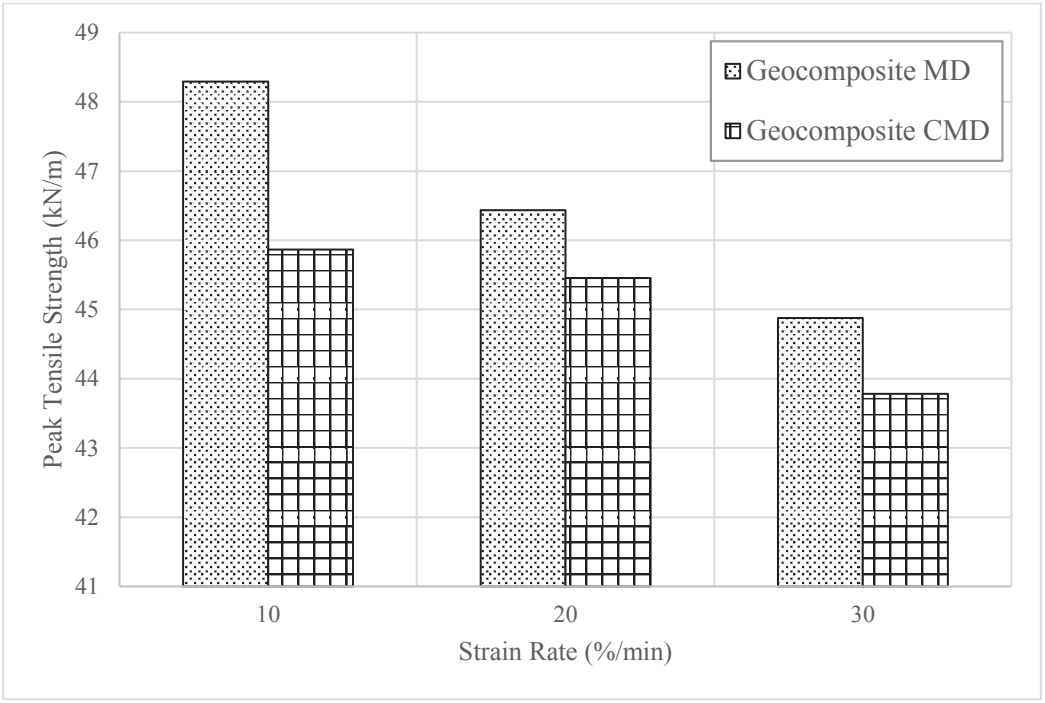

Figure 5-22 Relationship between tensile strength and strain rate for geocomposite MD and CMD tensile tests

Despite the geosynthetics being manufactured with different tensile strengths, they both exhibit the same anisotropic behaviour, with the UTS in the MD always exceeding the CMD regardless of the strain rate. An interesting trend to note is that as the strain rate increases from 10% per minute to 30% per minute, the variation between the UTS of the MD and CMD is reduced. The geogrid has a 4% variation at 10% per minute and a 1% variation at 30% per minute, therefore the reduction in variation as the strain rate increased was 3%. The same behaviour was observed for the geocomposite with the variation reducing also by 3%, between the strain rates of 10% per minute and 30% per minute.

This reduction in variation is likely due to the rate of the test affecting the speed at which the stiffening reaction occurs in the geosynthetic polymer. For example, at 30% strain rate the reaction would occur 3 times faster than the 10% strain rate, assuming isotropic behaviour of the polymer.

Although these results disagree with manufacturer's claims about the isotropic behaviour of the geosynthetics, they do show that both geosynthetics equal or exceed the published maximum tensile strength.

5.6 PERFORMANCE VERIFICATION OF NEWLY DESIGNED CLAMPING MECHANISM

As with all new designs and methods, it is important to verify the results to determine the degree of success. The newly design and manufactured tensile testing grips were modelled from an existing Capstan grip, and as such could be assumed to be effective in yielding accurate results. However, the attachment mechanism to the UTM was a bespoke design and as such, the results from this study are required to be verified.

The best way to verify the results obtained using these grips and attachments is to compare them with published values obtained when following a widely accepted testing standard. The secant modulus and tensile strength results presented in this study will be compared with the manufacturer's published specification for the geogrid and geocomposite. The test standard followed by the manufacturer to obtain their results was BS EN ISO 10319:2015.

Shown in Table 5-4 are the results from this study, the manufacturer's specifications and the variation between them. The tests involving the geogrid samples showed a 2-4% increase, over the manufacturer's specifications, in the secant modulus values obtained and approximately a 10% increase in values obtain for the tensile strength.

With the exception of the geocomposite MD tests, there is approximately a 10% variation between the manufacturer's specifications and the results from this study for all geocomposite tests.

As the geocomposite MD results appear to be a statistical outlier, the variation in the results obtained using these newly design and manufactured grips and attachments are corrected by including a 10% reduction factor in all results obtained.

Table 5-4 Tensile testing results verifying newly designed clamping mechanism

	Geogrid		**Geocomposite**	
Sample direction	MD	CMD	MD	CMD
Manufacturers claimed secant modulus at 2% strain (kN/m)	600	600	800	800
Calculated secant modulus at 2% strain (kN/m)	623	615	961	861
Variation between claimed and calculated secant modulus at 2% strain (%)	3.7	2.4	16.8	7.1
Manufacturer's claimed maximum tensile strength (kN/m)	30	30	40	40
Calculated maximum tensile strength (kN/m)	33	32	46	45
Variation between claimed and calculated maximum tensile strength (%)	10	9.4	13.1	11.1

Chapter 6: Results and Discussion – Model Testing

6.1 INTRODUCTION

The two topics in focus for this chapter are pullout testing and CBR testing, as both of these tests are required to understand how effective each type of reinforcement is in a known condition. These results can then be utilised for developing design guidelines that include geogrid or geocomposite as a solution for subgrade stabilisation. Section 6.2 begins with the pullout testing results for both geogrid and geocomposite. From Section 6.6, the focus will be on geogrid in isolation due to the absence of geocomposite data, a limitation discussed in Section 3.4.

6.2 PULLOUT TESTING

Interface friction properties of geogrid and geocomposite are important in determining their effectiveness for subgrade stabilisation. To determine this, the interface properties of the geogrid and geocomposite samples were placed at the subgrade-subbase interface where the geogrid and geocomposite are in contact with two different materials (fine-grained soil (subgrade soil) and coarse-grained soil (subbase material)).

This pullout test series has been designed first to determine interface friction properties between the geogrid and geocomposite and the subbase material, and the geogrid and geocomposite and the subgrade soil. These interface properties were then used to calculate the pullout resistance of the geogrid and geocomposite placed at the interface of the subgrade-subbase soil layers. Finally, the calculated pullout resistance values were compared with experimental values to validate the testing and calculation procedures.

These pullout tests were conducted according to the procedure outlined in Section 4.4. All tests were performed at a horizontal displacement rate of 1 mm per minute, and had a series of applied normal stresses: 50kPa, 100kPa, 200kPa and 400kPa, to simulate various possible field conditions. The test program is outlined in Table 6-1 and shows all of the variations in test samples completed to determine the effectiveness of the geogrid and geocomposite samples at the defined normal stresses, and the interface properties for the subbase and subgrade interactions. The data collected during each test variation was

used to obtain a representative (average) load and displacement curve for specific test conditions (e.g.: geogrid, MD, subgrade - subgrade, normal stress 50kPa).

Table 6-1 Number of pullout tests and their testing parameters

Type	No reinforcement				Geogrid				Geocomposite			
Normal Stress (kPa)	50	100	200	400	50	100	200	400	50	100	200	400
Number of tests Subgrade / Subgrade	3	3	3	3	3	3	3	3	3	3	3	3
Number of tests Subbase / Subbase	3	3	3	3	3	3	3	3	3	3	3	3
Number of tests Subbase / Subgrade	3	3	3	3	3	3	3	3	3	3	3	3

The geogrid and geocomposite samples were all prepared in the MD as this is the preferred direction that each material is laid in, due to the roll dimensions. The sample was 136mm wide and 304mm long (including grip section) and included four tensile ribs in the direction of travel. Small holes were cut in the fabric of the geocomposite to allow the screws to pass through for the attachment to the grip (Figure 6-1).

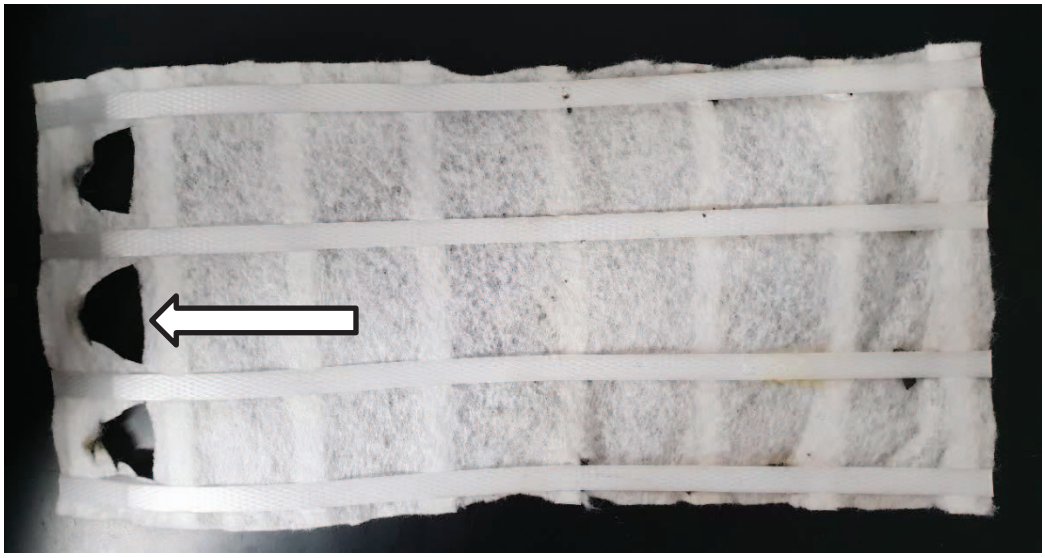

Figure 6-1 Geocomposite sample showing holes for screws to pass through for clamping attachment

The subgrade and subbase used for this study were the same materials outlined in Sections 5.2.1 and 5.2.2 respectively. The subbase material was prepared to suit the OMC condition and the subgrade material was prepared to suit a weak subgrade condition with

a CBR value ≤ 3. These conditions were maintained for all tests outlined in Table 6-1, as these conditions are representative of a common field condition where the use of a geogrid or geocomposite would yield maximum benefit.

Table 6-1 shows that three tests were conducted for each testing variation. The data obtained from these three tests was used to calculate an average for that particular variation. Furthermore, the tests involving no reinforcement were conducted to determine if any residual friction was present in the apparatus under the various normal stresses. It was confirmed that the vertical load equalled the horizontal load and therefore no correction factor for the friction was required to be applied to the results. Figures 6-2 to 6-7 depict the initialised horizontal force verses the horizontal displacement curves obtained for the test conditions summarised in Table 6-1.

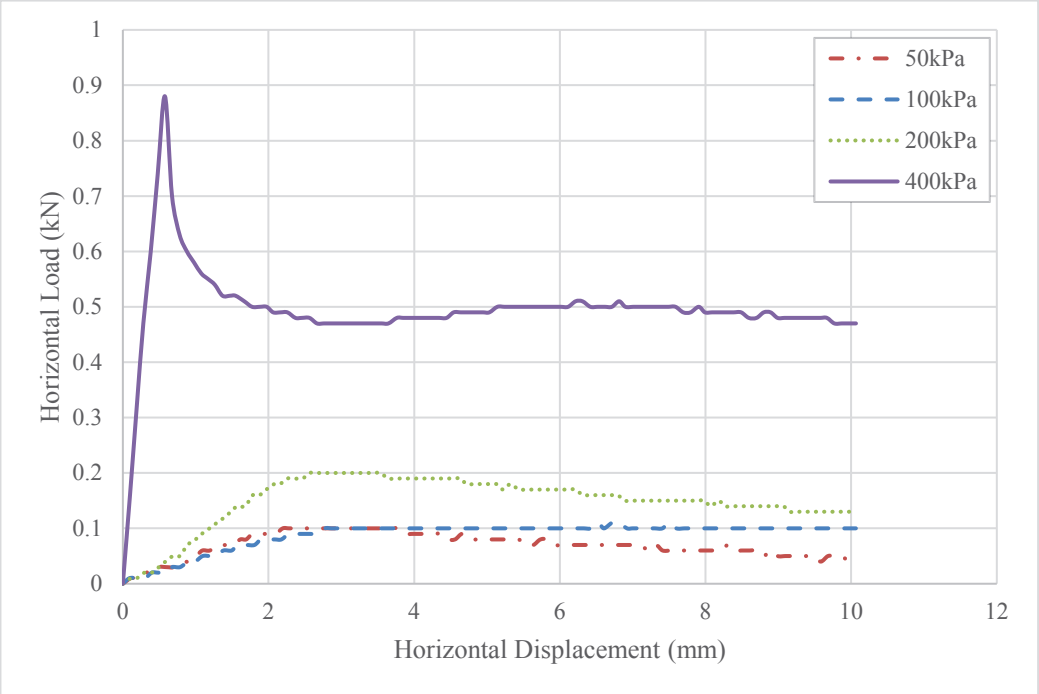

Figure 6-2 Relationship between horizontal force and horizontal displacement for geogrid placed in subgrade materials for pullout tests (subgrade - subgrade)

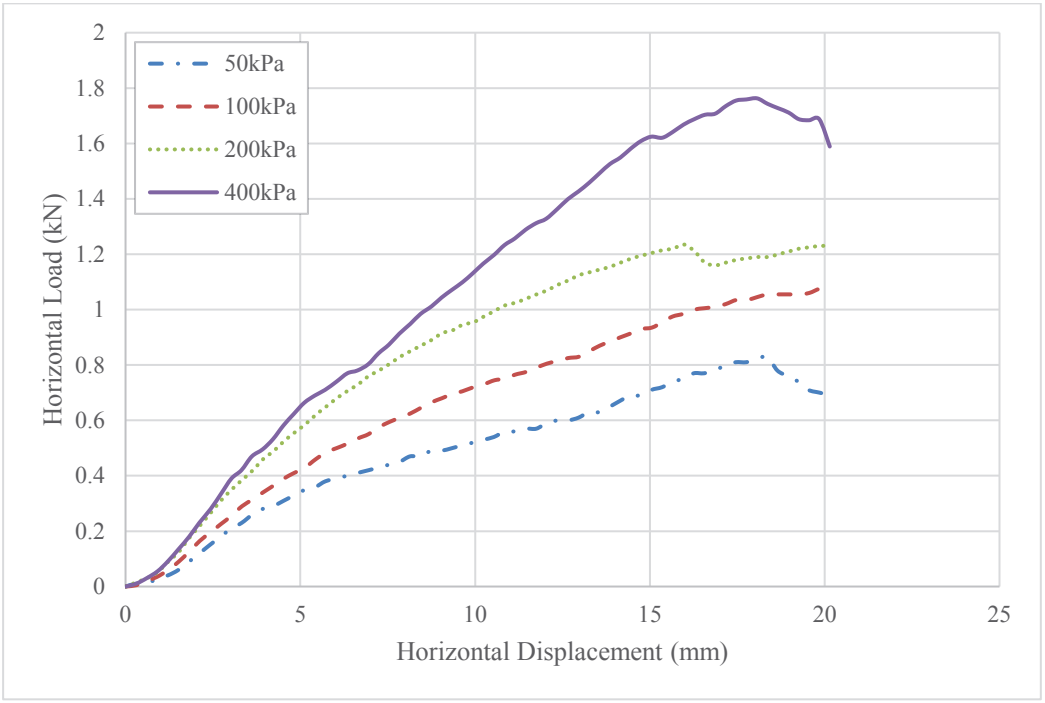

Figure 6-3 Relationship between horizontal force and horizontal displacement for geogrid placed in subgrade materials for pullout tests (subgrade - subbase)

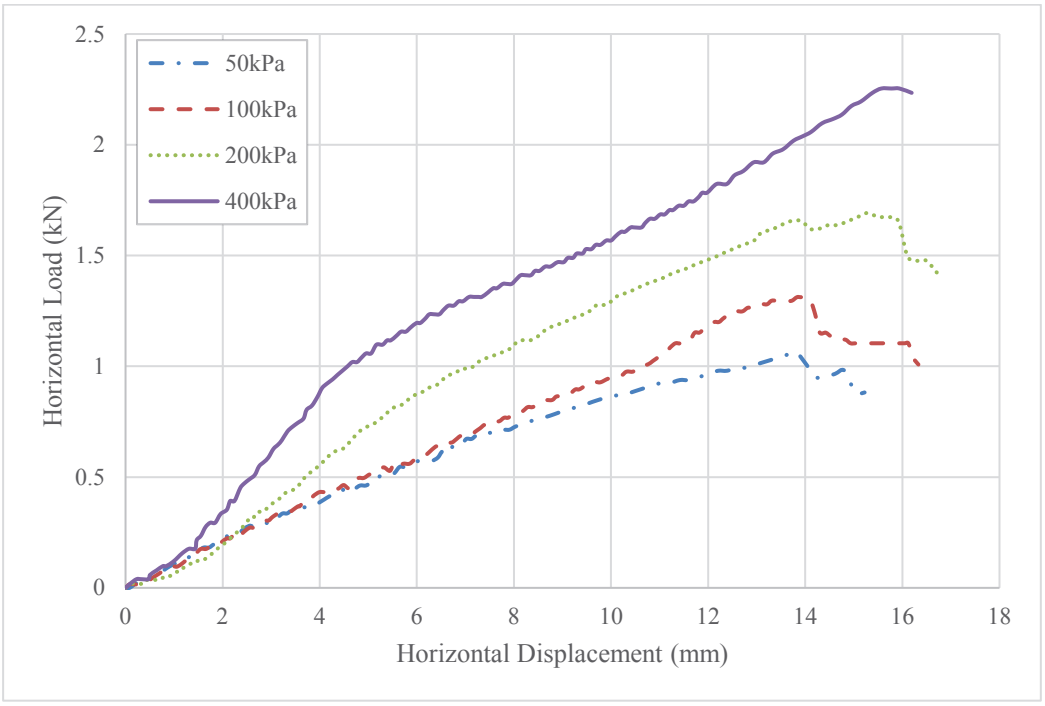

Figure 6-4 Relationship between horizontal force and horizontal displacement for geogrid placed in subgrade materials for pullout tests (subbase - subbase)

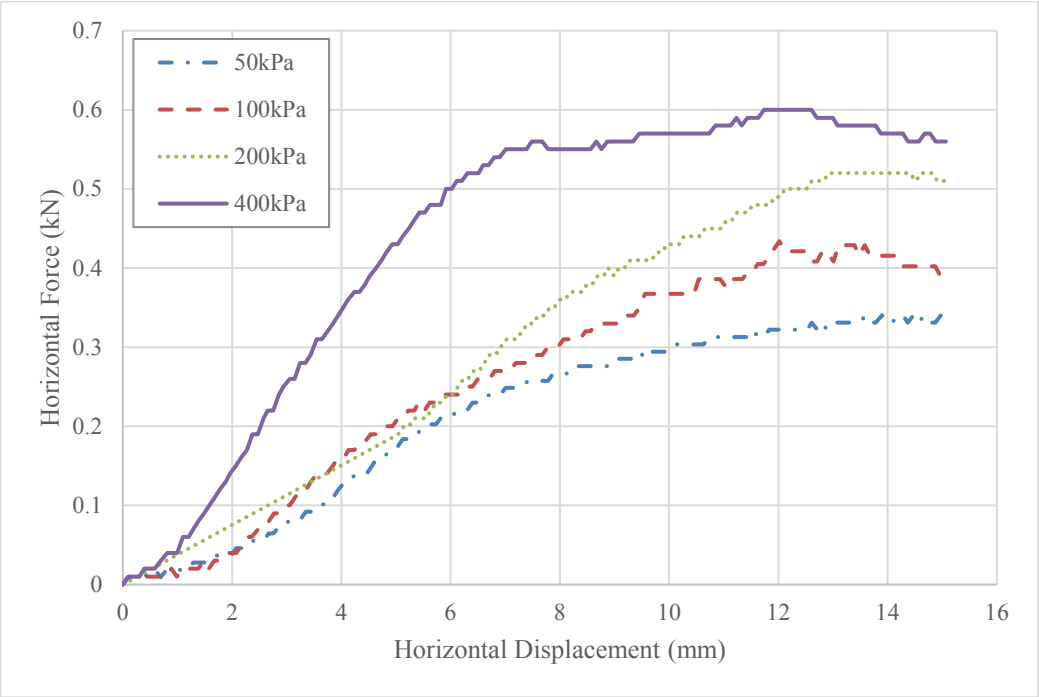

Figure 6-5 Relationship between horizontal force and horizontal displacement for geocomposite placed in subgrade materials for pullout tests (subgrade - subgrade)

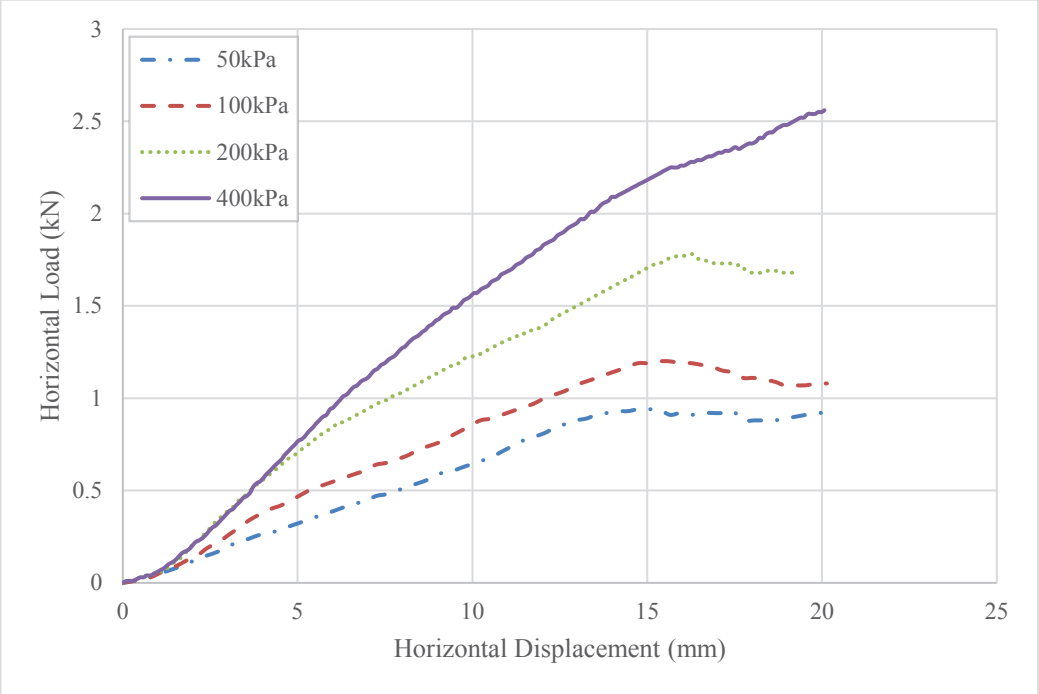

Figure 6-6 Relationship between horizontal force and horizontal displacement for geocomposite placed in subgrade materials for pullout tests (subgrade - subbase)

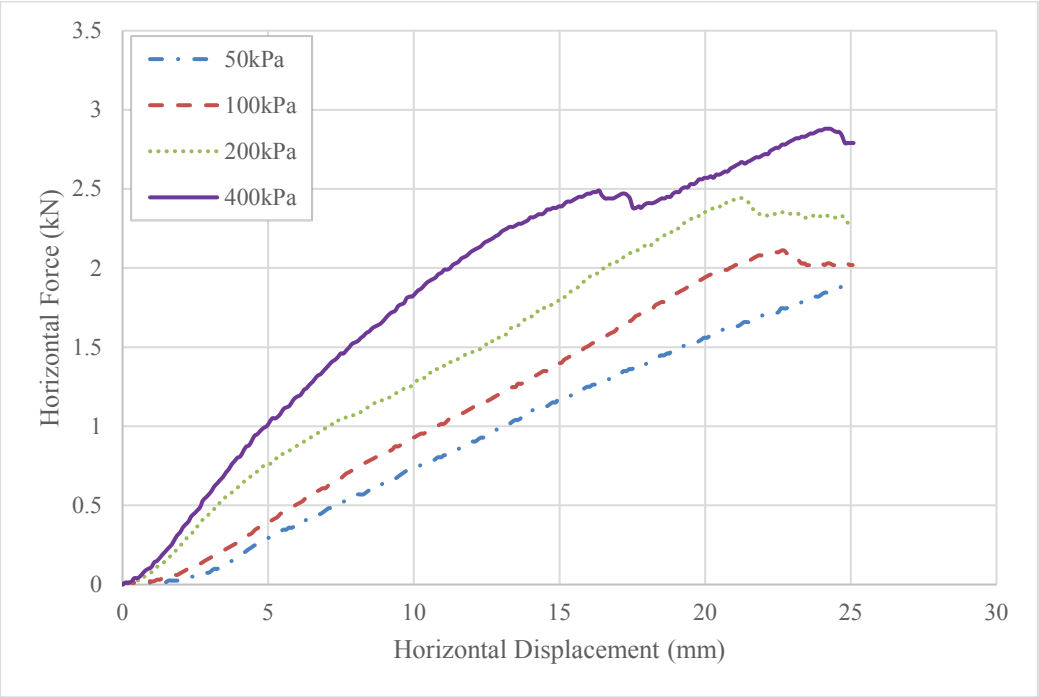

Figure 6-7 Relationship between horizontal force and horizontal displacement for geocomposite placed in subgrade materials for pullout tests (subbase - subbase)

6.3 FACTORS AFFECTING THE PULLOUT RESISTANCE

The pullout resistance is affected by different parameters such as confining stress (vertical stress acting on the sample), geosynthetic type (geogrid or geocomposite), and the physical properties of the soil or granular material. To investigate the effects of these factors on pullout resistance, the horizontal force (pullout force) in shown in Figures 6-2 to 6-7 was converted to pullout resistance using Equation 6.1 (ASTM D6706-01 (2013)) and graphs were replotted in Figures 6-8 to 6-13.

$$P_r = \frac{F_p \times n_g}{N_g} \qquad \textbf{Equation 6.1}$$

Where:

P_r: pullout resistance, kN/m

F_p: pullout (horizontal) force, kN

n_g: number of ribs per unit width of geogrid in the direction of the pullout force

N_g: number of ribs of geogrid test specimen in the direction of the pullout force

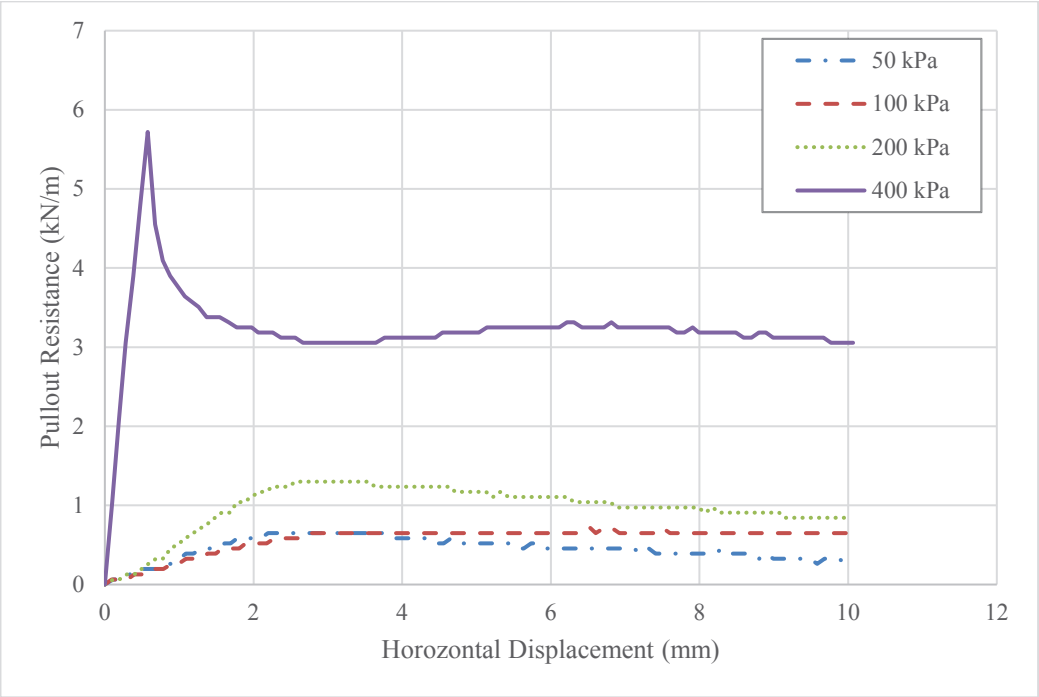

Figure 6-8 Variation of pullout resistance with horizontal displacement for geogrid placed in subgrade soil for pullout tests (subgrade - subgrade)

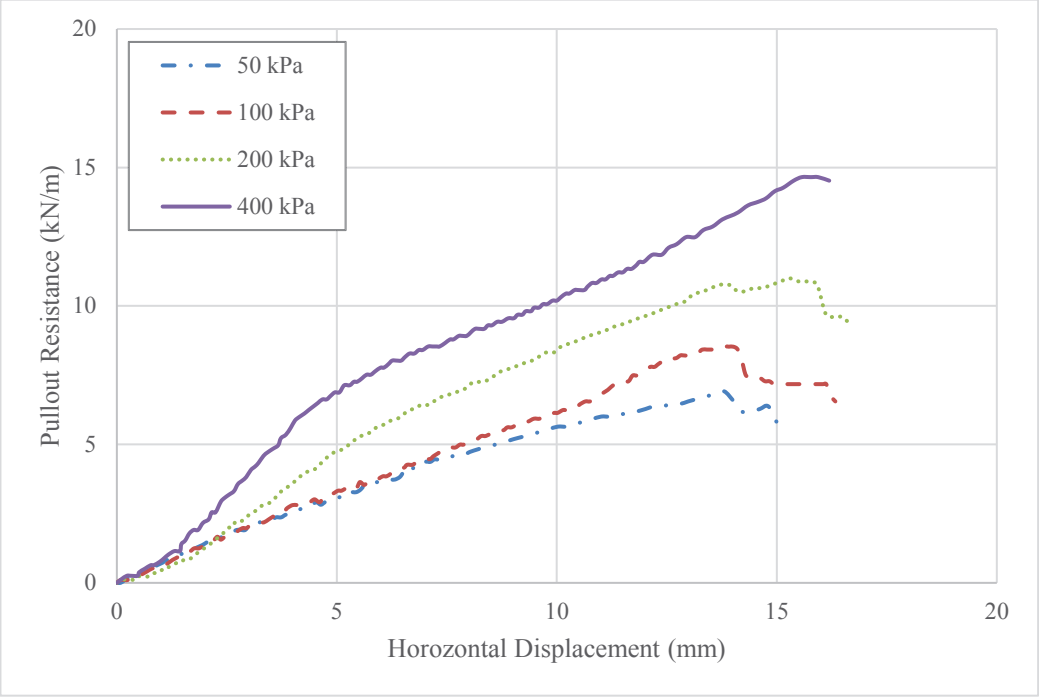

Figure 6-9 Variation of pullout resistance with horizontal displacement for geogrid placed in subbase soil for pullout tests (subbase - subbase)

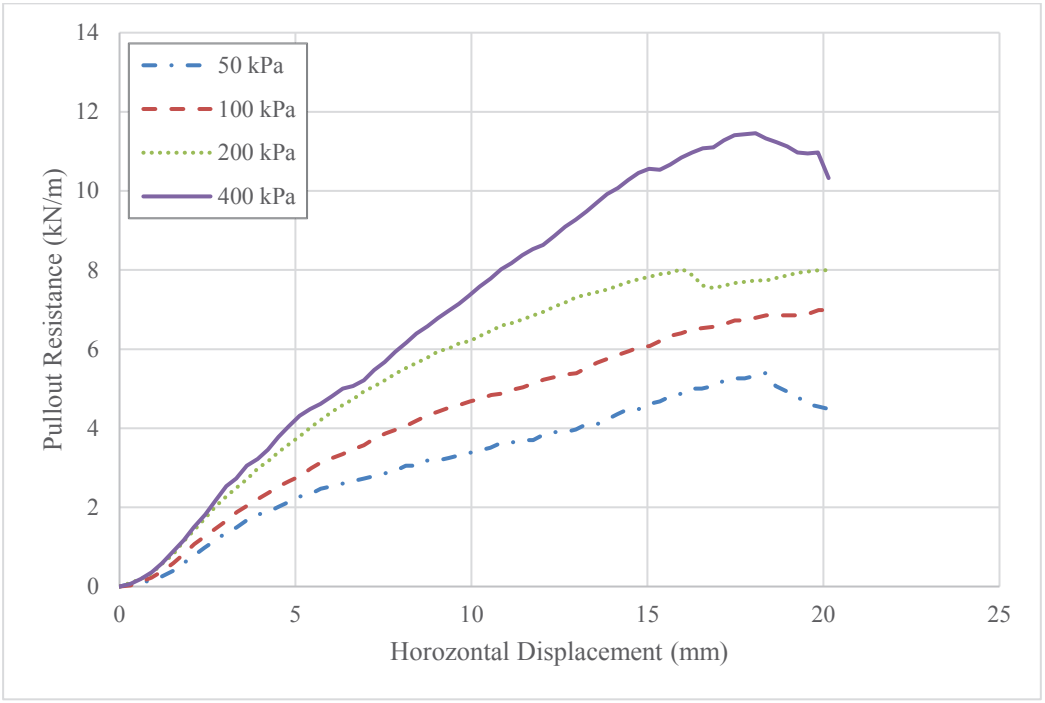

Figure 6-10 Variation of pull-out resistance with horizontal displacement for geogrid placed at interface for pullout tests (subgrade – subbase)

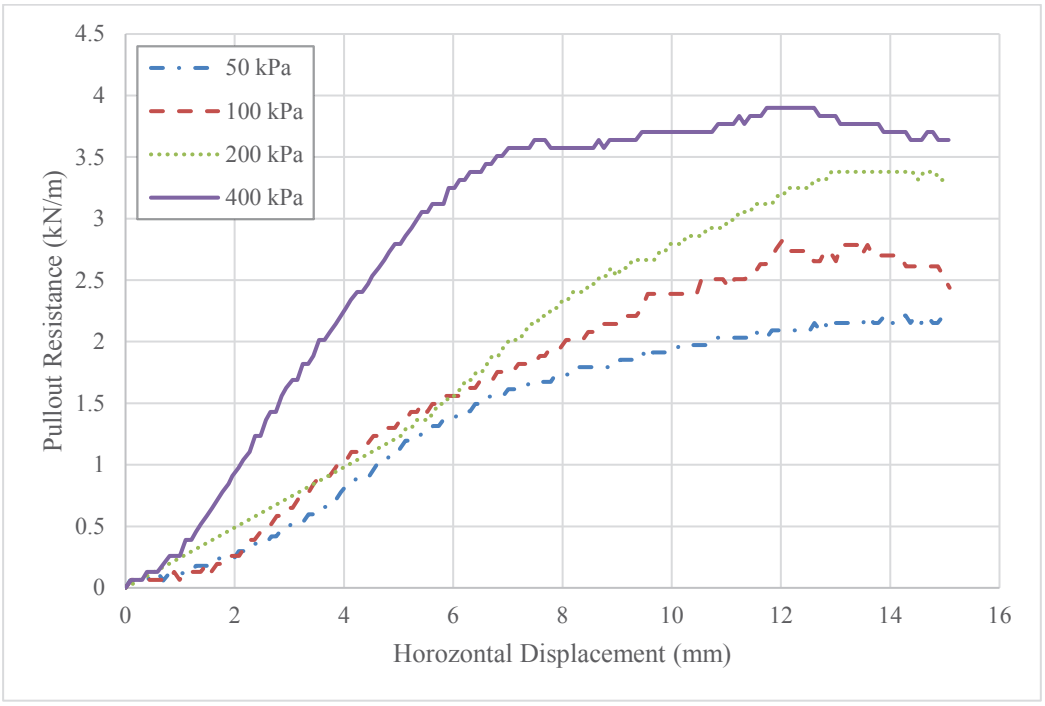

Figure 6-11 Variation of pullout resistance with horizontal displacement for geocomposite placed in subgrade soil for pullout tests (subgrade - subgrade)

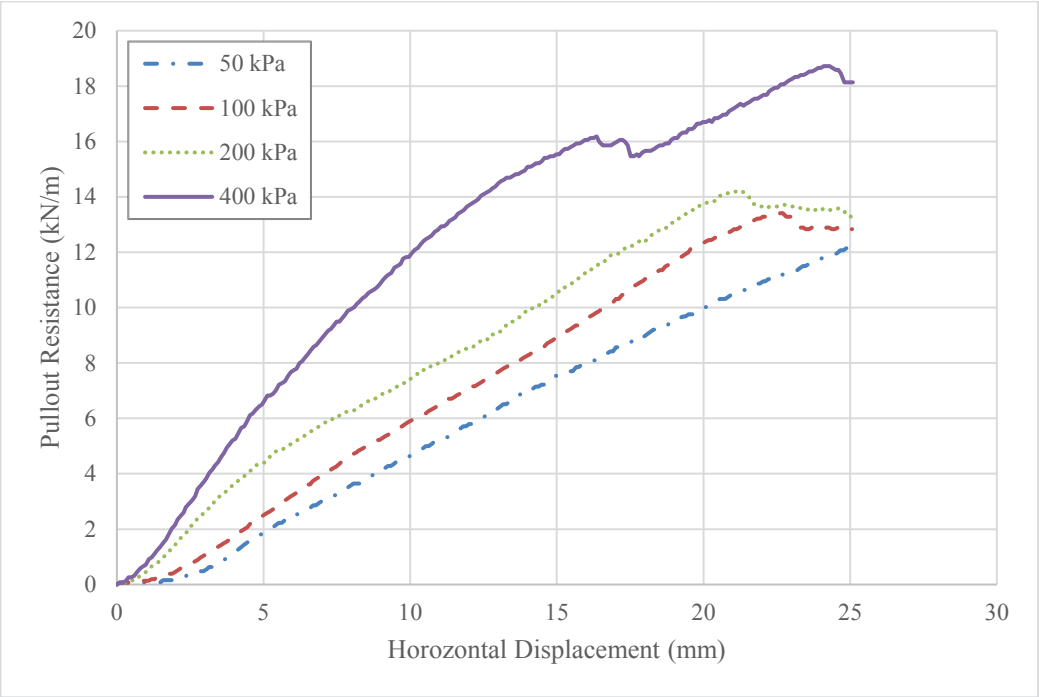

Figure 6-12 Variation of pullout resistance with horizontal displacement for geocomposite placed in subbase soil for pullout tests (subbase - subbase)

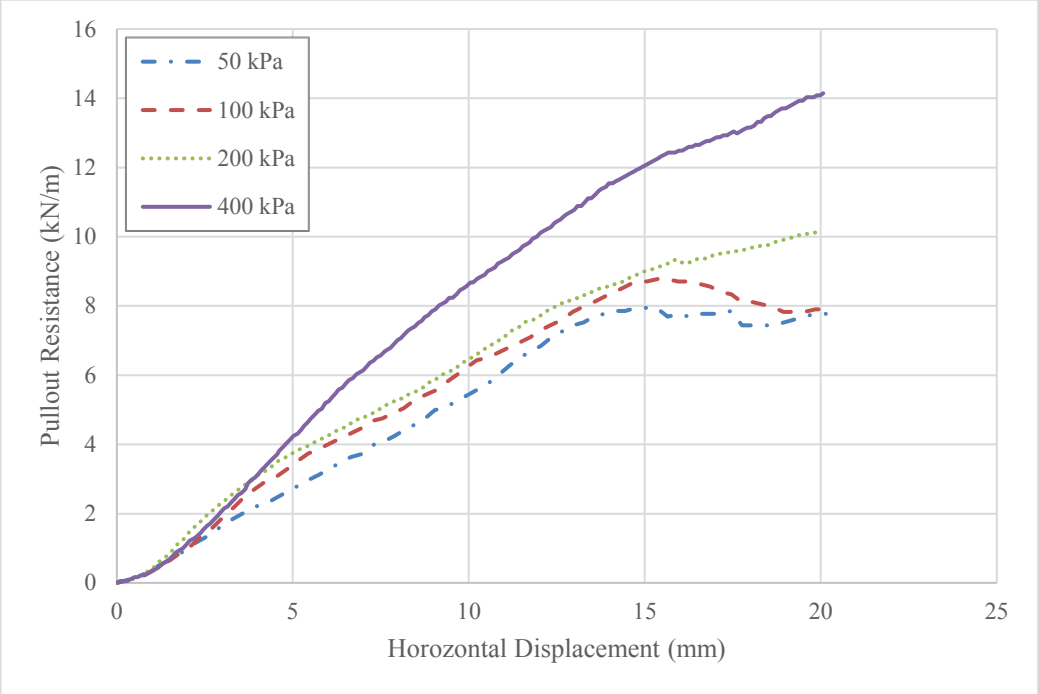

Figure 6-13 Variation of pull-out resistance with horizontal displacement for geocomposite placed at interface for pullout tests (subbase - subgrade)

It can be seen from Figures 6-8 to 6-13 that the pullout resistance increases with the increase in the vertical normal stress. This occurs irrespective of geosynthetic type (geogrid or geocomposite) and soil material (subgrade or subbase). What is also clear is that these results conform to friction theory: the larger the vertical normal stress on the geogrid or geocomposite, the larger the induced pullout resistance.

To investigate the effects of soil material (subbase or subgrade) on the pullout resistance, the pullout resistance at 10mm of horizontal displacement was obtained for 50kPa and 400kPa vertical stresses, different interface conditions (subgrade-subgrade, subbase-subbase, and subgrade-subbase), and for both geogrid and geocomposite. The results are shown in Figures 6-14 and 6-15.

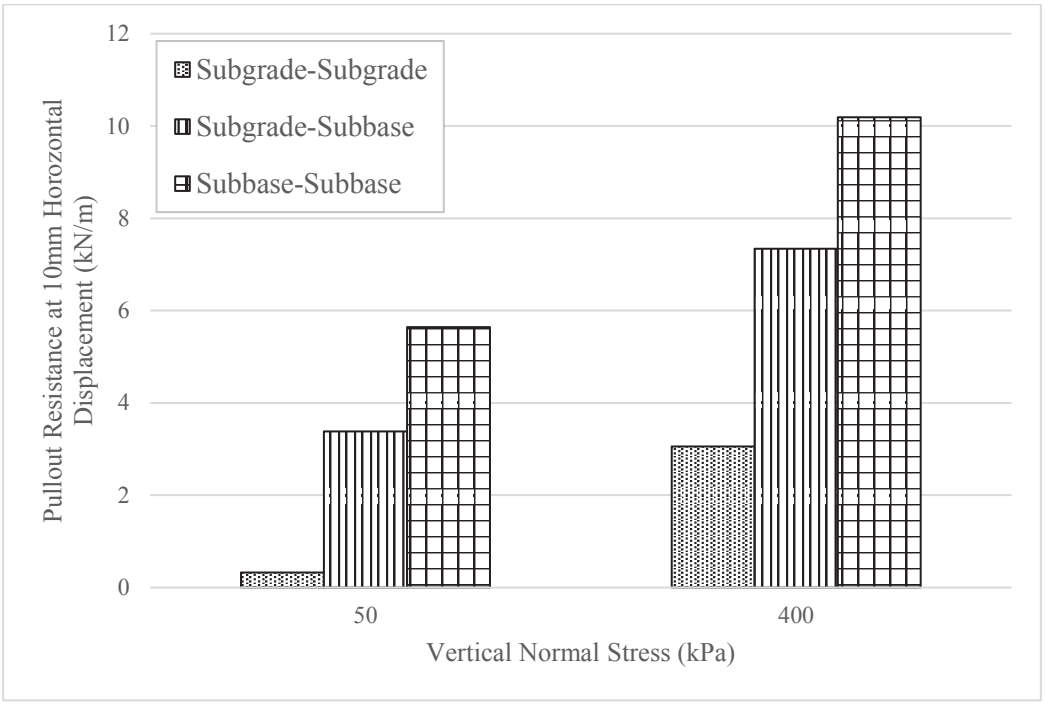

Figure 6-14 Effect of soil material on pullout resistance for geogrid

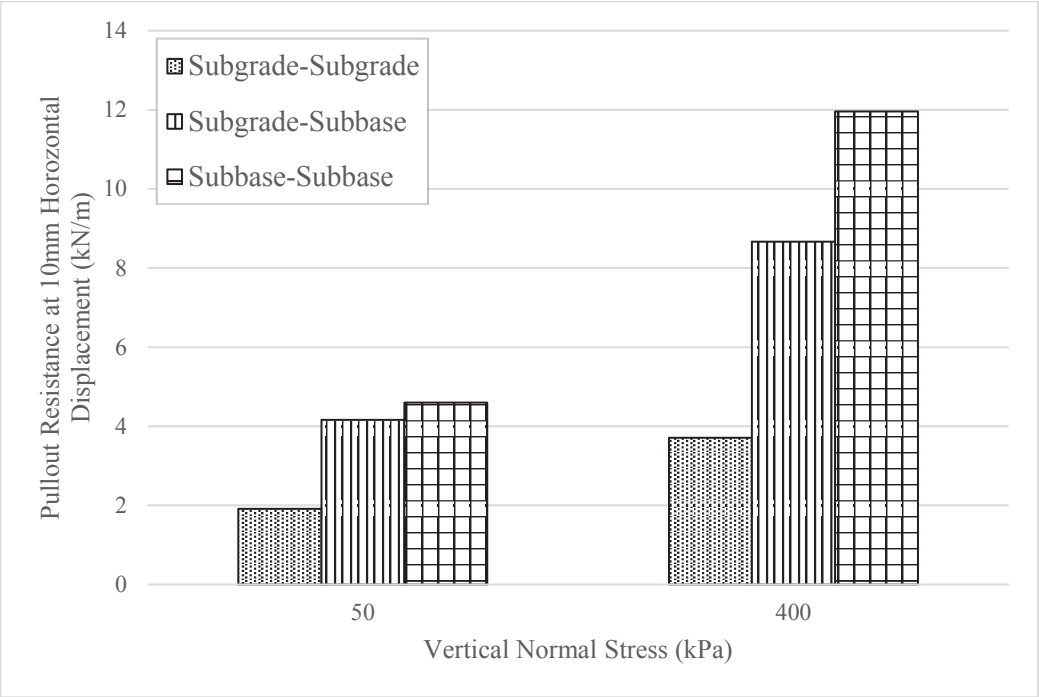

Figure 6-15 Effect of soil material on pullout resistance for geocomposite

As shown in Figures 6-14 and 6-15, irrespective of vertical normal stress and geosynthetic type, at 10mm of horizontal displacement the subbase-subbase condition provides a larger pullout resistance compared to subgrade-subgrade and subgrade-subbase conditions. Fourie and Fabian (1987) concluded that pullout resistance is directly proportional to normal stress. The results from this study agree with this conclusion and suggest reasons for this relationship. This increased pullout resistance is due to the friction and interlocking that occurs between the geosynthetic and the soil materials.

The increased friction and interlocking that occurs with the subbase material is due primarily to its larger particle size when compared to the subgrade. This larger particle size allows for increased interlocking with the geosynthetic and increased friction with both the restrained soil particles and the geosynthetic at the interface layer. Conversely, the subgrade-subgrade condition shows the lowest pullout resistance due to the high percentage of small clay particles providing low friction and interlocking ability with the surrounding restrained soil and geosynthetic.

Figures 6-14 and 6-15 show the results for the subgrade-subbase condition between the subgrade-subgrade and subbase-subbase conditions. With the different soil materials either side of the geosynthetic for these tests, and considering their differing interlocking and friction effectiveness, this was the expected result.

Variation can be seen between the magnitudes of the results when comparing the equivalent testing condition for each geosynthetic with the applied normal stress. The most obvious of variations is the subgrade-subgrade condition with 50kPa confining stress. This comparison shows the geocomposite is almost six times stronger in the same condition when compared to the geogrid. However, it is interesting to note that for all three conditions when subjected to 400kPa confining stress, the variation between the magnitudes of the results is only about 15%, in favour of the geocomposite.

The reason for this variation between the geogrid and geocomposite at low confining stress is due to the inclusion of the geotextile woven into the geocomposite. The inclusion of the geotextile increases the frictional surface area between the geocomposite and the soil materials, therefore increasing the pullout resistance. However, because of the inclusion of the geotextile, the interlocking ability between the soil materials and the geocomposite are reduced.

The variation in pullout resistance between the two products is also evident for the 400kPa confining stress where the geocomposite shows larger pullout resistance than the geogrid for all three testing conditions. However, the impact of the geotextile is less significant at the higher normal stress as the primary form of resistance at the higher normal stress is the interlocking between the geogrid and the soil materials.

6.4 THE EFFECT OF SOIL MATERIAL ON INTERFACE PROPERTIES

When considering the effectiveness of a geogrid or geocomposite in a pullout situation, the most important factor is how it interacts with the soil material. The properties to consider are its interlocking ability, and friction created between the soil material and the geogrid or geocomposite, as these properties directly relate to strength.

In this particular situation, it is important to remember that each geogrid or geocomposite sample tested has two sides in contact with the soil material. As this study was based on placing the geogrid or geocomposite sample at the interface layer, each side of the sample was in contact with a different soil material. This is important as each soil material has different physical properties and will therefore interact with the geogrid or geocomposite sample with different degrees of effectiveness. In the simulated field condition, the underside of the sample was in contact with the soft clay subgrade and the upper side in contact with the subbase.

In order to determine the interlocking and friction properties of each sample with both the subgrade and subbase, a series of tests were conducted where subgrade was used both above and below the geogrid and geocomposite sample. Similarly, the same test series was conducted for the subbase.

The force and displacement results from these tests, shown in Figures 6-2 and 6-4 (for the geogrid) and Figures 6-5 and 6-7 (for the geocomposite), were used to calculate the normal and shear stresses. Equation 6.2 (AS 1289.6.6.6-1998) was used to calculate the shear stress for each variation of soil and geosynthetic material.

$$\tau = F / A \qquad \textbf{Equation 6.2}$$

Where:

τ: shear stress (kN/m² or kPa)
F: the force applied (kN)
A: the cross-sectional area of the material (m²)

To calculate the shear stress, the cross-sectional area was required. As the geosynthetic has two sides in contact with the soil material, the effective area is double that of the geosynthetic sample that is inside the test area. The sample size used for this test series was 150mm x 150mm. Therefore, the total effective area is 45000mm², or 0.045m². With the normal stress and the shear stress calculated for each test series, the peak shear stress values were plotted against the normal stress values (Figure 6-16).

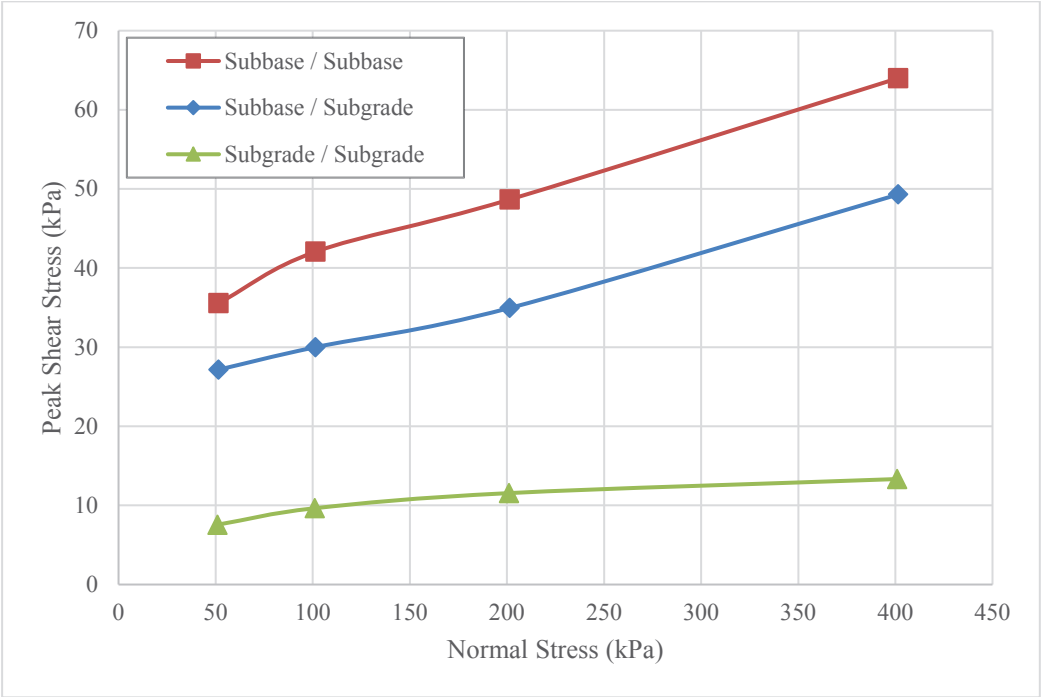

Figure 6-16: Relationship between normal stress and peak shear stress for geocomposite pullout testing

Figure 6-16 shows three conditions for the geocomposite sample, two of which have already been discussed, and the third condition shown is the subbase-subgrade or simulated field condition. The results from the simulated field condition can be seen between the subbase-subbase and subgrade-subgrade, which determines that the simulated field condition is weaker than the subbase-subbase condition, however is stronger than the subgrade-subgrade condition. These results agree with the trends seen in research by Wang et al., (2016) and were therefore expected, as the subgrade is a weak clay and the subbase is a stronger granular material.

Figures 6-5, 6-7 and 6-16 all show the results from the calculations and analysis for the geocomposite, and it is important to note that the same calculations and analysis were performed for the geogrid sample. Using these values, the friction angle and adhesion of each soil material were calculated and used to determine the effectiveness of each soil material with both the geogrid and geocomposite, as seen in Table 6-2. These values were obtained by applying a linear trendline to each condition in Figure 6-16 and using the equation of that trendline to determine the adhesion and calculate the friction angle.

Table 6-2 Friction angle and adhesion for both geogrid and geocomposite

	Subgrade - Subgrade	Subbase - Subbase
Geocomposite Friction Angle (degrees)	0.87	4.49
Geocomposite Adhesion (kPa)	7.7	32.8
Geogrid Friction Angle (degrees)	1.51	4.23
Geogrid Adhesion (kPa)	0.1	21.2

6.4.1 Estimating field conditions from interface properties

To estimate how a geogrid or geocomposite will perform in the field, specific material properties are required. How the geogrid or geocomposite material will interact with a soil material can be summarised by knowing its interface properties. In Section 6.4, the friction angle and adhesion properties were calculated and showed that when the geogrid and geocomposite were tested with the same soil material, it could be determined how that particular geogrid or geocomposite would interact with that particular soil material.

Two soil materials (physical properties outlined in Section 5.2) were tested in this study: a subgrade and a subbase. The raw load and displacement data was collected from all tests conducted and used to determine the effect that both soil materials had on the effectiveness of the particular geogrid or geocomposite. This determination consisted of calculating the peak shear stresses the geogrid and geocomposite were able to sustain with both the subbase and subgrade at various normal stress levels.

Shown in Figure 6-17 are the results from calculating the peak shear stress, using Equation 6.3 and the calculated data in Table 6-2, sustained by the geogrid sample when tested with the subgrade and the subbase individually. Figure 6-17 shows that as the normal stress increases from 50kPa to 400kPa, the peak shear stress values more than double for the subbase and increase five-fold for the subgrade.

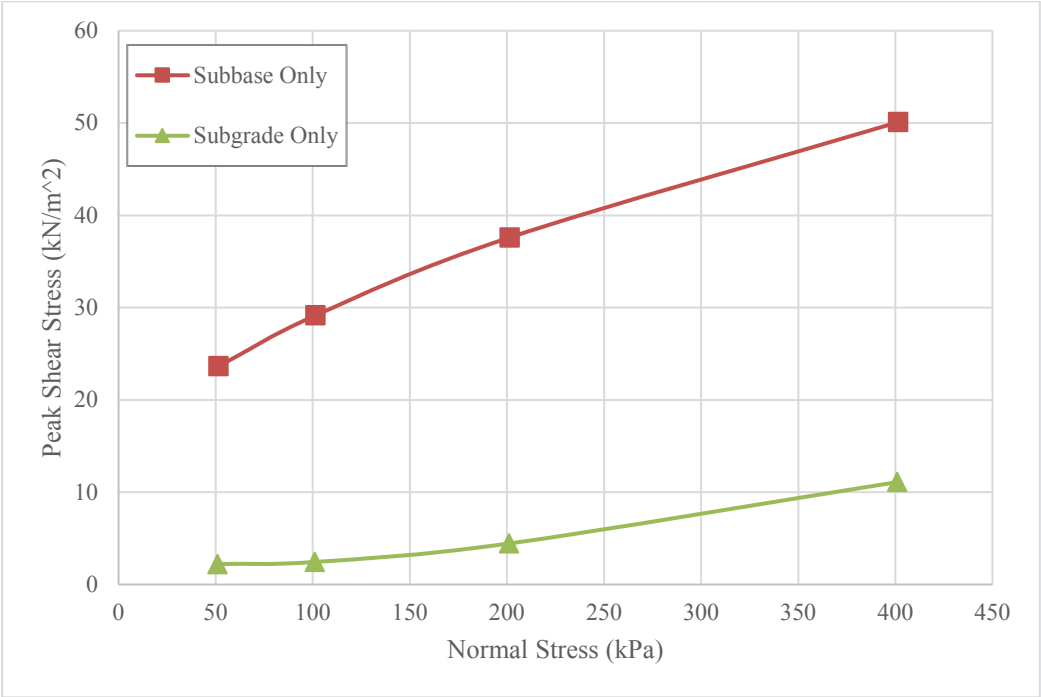

Figure 6-17 Relationship between peak shear stress and normal stress for geogrid at various normal stresses for subbase – subbase and subgrade - subgrade

$\tau = c' + \sigma' \tan \phi'$ **Equation 6.3**

Where:

τ: shear stress (kPa)

c': effective adhesion (kPa)

σ': effective normal stress (kPa)

ϕ': friction angle (degrees)

As the aim of this test series was to estimate how effective the geogrid will be in the field, an effectiveness criterion was established. This criterion was defined as the peak load, in kN, at normal stress values of 50kPa, 100kPa, 200kPa and 400kPa. This criterion was selected due to the data collected from the subgrade - subbase or simulated field condition test series, at each of the defined normal stress values. The data obtained from this test series was load (kN) and displacement (mm).

In order to determine that an accurate prediction of the simulated field condition can be obtained from the separate subgrade and subbase only trials, the peak shear stress

values needed to be back calculated into a load value (kN). This was achieved by using the shear stress values calculated from Equation 6.3 at each of the defined normal stress values and multiplying it by the cross-sectional area of 150mm x 150mm or 0.0225m², used in the simulated field condition trials. This calculation was performed for both the subgrade and subbase at the same normal stress value, with the final step being the addition of these load values to compare with the measured simulated field condition value. Figure 6-18 shows the results for the measured values from the test series and the calculated values using the previously mentioned procedure.

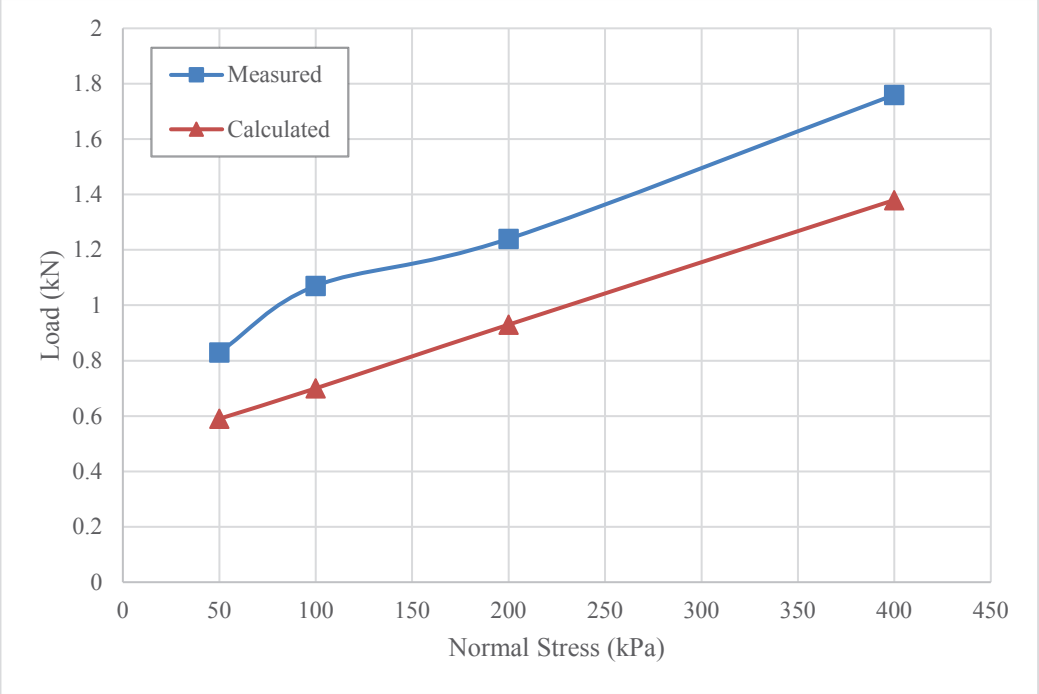

Figure 6-18 Relationship between measured and calculated loads at various normal stress values for geogrid pullout tests

This series of calculations was completed for both the geogrid and the geocomposite with the results for the geocomposite shown in Figure 6-19.

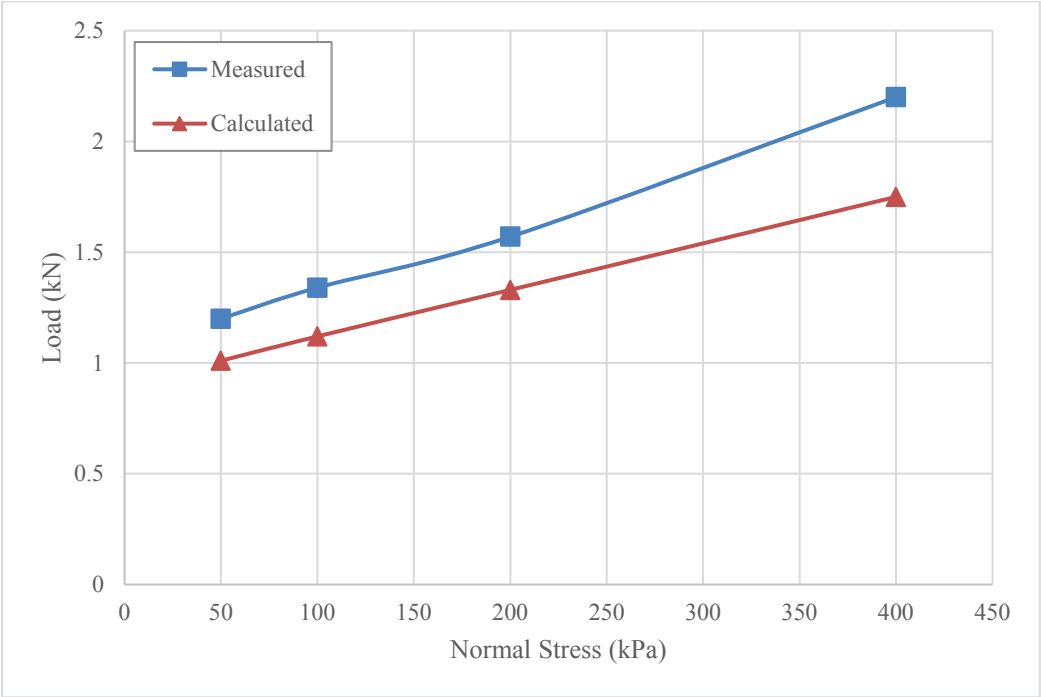

Figure 6-19 Relationship between measured and calculated loads at various normal stress values for geocomposite pullout tests

Both Figure 6-18 and Figure 6-19 show a disparity between the measured and calculated values, with the measured value always exceeding the calculated value. For the geogrid the measured value exceeds the calculated value by approximately 25%, and for the geocomposite the measured value exceeds the calculated value by approximately 15%.

There could be a number of reasons for this disparity between the measured and calculated values. The area value used in the calculation is the cross-sectional area at the interface layer. Using this value may not account for the vacant area between the ribs in the geogrid sample. This is an important consideration as within this vacant area there is no friction between the soil material and geogrid, helping to resist the shear. Another reason for the difference in the values may be due to the compaction in the sample preparation phase. When compacting the subbase material that sits above the geogrid sample, it is possible to force it through the aperture and into the subgrade. Therefore, when performing the pullout test, it is not certain that the geogrid perfectly separates the subgrade and subbase. As both of these soil materials have vastly different properties, one of the materials may have resisted the pullout force to a greater degree.

Although there is variation between the measured and calculated values, the difference is consistent. As the measured value always exceeds the calculated value, a degree of safety already exists when considering design criteria. Therefore, when

performing estimation calculations for design guidelines, a correction factor is able to be applied to bring the calculated value closer to the measured value.

The geogrid measured value was approximately 25% higher than the calculated value and therefore Equation 6.4 can be used to more accurately estimate the peak load at any given normal stress. The geocomposite measured value was approximately 15% higher than the calculated value and therefore Equation 6.5 can be used to more accurately estimate the peak load at any given normal stress.

$\tau = c' + \sigma' \tan \phi'$

or

$\tau = F / A$

or

$F = \tau \times A$

$F = 1.25(\tau \times A)$ **Equation 6.4**

$F = 1.15(\tau \times A)$ **Equation 6.5**

Where:

F: force (kN)

τ: shear stress (kN/m²)

A: cross-sectional area (m²)

As shown in Figure 6-20 using Equation 6.4, and Figure 6-21 using Equation 6.5, the new calculated result is significantly more accurate as it is much closer to the measured value whilst still allowing a safety factor.

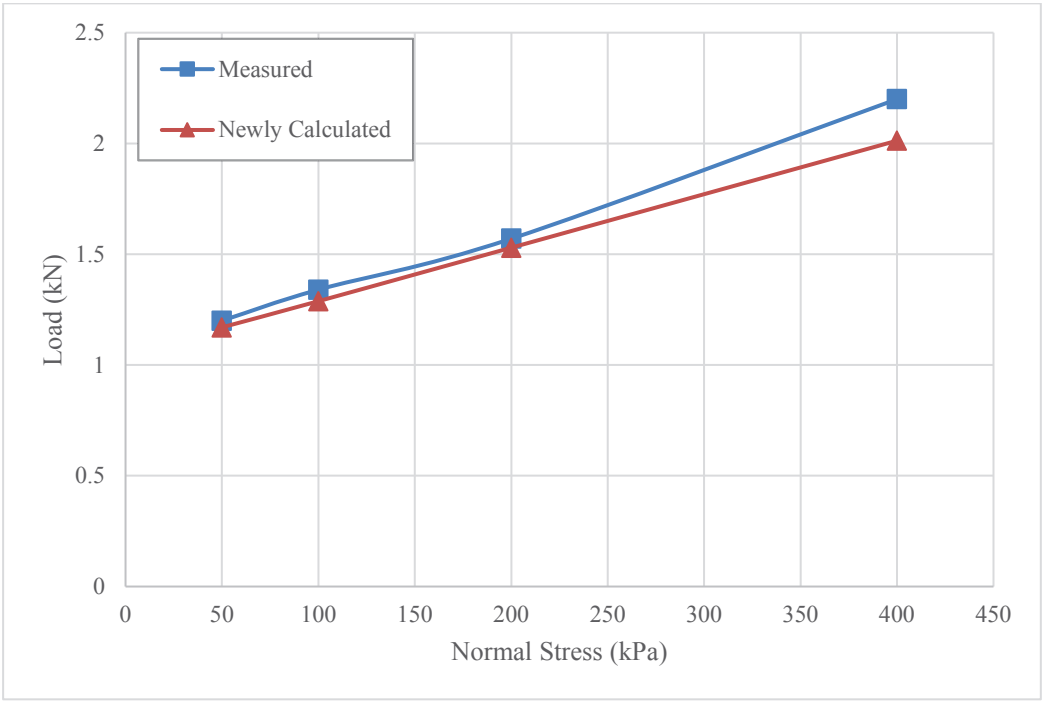

Figure 6-20 Relationship between measured and newly calculated loads at various normal stress values for geogrid pullout tests

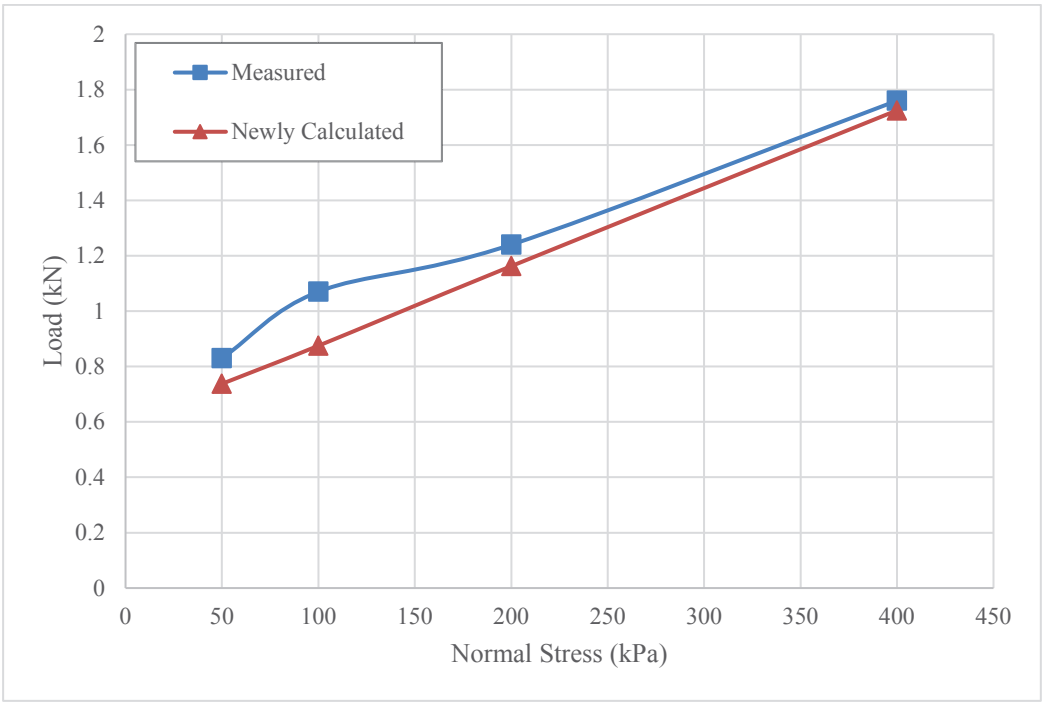

Figure 6-21 Relationship between measured and newly calculated loads at various normal stress values for geocomposite pullout tests

6.5 CALIFORNIA BEARING RATIO (CBR) TESTING

The inclusion of geogrid in any design is primarily to improve the strength. When considering foundation strength, a widely accepted measure of strength is its bearing capacity. To ascertain this value, a CBR test can be performed and this value used for analysis and comparison.

This series of tests were conducted according to the methodology outlined in Chapter 3, using the equipment detailed in Chapter 4. Table 6-3 outlines the tests performed during this research to determine the performance of the geogrid and the effect of the variations in subbase layer thickness.

Table 6-3 Summary of the CBR tests performed: conditions and number of tests

Geogrid Samples	No Cover	50mm Cover	100mm Cover	200mm Cover
Without Geogrid	3	3	3	3
With Geogrid	3	3	3	3
With Strain Gauges	0	2	2	2
With Tactile Sensors	2	0	2	0
Repeatability Trials	2	2	0	0

As mentioned in Chapter 4, a series of tests were conducted using pressure sensors. The purpose of these tests was to determine the extent of the boundary effect and, therefore, how effective the newly designed CBR mould was in reducing this testing error. This measurement was represented in the I-scan pressure mapping software as a visual colour change from light blue to red as the pressure increased. Figure 6-22 shows a screen capture from the software at the conclusion of a test where a geogrid sample was included with a 100mm subbase cover layer, and the software set to maximum sensitivity. The image is shown in the same orientation that the sensor was embedded in the sample.

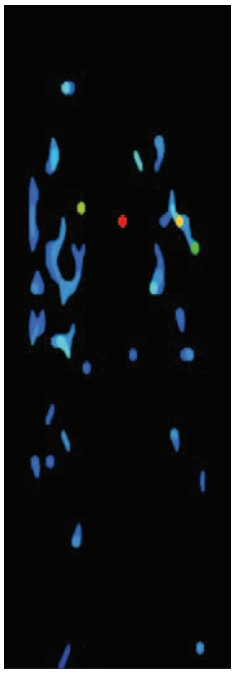

Figure 6-22 Screen capture image of Tekscan output file showing pressure location for CBR tests

As the screen was calibrated to black at the beginning of the test, is easy to see a colour change approximately 1/3 of the distance from the top in Figure 6-22. These blue, green, yellow and red colours are present and therefore indicating an increase in pressure through this region. The distance from the top corresponds directly with the interface layer where the geogrid was embedded between the subgrade and subbase. This was the expected outcome: the geogrid acted to distribute the stress more uniformly across the soil sample at the interface layer, reducing the permanent deformation in both the subbase and subgrade layers.

Further data collection was performed using the strain gauges defined in Section 4.5 and attached as per Figure 4-6. For each sample utilising these strain gauges, five gauges per sample were attached, three in the MD and two in the CMD. Whilst data was successfully obtained from these tests, during the compaction of the subbase material some of the connections between the strain gauge and the data collection apparatus were destroyed. The results from the remaining strain gauges were obtained, however nothing meaningful was able to be determined through analysis of these results.

To ensure that the proposed method and procedure detailed in Chapter 3 would yield reliable results, a series of initial repeatability trials were conducted. Table 6-3 mentioned two tests with no cover layer and two tests with 50mm cover layer. The results

of these tests are shown in Figure 6-23. These results shown were achieved by following the procedure outlined in Chapter 3 with the additional step of removing 120mm of subgrade between each test. Through the inclusion of this step in the procedure, repeatable and reliable results were obtained for all subsequent tests.

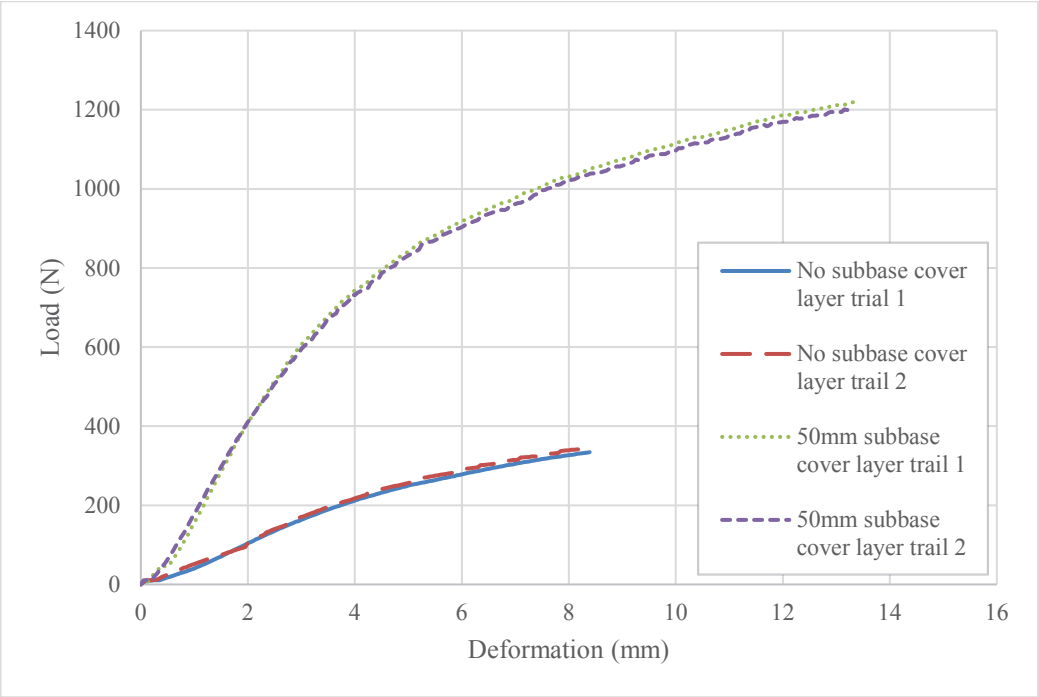

Figure 6-23 Relationship between load and deformation for repeatability trials with and without subbase cover for CBR tests

6.5.1 The effect of including geogrid at the interface layer

The results obtained from the UTM in their raw form were load (N) and displacement (mm), where the displacement was directly equal to the deformation due to the plunger. As the data collection was consistent across all tests, a direct comparison of the results was possible. This study focused on the test results up to 10mm of penetration as all tests conducted achieved this value.

The initial test series included only one variation: the cover layer depth. In this test series, no geogrid reinforcement was included to obtain values for the specified simulated field condition without reinforcement. Obtaining these values was critical, as without these values, quantifying the strength gains resulting from the geogrid inclusion would not have been possible.

Figure 6-24 shows the load and deformation curve for the unreinforced simulated field condition with the subbase cover layer depths of 0mm (subgrade only), 50mm,

100mm and 150mm. The trend observed in Figure 6-24 shows that the load increases with cover layer depth. This was the expected trend, as stronger subbase material is capable of sustaining a higher load than the weak clay subgrade. Therefore, as the subbase layer thickness increases, the direct load on the subgrade is reduced, allowing the overall condition to achieve a higher load carrying capacity.

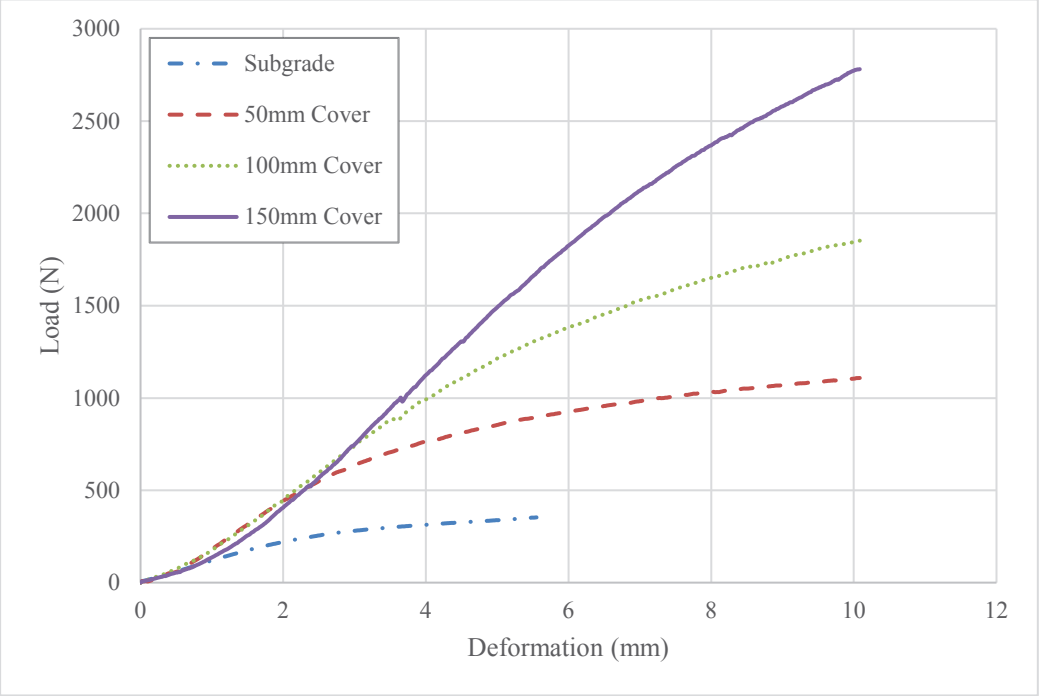

Figure 6-24 Relationship between load and deformation with various cover layer thicknesses and without geogrid reinforcement for CBR tests

To quantify the strength gains resulting from the addition of the geogrid, the previous test series was repeated with one variation: the inclusion of the geogrid reinforcement at the interface layer. Furthermore, as the geogrid relies on interlocking with soil materials on both surfaces, the 0mm subbase cover layer was not tested.

Figure 6-25 shows the same trend that exists in Figure 6-24 with a significant increase in peak load at 10mm of deformation for each of the three subbase layer thicknesses. As the only variation in this test series was the inclusion of the geogrid at the interface layer, the increase in load can only be due to the interaction of the geogrid with the soil materials. This trend agrees with results found in a study conducted by Asha, M.N. and Latha, G.M. (2010).

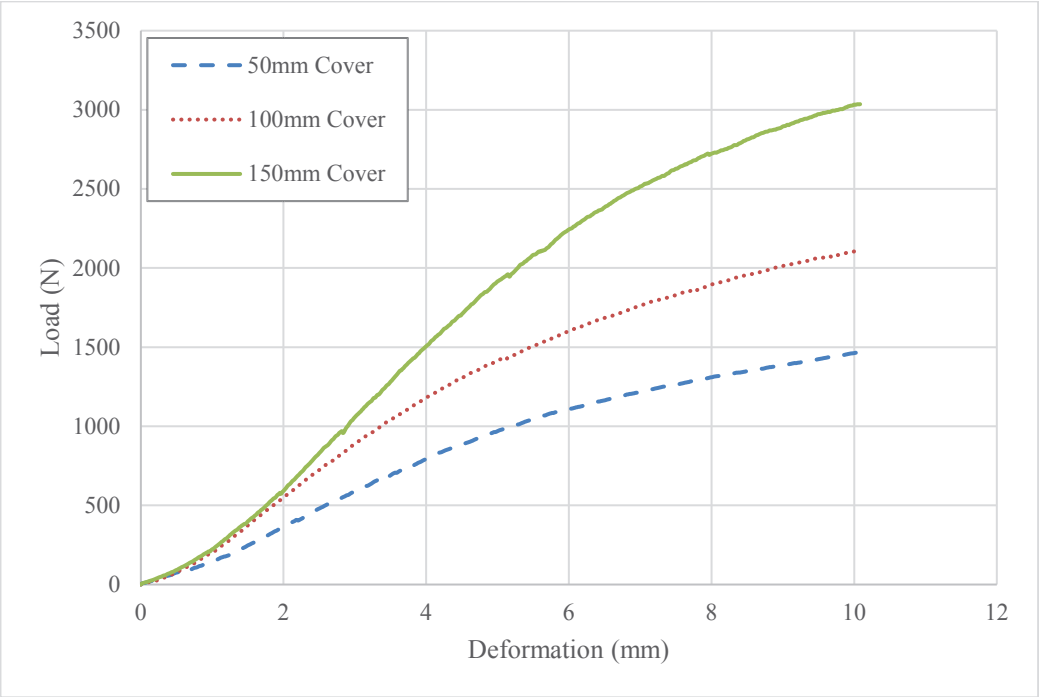

Figure 6-25 Relationship between load and deformation with various cover layer thicknesses and geogrid reinforcement for CBR tests

6.5.2 The effect of cover layer thickness on geogrid performance

With the trend of increasing cover layer thickness improving the load carrying capacity confirmed, the effectiveness of the geogrid with the various cover layer thicknesses could be quantified.

Figure 6-26 shows the peak load values for both the reinforced and unreinforced test series at each cover layer thickness tested. These values show that whilst there is an increase in load as the cover layer increases, the relative change due to the inclusion of the geogrid deceases – showing that the inclusion of the geogrid is most effective with a smaller cover layer thickness.

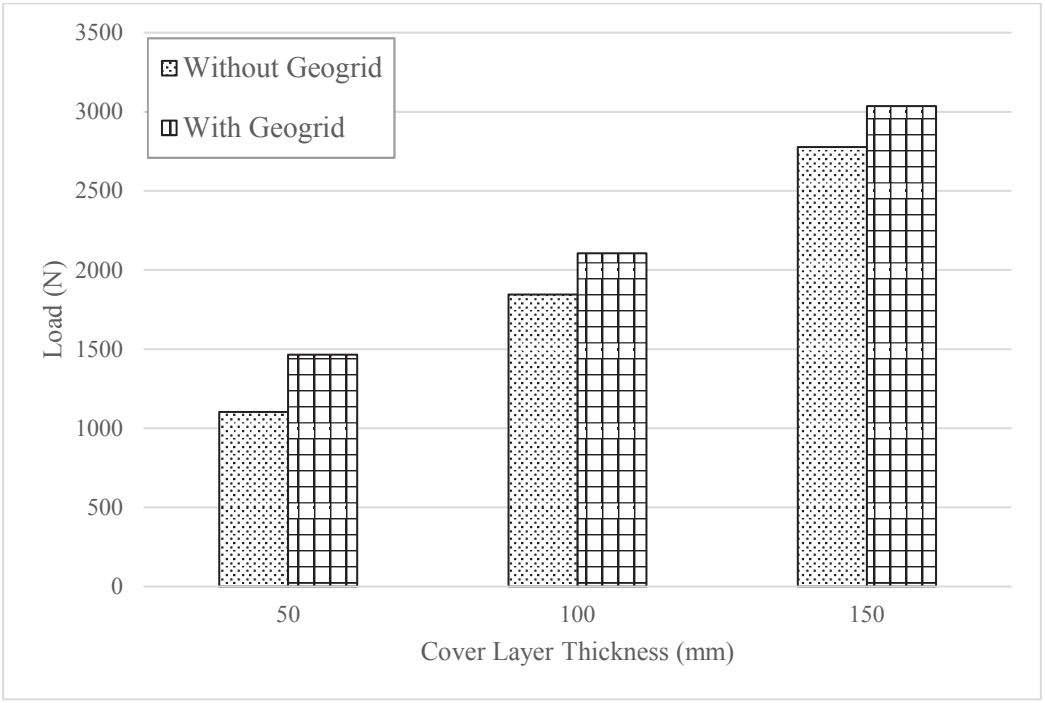

Figure 6-26 Variation between load and cover layer thickness with and without geogrid reinforcement at the interface layer for CBR tests

With the obvious decrease in geogrid performance as cover layer thickness increases (shown in Figure 6-26), it was important to quantify this factor for future verification of this testing model. A calculation was performed to determine the percentage increase in load due to the inclusion of the geogrid for each cover layer thickness.

Figure 6-27 shows the percentage increase in load carrying capacity for each cover layer thickness variation. Approximately a 25% increase was calculated for the 50mm cover layer, with this value decreasing to approximately 12% for the 100mm and approximately 9% for the 150mm cover layer.

The performance of the geogrid is determined by its interlocking ability with the surrounding soil material, which activates the membrane effect on the tensile face of the geogrid. This effect is most noticeable in this research with a 50mm subbase cover layer as the normal stress induced in the sample at the surface of the subbase is readily transferred to the geogrid at the interface layer. There is only a small reduction in the load transfer that occurs with the thin cover layer, therefore allowing a large degree of the induced load to act on the geogrid and readily activate the interlocking at the interface, maximising the tensile capabilities of the geogrid. This finding agrees with Duncan-Williams and Attoh-Okine (2008) as they also discovered that the membrane effect was mobilised to a higher degree with a thinner cover layer.

Despite the significant strength gain of 25% due to the geogrid with the 50mm cover layer, the effectiveness of the geogrid with 150mm of subbase cover is less than half at approximately 9% (Figure 6-27). This decrease in effectiveness occurs due to the normal stress induced in the subbase material at the surface, failing to activate the geogrid at the interface layer to the same degree as the thinner 50mm subbase cover layer.

The results in Figure 6-26 and 6-27 show that the inclusion of geogrid does increase the strength of the subgrade irrespective of the normal stress or cover layer thickness. However, the most important finding from this research is shown when comparing the peak load values for the 50mm cover layer and 150mm cover layer with the geogrid in Figure 6-26. These values show that more than 50% the subgrade strength for the 150mm cover layer without geogrid can be achieved using only 50mm of the subbase material with geogrid. This results in significant financial and environmental savings without compromising on subgrade strength.

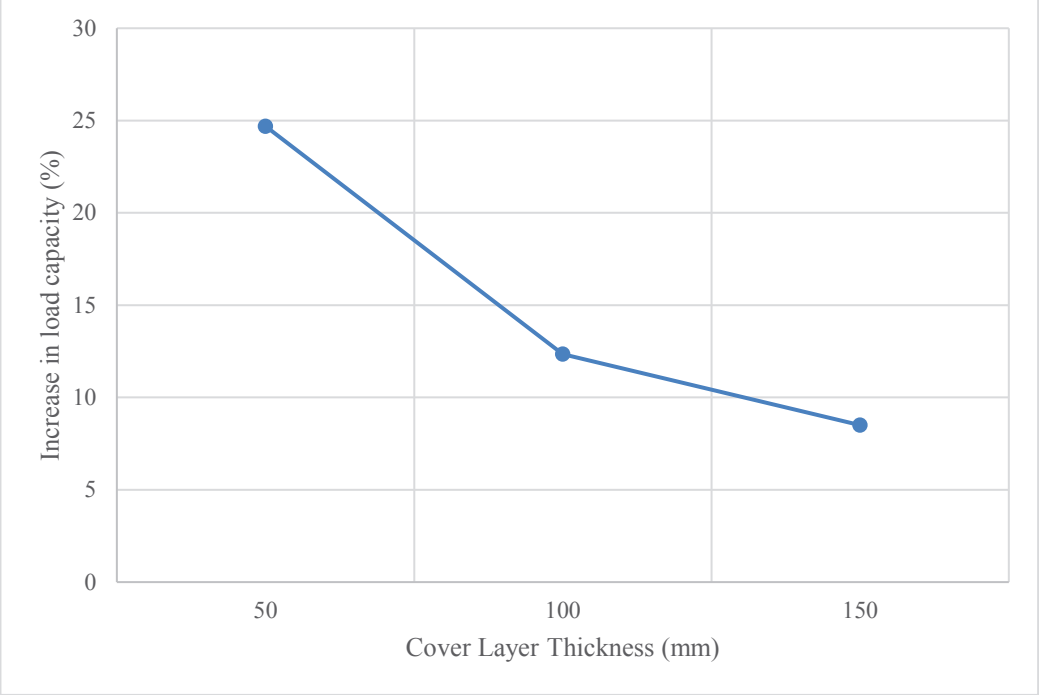

Figure 6-27 Relationship between the percentage increase in load capacity with variation in cover layer thickness and geogrid at the interface for CBR tests

Chapter 7: Conclusions and Recommendations

7.1 CONCLUSION

This research was designed to assess the effectiveness of two different geosynthetics – a geogrid and a geocomposite – as a weak subgrade stabiliser. The objectives of this study were to develop laboratory testing methods to assess the performance of geogrid and geocomposite stabilised subgrade. Once these testing procedures are verified and the tests results are correlated with large-scale model tests and field tests, they can be used for developing design guidelines and to assess performance of a given geogrid or geocomposite product.

The following sections in this chapter conclude major findings of this research while emphasising the achievement of each research objectives outlined in section 1.3.

7.1.1 Tensile properties of geogrid and geocomposite

As a part of the first objective of this research, a set of clamps (to grip the geogrid and geocomposite) and a set of attachments (to connect the clamps to the UTM), were designed and manufactured. This apparatus was then used to perform a series of tensile tests on geogrid and geocomposite samples to determine their tensile strength and secant modulus as these are critical factors that affect the material properties. The laboratory measured values were used to calculate the secant modulus and tensile strength of both geogrid and geocomposite and were compared with the manufacturer-specified values of each product. The good agreement between these values suggests that the newly designed and built clamps and testing procedure are both acceptable to determine tensile properties of a given geogrid or geocomposite product. Further, the following conclusions were made from the series of tensile tests conducted using this set of clamps and testing procedures:

- A video extensometer can effectively be used as non-contact method to measure tensile strain of a geogrid or geocomposite during a tensile test.

- The secant modulus is effected by the strain rate used in the test. This is evident as the modulus increases with the increase in the strain rate. Therefore, it is important use a standard strain rate in tensile tests on geogrid or geocomposite products.
- The test results suggest that both the geogrid and the geocomposite are stronger in the MD despite the manufacturer's claim that they are isotropic. The geogrid secant modulus measured in the CMD was approximately 2-3% lower when compared to that of MD. However, for the geocomposite, this difference was approximately 12-14% lower. Therefore, it is recommended to calculate the secant modulus and tensile strength in both the MD and CMD for any given geogrid or geocomposite product.

7.1.2 Pullout tests on geogrid and geocomposite

The objective of the pullout tests was to investigate the pullout tensile resistance and interlocking effect of different geogrid products. This objective was achieved in two stages.

First the geogrid and geocomposite product were both tested according to the methodology outlined in Section 4.4, and their tensile properties were successfully obtained by calculating the maximum tensile resistance. The second phase in achieving this objective was to determine the interlocking effect the geogrid and geocomposite had with each soil material. The following conclusions were made from the series of pullout tests conducted on the geogrid and geocomposite:

- A comparative analysis was undertaken using the raw data and it was determined that both products exhibited the same trend, being that maximum pullout resistance increases as both horizontal displacement and normal stress increases. However, as the geocomposite returned higher load and pullout resistance values, it was determined to be a more effective product for the conditions and soil materials used in this study.
- Through analysing the interface properties between each of the various combinations of geogrid and geocomposite with both the subgrade and subbase materials, the friction angle and adhesion that occurred for each of these test variations was calculated. Using the interface properties and the application of a correction factor, accurate results using the proposed testing method were achieved.

- By utilising the calculations proposed in Sections 6.5 and 6.6, and this testing model, the behaviour of the geogrid or geocomposite sample in a similar field condition can be predicted.

As the results of the testing proved that the small-scale laboratory model utilised in this research was able to accurately predict the geogrid and geocomposite performance in the simulated field condition, it is reasonable to assume that this will accurately scale to a field trial.

7.1.3 CBR tests on geogrid reinforced subgrade model

The objectives of the CBR testing were the design and manufacture of a larger than standard CBR mould to reduce the boundary effect, and development of a testing model to assess the performance of geogrid as a subgrade reinforcement.

The first part of this objective was successful following the methodology in Section 3.2 and in-depth procedure outlined in Section 4.2. The second part of this objective was achieved through a testing regime outlined in Section 4.2 and Table 4-1, consisting of the inclusion and exclusion of geogrid reinforcement whilst varying the subbase cover layer thickness to assess the geogrid performance. The following conclusions were made from the series of CBR tests conducted using the new CBR mould and varying the cover layer thickness:

- The inclusion of geogrid at the interface layer did improve the strength of the foundation by approximately 25% with a 50mm subbase cover layer. However, despite the subgrade strength increasing for all cover layer depths tested, the effectiveness of the geogrid became less apparent. This was evident as with 150mm of subbase cover, the inclusion of the geogrid only contributed an extra 9% to the overall strength.
- The boundary effect is only present at the interface layer as is evident from Figure 6-22. However, further quantitative analysis is required to quantify the exact reduction in the boundary effect due to the larger mould size.

In conclusion, the research process followed in this study successfully achieved the objectives outlined in Section 1.3. This research shows that accurate physical

properties of geogrid and geocomposite samples, and soil materials, can be obtained and used to predict geogrid or geocomposite performance in the field.

7.2 RECOMMENDATIONS

It is recommended that research be undertaken to further verify and enhance the proposed testing apparatus and procedures used in this research to assess the effectiveness of geogrid and geocomposite as a subgrade reinforcement product. The following recommendations for further research should be followed with the desired aim to develop design guidelines for geogrid use in pavement:

- Test simulated model pavements in the modified CBR mould with repeated loading to assess the performance.
- Optimise this small scale model with a focus on required layer thickness to induce optimum tension in the geogrid
- Test a larger range of geogrid and geocomposite products according to the proposed testing procedure. These tests may also involve using some clear soil simulated soil media to better view and understand the interlocking effect.
- Perform large-scale laboratory and field tests on geogrid and geocomposite reinforced subgrade pavements and develop performance correlations between the proposed small scale model tests and large scale laboratory and field tests.
- Develop numerical models to simulate the performance of pavement with geogrid reinforced subgrade and validate them from small- and large-scale laboratory testing, and field tests.

References

Abu-Farsakh, M., Coronel, J. and Tao, M. (2007). Effect of Soil Moisture Content and Dry Density on Cohesive Soil–Geosynthetic Interactions Using Large Direct Shear Tests. *Journal of Materials in Civil Engineering*, 19(7), pp.540-549.

Abu-Farsakh, M., Chen, Q. and Sharma, R. (2013). An experimental evaluation of the behavior of footings on geosynthetic-reinforced sand. *Soils and Foundations*, 53(2), pp.335-348.

Abu-Farsakh, M., Gu, J., Voyiadjis, G. and Chen, Q. (2014). Mechanistic–empirical analysis of the results of finite element analysis on flexible pavement with geogrid base reinforcement. *International Journal of Pavement Engineering*, 15(9), pp.786-798.

Adams, M. and Collin, J. (1997). Large Model Spread Footing Load Tests on Geosynthetic Reinforced Soil Foundations. *Journal of Geotechnical and Geoenvironmental Engineering*, 123(1), pp.66-72.

Al-Qadi, I., Lahouar, S., Loulizi, A., Elseifi, M. and Wilkes, J. (2004). Effective Approach to Improve Pavement Drainage Layers. *Journal of Transportation Engineering*, 130(5), pp.658-664.

Al-Qadi, I., Dessouky, S., Kwon, J. and Tutumluer, E. (2008). Geogrid in Flexible Pavements. *Transportation Research Record: Journal of the Transportation Research Board*, 2045(1), pp.102-109.

Arulrajah, A., Rahman, M.A., Piratheepan, J., Bo, M.W. and Imteaz, M.A. (2013). Evaluation of interface shear strength properties of geogrid-reinforced construction and demolition materials using a modified large-scale direct shear testing apparatus. *Journal of Materials in Civil Engineering*, *26*(5), pp.974-982.

AS 1289, (2014). Standard methods of testing soils for engineering purposes. Council of Standards Australia.

Asha, M.N. and Latha, G.M. (2010). Modified CBR Tests on Geosynthetic Reinforced Soil-aggregate Systems. *strain (kN/m)*, *151*(588), p.319.

ASTM D6706-01, (2013). Standard test method for measuring geosynthetic pullout resistance in soil. ASTM International, West Conshohocken, PA, USA.

ASTM D6637/D6637M, (2015). Standard test method for determining tensile properties of geogrids by the single or mildti-rib tensile method. ASTM International, West Conshohocken, PA, USA.

Austroads, (2008a). Future development of Austroads pavement design guidelines, by G Jameson, Austroads internal report, Austroads, Sydney, NSW.

Austroads, (2008b). Guide to pavement technology part 2: pavement structural design, by G Jameson, APT98/08, Austroads, Sydney, NSW.

Austroads, (2012). Austroads Guide to Pavement Technology Part 2: Pavement Structural Design. Austroads Inc. Sydney, Australia.

Barbieri, D., Hoff, I. and Mørk, M. (2019). Innovative stabilization techniques for weak crushed rocks used in road unbound layers: A laboratory investigation. *Transportation Geotechnics*, 18, pp.132-141.

Ezzein, F. and Bathurst, R. (2014). A new approach to evaluate soil-geosynthetic interaction using a novel pullout test apparatus and transparent granular soil. *Geotextiles and Geomembranes*, 42(3), pp.246-255.

Bathurst, R. and Ezzein, F. (2016). Geogrid pullout load–strain behaviour and modelling using a transparent granular soil. *Geosynthetics International*, 23(4), pp.271-286.

Berg, R. R., Christopher, B. R., & Perkins, S. W. (2000). Geosynthetic reinforcement of the aggregate base course of flexible pavement structures. *GMA White Paper II, Geosynthetic Materials Association, Roseville, MN, USA*, 130.

Bergado, D., Chai, J., Abiera, H., Alfaro, M. and Balasubramaniam, A. (1993). Interaction between cohesive-frictional soil and various grid reinforcements. *Geotextiles and Geomembranes*, 12(4), pp.327-349.

Bhutta, S. A. (1998). *Mechanistic-empirical pavement design procedure for geosynthetically stabilized flexible pavements* (Unpublished doctoral dissertation). Virginia Polytechnic Institute and State University, Blacksburg, Va.

Bloise, N., & Ucciardo, S. (2000). On site test of reinforced freeway with high-strength geosynthetics. In *Second European geosynthetics conference* (Vol. 1, pp. 369-371).

BS EN ISO 10319, (2015). Geosynthetics - Wide-width tesile test. The British Standards Institution.

Cancelli, A., & Montanelli, F. (1999). *In-ground test for geosynthetic reinforced flexible paved roads* (No. Volume 2).

Cook, J. and Andrews, C. (2015). The benefits of stabilisation geogrids in whole pavement construction. *Proceedings of the Institution of Civil Engineers - Civil Engineering*, 168(6), pp.29-34.

Celauro, B., Bevilacqua, A., Lo Bosco, D. and Celauro, C. (2012). Design Procedures for Soil-Lime Stabilization for Road and Railway Embankments. Part 1-Review of Design Methods. *Procedia - Social and Behavioral Sciences*, 53, pp.754-763.

Cuelho, E. and Perkins, S. (2017). Geosynthetic subgrade stabilization – Field testing and design method calibration. *Transportation Geotechnics*, 10, pp.22-34.

Das, B. (2016). Use of geogrid in the construction of railroads. *Innovative Infrastructure Solutions*, 1(1).

Davies, M. C. R., & Bridle, R. J. (1990). Predicting the Permanent Deformation of Reinforced Flexible Pavement Subject to Repeated Loading. *Performance of Reinforced Soil Structures*, pp.421-425.

Demir, A., Laman, M., Yildiz, A. and Ornek, M. (2013). Large scale field tests on geogrid-reinforced granular fill underlain by clay soil. *Geotextiles and Geomembranes*, 38, pp.1-15.

Duncan-Williams, E. and Attoh-Okine, N. (2008). Effect of geogrid in granular base strength – An experimental investigation. *Construction and Building Materials*, 22(11), pp.2180-2184.

El-Ashwah, A., Awed, A., El-Badawy, S. and Gabr, A. (2019). A new approach for developing resilient modulus master surface to characterize granular pavement materials and subgrade soils. *Construction and Building Materials*, 194, pp.372-385.

Farrag, K., Acar, Y. and Juran, I. (1993). Pull-out resistance of geogrid reinforcements. *Geotextiles and Geomembranes*, 12(2), pp.133-159.

Ferrotti, G., Canestrari, F., Virgili, A. and Grilli, A. (2011). A strategic laboratory approach for the performance investigation of geogrids in flexible pavements. *Construction and Building Materials*, 25(5), pp.2343-2348.

Floss, R., & Gold, G. (1994). Causes for the improved bearing behaviour of the reinforced two-layer system. In *Fifth International Conference on Geotextiles, Geomembranes and Related Products* (Vol. 1, pp. 147-150).

Fourie, A. and Fabian, K. (1987). Laboratory determination of clay-geotextile interaction. *Geotextiles and Geomembranes*, 6(4), pp.275-294.

Giroud, J.P. and Noiray, L., (1981). Geotextile-reinforced unpaved road design. *Journal of Geotechnical and Geoenvironmnetal Engineering, 107*(ASCE 16489).

Giroud, J. P., Ah-Line, C., & Bonaparte, R. (1984). Design of unpaved roads and trafficked areas with geogrids. In *Polymer grid reinforcement* (pp. 116-127). Thomas Telford Publishing.

Giroud, J. and Han, J. (2004). Design Method for Geogrid-Reinforced Unpaved Roads. I. Development of Design Method. *Journal of Geotechnical and Geoenvironmental Engineering*, 130(8), pp.775-786.

Guido, V., Chang, D. and Sweeney, M. (1986). Comparison of geogrid and geotextile reinforced earth slabs. *Canadian Geotechnical Journal*, 23(4), pp.435-440.

Haas, R., Walls, J. and Carroll, R.G., (1988). Geogrid reinforcement of granular bases in flexible pavements. *Transportation research record*, *1188*, pp.19-27.

Hicks, R.G. and Monismith, C.L., (1971). Factors influencing the resilient response of granular materials. *Highway research record*, (345).

Hufenus, R., Rueegger, R., Banjac, R., Mayor, P., Springman, S. M., & Brönnimann, R. (2006). Full-scale field tests on geosynthetic reinforced unpaved roads on soft subgrade. *Geotextiles and Geomembranes*, 24(1), pp.21-37.

Infante, D. U., Martinez, G. A., Arrúa, P., & Eberhardt, M. (2016). Behaviour of geogrid reinforced sand under vertical load. *International Journal of Geomate*, *10*(21), pp.1862-1868.

Jahandari, S., Saberian, M., Zivari, F., Li, J., Ghasemi, M. and Vali, R. (2017). Experimental study of the effects of curing time on geotechnical properties of stabilized clay with lime and geogrid. *International Journal of Geotechnical Engineering*, 13(2), pp.172-183.

JGS 0942, (2009). Tests on geosynthetics - pull out test for geosynthetics. The Japanese Geotechnical Society, Japan.

Khing, K., Das, B., Puri, V., Cook, E. and Yen, S. (1993). The bearing-capacity of a strip foundation on geogrid-reinforced sand. *Geotextiles and Geomembranes*, 12(4), pp.351-361.

Kim, D. and Frost, J. (2011). Effect of geotextile constraint on geotextile/geomembrane interface shear behavior. *Geosynthetics International*, 18(3), pp.104-123.

Kumar, S., Solanki, C. H., & Pandey, B. K. (2015). Behaviour of prestressed geotextilereinforced fine sand bed supporting an embedded square footing. *International Journal of Geomate*, *8*(2), pp.1257-1262

Kwon, J. and Tutumluer, E. (2009). Geogrid Base Reinforcement with Aggregate Interlock and Modeling of Associated Stiffness Enhancement in Mechanistic Pavement Analysis. *Transportation Research Record: Journal of the Transportation Research Board*, 2116(1), pp.85-95.

Lee, K. and Manjunath, V. (2000). Soil-geotextile interface friction by direct shear tests. *Canadian Geotechnical Journal*, 37(1), pp.238-252.

Liu, C., Zornberg, J., Chen, T., Ho, Y. and Lin, B. (2009). Behavior of Geogrid-Sand Interface in Direct Shear Mode. *Journal of Geotechnical and Geoenvironmental Engineering*, 135(12), pp.1863-1871.

Liu, C., Yang, K. and Nguyen, M. (2014). Behavior of geogrid–reinforced sand and effect of reinforcement anchorage in large-scale plane strain compression. *Geotextiles and Geomembranes*, 42(5), pp.479-493.

Lopes, M. and Ladeira, M. (1996). Influence of the confinement, soil density and displacement rate on soil-geogrid interaction. *Geotextiles and Geomembranes*, 14(10), pp.543-554.

McCartney, J., Zornberg, J. and Swan, R. (2009). Analysis of a Large Database of GCL-Geomembrane Interface Shear Strength Results. *Journal of Geotechnical and Geoenvironmental Engineering*, 135(2), pp.209-223.

Miyata, Y. and Bathurst, R. (2012). Reliability analysis of soil-geogrid pullout models in Japan. *Soils and Foundations*, 52(4), pp.620-633.

Moayed, R.Z. and Nazari, M., (2011). Effect of Utilization of Geosynthetic on Reducing the Required Thickness of Subbase Layer of a Two Layered Soil. *World Academy of Science, Engineering and Technology*, *49*(175), pp.963-967.

Montanelli, F. I. L. I. P. P. O., Zhao, A., & Rimoldi, P. (1997, March). Geosynthetic-reinforced pavement system: testing and design. In *Proceeding of Geosynthetics* (Vol. 97, pp. 619-632).

Müller, W.W. and Saathoff, F., (2015). Geosynthetics in geoenvironmental engineering. *Science and technology of advanced materials*, *16*(3), p.034605.

Naeini, S., and Moayed, R. Z. (2009). Effect of plasticity index and reinforcement on the CBR value of soft clay. *International Journal of Civil Engineering, 7*(2), pp.124-130.

Ochiai, H., Otani, J., Hayashic, S. and Hirai, T. (1996). The pull-out resistance of geogrids in reinforced soil. *Geotextiles and Geomembranes*, 14(1), pp.19-42.

Ornek, M., Laman, M., Demir, A. and Yildiz, A. (2012). Prediction of bearing capacity of circular footings on soft clay stabilized with granular soil. *Soils and Foundations*, 52(1), pp.69-80.

Patra, C., Das, B. and Atalar, C. (2005). Bearing capacity of embedded strip foundation on geogrid-reinforced sand. *Geotextiles and Geomembranes*, 23(5), pp.454-462.

Paul, R., and Grove, R. (2008). Guide to road design: part 7: geotechnical investigation and design

Perkins, S. (1999). Mechanical Response of Geosynthetic-Reinforced Flexible Pavements. *Geosynthetics International*, 6(5), pp.347-382.

Perkins, S. and Ismeik, M. (1997). A Synthesis and Evaluation of Geosynthetic-Reinforced Base Layers in Flexible Pavements- Part II. *Geosynthetics International*, 4(6), pp.605-621.

Perkins, S. W., Christopher, B. R., Cuelho, E. L., Eiksund, G. R., Hoff, I., Schwartz, C. W., ... & Watn, A. (2004). Development of design methods for geosynthetic reinforced flexible pavements. *report prepared for the US Department of Transportation Federal Highway Administration, Washington, DC, FHWA Report Reference Number DTFH61-01-X-00068, 263p*.

Powell, W., Keller, G. and Brunette, B. (1999). Applications for Geosynthetics on Forest Service Low-Volume Roads. *Transportation Research Record: Journal of the Transportation Research Board*, 1652(1), pp.113-120.

Qian, Y., Han, J., Pokharel, S. K., & Parsons, R. L. (2010). Experimental study on triaxial geogrid-reinforced bases over weak subgrade under cyclic loading.

GeoFlorida 2010: Advances in Analysis, Modeling and Design (Geotechnical Special Publication 199), 1208-1216.

Rajesh, U., Sajja, S. and Chakravarthi, V. (2016). Studies on Engineering Performance of Geogrid Reinforced Soft Subgrade. *Transportation Research Procedia*, 17, pp.164-173.

Richeton, J., Ahzi, S., Vecchio, K., Jiang, F. and Makradi, A. (2007). Modeling and validation of the large deformation inelastic response of amorphous polymers over a wide range of temperatures and strain rates. *International Journal of Solids and Structures*, 44(24), pp.7938-7954.

Schuettpelz, C., Fratta, D. and Edil, T. (2009). Evaluation of the Zone of Influence and Stiffness Improvement from Geogrid Reinforcement in Granular Materials. *Transportation Research Record: Journal of the Transportation Research Board*, 2116(1), pp.76-84.

Sellmeijer, J. B. (1990). Design of geotextile reinforced paved roads and parking areas. In *Proceedings of the Fourth International Conference on Geotextiles, Geomembranes and Related Products* (pp. 177-182).

Singh, P. and Gill, K.S., (2012). CBR Improvement of clayey soil with Geogrid Reinforcement. *International Journal of Emerging Technology and Advanced Engineering*, *2*(6), pp.456-462.

Steward, J., Williamson, R. and Mohney, J., (1977). *Guidelines for use of fabrics in construction and maintenance of low-volume roads* (No. FHWA-TS-78205).

Subaida, E., Chandrakaran, S. and Sankar, N. (2009). Laboratory performance of unpaved roads reinforced with woven coir geotextiles. *Geotextiles and Geomembranes*, 27(3), pp.204-210.

Sugimoto, M., Alagiyawanna, A. and Kadoguchi, K. (2001). Influence of rigid and flexible face on geogrid pullout tests. *Geotextiles and Geomembranes*, 19(5), pp.257-277.

The World Factbook. (2018). Retrieved 26 November 2018, from Central Intelligence Agency,https://www.cia.gov/library/publications/the-world-factbook/geos/as.html

Wang, Z., Jacobs, F. and Ziegler, M. (2016). Experimental and DEM investigation of geogrid–soil interaction under pullout loads. *Geotextiles and Geomembranes*, 44(3), pp.230-246.

Watts, G. R. A., Blackman, D. I., & Jenner, C. G. (2004). The performance of reinforced unpaved sub-bases subjected to trafficking.

Webster, S.L. (1993). *Geogrid reinforced base courses for flexible pavements for light aircraft: Test section constuction, behaviour under traffic, laboratory tests, and design criteria* (No. WES/TR/GL-93-6). Army Engineer Waterways Experiment Station Vicksburg Ms Geotechnical Lab.

Werkmeister, S., Dawson, A.R. and Wellner, F., (2004). Pavement design model for unbound granular materials. *Journal of Transportation Engineering*, *130*(5), pp.665-674.

Zornberg, J.G., (2011). Advances in the use of geosynthetics in pavement design. *Geosynthetics India*, 11, pp.23-24.

Zornberg, J., & Gupta, R. (2010). Geosynthetics in pavements: North American contributions. In *Theme Speaker Lecture, Proceedings of the 9th International Conference on Geosynthetics, Guarujá, Brazil, May* (Vol. 1, pp. 379-400).